CHAPTER 6: System Throughput and SNR / Exposure Time Estimation

In This Chapter...

6.1 System Throughput

A decision on a suitable exposure time will require the combination of

- The overall spectral response of the system (Figure 2.4).
- The spectral transmission of the filters (Chapter 3 and Appendix A).
- The spectral energy distribution and spatial profile of the target.
- The point response function and pixel size of the instrument (Chapter 5).
- Criteria for specifying desirable charge levels.

When the transmissions of filters $T(\lambda)$ are combined with the overall system response $Q(\lambda)$, we obtain detective quantum efficiency plots (electrons-per-photon as a function of λ) for each filter. These DQE plots link the output of the CCD to the photon flux at the input to an unobscured 2.4 m telescope.

These calibrations exist in the STScI Calibration Data Base, and are accessible with the STSDAS SYNPHOT package or with the XCAL software. The XCAL and SYNPHOT Users Guides should be consulted for further details. We include here a sufficient calibration for exposure planning.

In Table 6.1 the dimensionless efficiency and the mean wavelength for each filter are tabulated together with the effective width, the equivalent Gaussian dimensionless width, the maximum transmission, the derivative of the mean wavelength with respect to spectral index, the pivot wavelength, average wavelength, and wavelength of maximum transmission. The parameters are defined as follows. The dimensionless efficiency is

$$\int Q(\lambda)T(\lambda)d\lambda/\lambda$$

The mean wavelength is defined in Schneider, Gunn, and Hoessel Ap. J., 264, 337 (1983)

$$\bar{\lambda} = \exp\left[\frac{\int Q(\lambda)T(\lambda)\log_e(\lambda)d\lambda/\lambda}{\int Q(\lambda)T(\lambda)d\lambda/\lambda}\right]$$

This rather unconventional definition has the property that the correspondingly defined mean frequency is just $c/\bar{\lambda}$. It is in some sense halfway between the conventional frequency mean and the wavelength mean. The pivot wavelength is defined as

$$\lambda_p = \left[\frac{\int Q(\lambda)T(\lambda)\lambda d\lambda}{\int Q(\lambda)T(\lambda)d\lambda/\lambda}\right]^{1/2}$$

The effective dimensionless Gaussian width is defined implicitly by

$$\sigma^2 = \left[\frac{\int_{\bar{\lambda}(1-5\sigma)}^{\bar{\lambda}(1+5\sigma)} Q(\lambda)T(\lambda)\left[\log_e\left(\frac{\lambda}{\bar{\lambda}}\right)\right]^2\frac{d\lambda}{\lambda}}{\int_{\bar{\lambda}(1-5\sigma)}^{\bar{\lambda}(1+5\sigma)} Q(\lambda)T(\lambda)\frac{d\lambda}{\lambda}}\right]$$

where the integration limits eliminate unrealistic contributions from imperfect blocking far from the bandpass. The effective width of the bandpass is

$$\delta\bar{\lambda} = 2[2\log_e 2]^{1/2}\sigma\bar{\lambda}$$

The final two columns in Table 6.1 are defined as follows. In the next-to-last column $m_{e/sec}$ is the zero-point magnitude for 1 $e^- s^{-1}$ (with AB_V=0). The final column gives t_{wfsky}, which is the exposure time (in seconds) needed to make the sky noise equal to 5 e^- RMS (i.e. ~read noise) in the WFC for a sky level of V=23.3 mag $arcsec^{-2}$.

Table 6.1: System Efficiencies and Zeropoints. See Section 6.1 for definitions. [a]

Filter	$\int QTd\lambda/\lambda$	$\bar{\lambda}$	$\delta\bar{\lambda}$	σ	QT_{max}	$d\bar{\lambda}/d\alpha$	λ_p	$\langle\lambda\rangle$	λ_{max}	$m_{e/sec}$	t_{wfsky}
F122M	0.00012	1419.7	438.2	0.1311	0.00118	24.40	1748.5	2018.0	1258	18.69	1.7E+06
F130LP	0.09178	5115.8	4776.0	0.3965	0.12977	804.10	5786.6	6107.1	6386	25.90	
F160AW	0.00021	1491.8	448.9	0.1278	0.00065	24.36	1517.3	1530.4	1406	19.30	9.5E+05
F160BW	0.00021	1491.8	448.9	0.1278	0.00065	24.36	1517.3	1530.4	1406	19.30	9.5E+05
F165LP	0.08841	5195.6	4541.2	0.3712	0.12633	715.80	5817.0	6118.8	6386	25.86	
F170W	0.00057	1749.8	545.5	0.1324	0.00178	30.67	1824.6	1872.6	1834	20.38	3.5E+05
F185W	0.00035	1952.9	335.0	0.0729	0.00188	10.37	1971.9	1983.1	1936	19.86	9.1E+06
F218W	0.00057	2191.6	387.9	0.0752	0.00275	12.38	2205.2	2212.2	2248	20.38	5.6E+06
F255W	0.00078	2585.8	393.2	0.0646	0.00452	10.78	2597.3	2603.1	2546	20.73	4.1E+06
F300W	0.00519	2942.8	735.8	0.1062	0.01838	33.17	2981.9	3002.7	2866	22.78	7.1E+04
F336W	0.00403	3342.2	381.1	0.0484	0.02872	7.84	3359.4	3369.2	3456	22.51	3.3E+04
F343N	0.00006	3432.9	27.3	0.0034	0.00691	0.04	3440.4	3445.6	3432	17.94	2.2E+06
F375N	0.00006	3737.5	27.3	0.0031	0.00774	0.04	3743.0	3746.7	3737	17.94	9.0E+05
F380W	0.00693	3964.4	673.0	0.0721	0.03406	20.61	3984.8	3995.0	3994	23.10	7.8E+03
F390N	0.00029	3888.7	45.2	0.0049	0.01880	0.10	3889.6	3890.3	3885	19.65	1.9E+05
F410M	0.00164	4090.1	146.7	0.0152	0.03619	0.95	4092.6	4093.9	4098	21.53	3.3E+04
F437N	0.00019	4370.3	25.3	0.0025	0.02681	0.03	4369.6	4369.7	4368	19.19	1.8E+05
F439W	0.00501	4299.8	473.3	0.0467	0.03436	9.40	4309.6	4314.4	4186	22.74	6.9E+03
F450W	0.01501	4519.1	956.6	0.0899	0.07955	36.52	4555.1	4572.9	5066	23.94	2.3E+03
F467M	0.00216	4668.7	166.7	0.0152	0.04825	1.07	4669.9	4670.5	4732	21.83	1.6E+04
F469N	0.00023	4694.4	24.9	0.0022	0.03267	0.02	4694.5	4694.5	4699	19.40	1.5E+05
F487N	0.00029	4865.1	25.8	0.0023	0.04239	0.03	4865.4	4865.8	4866	19.65	8.5E+04
F502N	0.00037	5012.2	26.8	0.0023	0.05226	0.03	5013.1	5013.1	5008	19.92	6.7E+04
F547M	0.01224	5476.3	483.1	0.0375	0.10577	7.69	5484.0	5487.8	5566	23.71	2.0E+03
F555W	0.02727	5397.5	1226.4	0.0965	0.10312	50.26	5447.9	5473.3	5536	24.58	9.0E+02
F569W	0.02139	5614.2	965.7	0.0730	0.10587	29.96	5644.9	5660.3	5536	24.32	8.8E+02
F588N	0.00133	5893.5	49.0	0.0035	0.12054	0.07	5893.5	5893.6	5894	21.30	1.4E+04
F606W	0.04191	5935.0	1497.3	0.1071	0.13468	68.12	6002.3	6036.1	6194	25.05	4.5E+02
F622W	0.02649	6162.8	916.5	0.0632	0.13123	24.58	6187.5	6199.8	6416	24.55	7.1E+02
F631N	0.00078	6306.4	30.8	0.0021	0.11709	0.03	6306.4	6306.4	6306	20.73	2.4E+04
F656N	0.00045	6563.7	21.4	0.0014	0.10379	0.01	6563.7	6564.0	6561	20.13	3.4E+04
F658N	0.00063	6590.1	28.5	0.0018	0.10574	0.02	6590.8	6590.9	6596	20.49	2.4E+04
F673N	0.00104	6732.1	47.2	0.0030	0.11134	0.06	6732.2	6732.3	6736	21.04	1.5E+04
F675W	0.02169	6695.9	865.6	0.0549	0.12770	20.18	6716.1	6726.2	6634	24.34	7.1E+02
F702W	0.03206	6867.8	1382.5	0.0855	0.13397	50.19	6918.8	6944.5	6514	24.76	4.8E+02
F785LP	0.00780	8617.0	1331.7	0.0656	0.04378	37.11	8654.8	8673.9	8306	23.23	1.6E+03
F791W	0.01589	7826.3	1205.0	0.0654	0.09120	33.46	7860.5	7877.7	7364	24.00	7.9E+02
F814W	0.01799	7920.9	1488.8	0.0798	0.09937	50.47	7973.0	7999.5	7266	24.13	7.0E+02
F850LP	0.00395	9072.1	985.8	0.0461	0.03491	19.32	9091.6	9101.6	8800	22.49	2.9E+03
F953N	0.00012	9544.7	52.5	0.0023	0.01651	0.05	9544.7	9544.8	9526	18.69	9.6E+04
F1042M	0.00012	10183.5	365.0	0.0152	0.00359	2.36	10188.8	10191.1	10110	18.69	8.7E+04
FQUVN-A	0.00028	3765.4	73.1	0.0082	0.01122	0.26	3766.0	3766.6	3803	19.61	4.7E+05
FQUVN-B	0.00028	3830.2	57.1	0.0063	0.01465	0.15	3830.7	3831.3	3827	19.61	1.9E+05
FQUVN-C	0.00038	3912.9	59.3	0.0064	0.01949	0.16	3914.4	3915.0	3907	19.94	1.4E+05
FQUVN-D	0.00045	3992.3	63.5	0.0068	0.02244	0.18	3992.9	3993.2	3992	20.13	1.2E+05
FQCH4N-A	0.00075	~5433	~38	0.0028	0.09356	0.04	-	-	5443	20.68	3.3E+04
FQCH4N-B	0.00082	~6193	~44	0.0028	0.11360	0.05	-	-	6205	20.78	2.3E+04
FQCH4N-C	0.00062	~7274	~51	0.0024	0.09075	0.04	-	-	7279	20.48	2.5E+04
FQCH4N-D	0.00026	~8929	~64	0.0067	0.03334	0.39	-	-	8930	19.53	4.4E+04
POLQ_par	0.06005	5570.9	4184.5	0.3190	0.09298	566.81	6076.2	6323.3	6476	25.44	
POLQ_per	0.01299	7027.7	5153.2	0.3114	0.03744	681.43	7541.1	7766.0	7839	23.78	

a. It is anticipated the values for filters F160BW and FQCH4N will be updated in mid-1996.

Table 6.2: AB_ν as a Function of Wavelength. AB_ν is defined as a color-dependent correction from V magnitude to AB magnitude at frequency ν. Wavelength (Å) runs along the top; spectral classes run down the leftmost column. The second column contains B-V. See Section 6.3.

	B-V	1500	2000	2500	3000	3500	4000	4500	5000	6000	7000	8000	9000	10000
sky	1.10	2.45	5.46	5.46	3.12	2.00	1.03	0.55	0.18	-0.11	-0.33	-0.55	-0.65	-0.75
B0	-0.31	-1.60	-1.50	-1.20	-0.78	-0.62	-0.46	-0.36	-0.22	0.16	0.46	0.76	0.96	1.17
A0	0.00	2.22	1.35	1.11	1.21	1.00	-0.23	-0.16	-0.09	0.11	0.22	0.33	0.36	0.4
F0	0.27	7.22	4.10	3.11	1.99	1.38	0.29	0.06	0.03	0.03	0.05	0.08	0.09	0.1
G0	0.58	8.9	6.35	4.61	2.46	1.63	0.67	0.26	0.08	-0.04	-0.12	-0.21	-0.23	-0.25
K0III	1.07	13	10.3	8.11	5.46	2.13	1.16	0.46	0.2	-0.24	-0.42	-0.61	-0.66	-0.72
M0III	1.60	15	12.3	9.36	6.21	4.63	2.26	0.96	0.51	-0.46	-0.76	-1.06	-1.12	-1.19
gE	1.00	6.82	6.41	5.43	3.63	2.49	1.40	0.55	0.21	-0.19	-0.52	-0.81	-1.07	-1.29
Sa	0.80	5.40	4.80	4.10	3.00	2.01	1.12	0.44	0.19	-0.17	-0.44	-0.7	-0.95	-1.16
Sbc	0.60	4.03	3.18	2.86	2.46	1.54	0.84	0.34	0.17	-0.14	-0.37	-0.6	-0.84	-1.04
Scd	0.45	2.67	2.29	2.15	1.76	1.35	0.65	0.28	0.13	-0.11	-0.26	-0.39	-0.47	-0.58
Ir I	0.30	1.77	1.40	1.36	1.24	0.94	0.43	0.34	0.17	0.13	-0.04	-0.21	-0.33	-0.45

6.2 On-Line Exposure Time Calculator

We note that most of the calculations below are incorporated in the on-line WFPC2 Exposure Time Calculator (ETC) program, which is available on the WFPC2 WWW pages at

`http://www.stsci.edu/ftp/instrument_news/WFPC2/wfpc2_top.html`

on the software tools page.

To use this program, one merely fills out an “HTML” form giving the target information (e.g. magnitude and color), camera configuration (PC or WFC, desired gain setting, and filter), and either the exposure time or the desired signal-to-noise ratio. As of this writing there are separate HTML forms for point sources, extended sources, point source with background light, and extended targets with background light. After filling out the form the user then clicks on “calculate” and the program returns the resulting signal-to-noise ratio if the exposure time was specified, or vice versa. Examples of completed HTML forms and results are shown in “Sample SNR Calculations” on page 123. Note that clicking on any colored text on the HTML form will give a description of that item.

The ETC program handles sources with stellar spectra, power law sources, and emission line sources; point sources and extended sources; and sources superposed on a diffuse stellar background. The program also returns advice on CR-SPLITing, use of CLOCKS=YES, and warnings about saturation, if appropriate. The program currently (Version 2.0) assumes stellar data will be analyzed by PSF fitting. Results are typically accurate to a few percent.

While observers should familiarize themselves with the material below, most will find the ETC program faster and easier to use for actual calculations. The ETC program will also be updated to reflect any changes in instrument performance, so observers can be assured of up-to-the-minute information.

6.3 Target Count Rates

We now consider estimation of count rates for objects with stellar, power law, and emission line spectra.

6.3.1 Count Rates for Stellar Sources

To estimate the number of electrons collected from a point source of apparent visual magnitude V, one can use the equation:

$$N = 2.5 \times 10^{11} \cdot t \cdot [\int Q(\lambda) T(\lambda) d\lambda / \lambda] \times 10^{-0.4(V + AB_\nu)} \qquad (6.1)$$

where t is the exposure time in seconds, the QT integral is given in Table 6.1, and AB_ν is given in Table 6.2 as a function of spectral type and wavelength for some example spectral energy distributions. The quantity AB_ν is a color-dependent correction from V magnitude to AB magnitude at frequency ν. The AB magnitude system is defined as (Oke and Gunn 1983)

$$AB = V + AB_\nu = -2.5 \cdot \log F_\nu - 48.60$$

where F_ν is the flux in erg cm^{-2} s^{-1} Hz^{-1}.

Equation 6.1 may be trivially rewritten to give the count rate R_{object} in units of e$^-$ s^{-1} pixel^{-1} for a target with a stellar spectrum as:

$$R_{object} = 2.5 \times 10^{11} \cdot [\int Q(\lambda) T(\lambda) d\lambda / \lambda] \cdot 10^{-0.4(V + AB_\nu)} \qquad (6.2)$$

6.3.2 Count Rates for Power Law Sources

If one knows the spectral index α (which is zero for a source with a flat continuum), $V+AB_\nu$ can also be calculated as the monochromatic Oke system magnitude at the corrected mean wavelength of the filter:

$$V + AB_\nu = -2.5\log_{10}(S_\nu[\bar{\lambda} + \alpha(d\bar{\lambda}/d\alpha)]) - 48.6$$

where S_ν is the flux in ergs cm^{-2} s^{-1} Hz^{-1} as in Oke and Gunn, Ap. J., 266, 713 (1983) at the effective mean wavelength of the filter $\bar{\lambda} + \alpha(d\bar{\lambda}/d\alpha)$. It can be shown that

$$\frac{d\bar{\lambda}}{d\alpha} = \bar{\lambda}\sigma^2$$

if the integrands are weighted by a source with spectral index α in the definition of λ. See also Koornneef, J., et al. "Synthetic Photometry and the Calibration of the Hubble Space Telescope" in Highlights of Astronomy (7, 833, J.-P. Swings Ed (1983). Combining the above equations gives

$$R_{object} = 6.9 \times 10^{30} \cdot [\int Q(\lambda)T(\lambda)d\lambda/\lambda] \cdot S_\nu\left(\bar{\lambda} + \alpha\frac{d\bar{\lambda}}{d\alpha}\right) \qquad (6.3)$$

6.3.3 Count Rates for Emission Line Sources

The count rate in units of e^- s^{-1} for a monochromatic emission line is given by

$$R_{object} = 2.3 \times 10^{12} \cdot (QT) \cdot F \cdot \lambda \qquad (6.4)$$

where F is the emission line flux in units of ergs cm^{-2} s^{-1}, and λ is the wavelength of the line in Angstroms. The quantity QT is the (system + filter) quantum efficiency at the wavelength of the line, which can be determined from inspection of the figures in section A.2, "Passbands including the System Response", on page 211. For lines near the maxima of the filter transmission curves, it should be sufficient to use QT_{max} from Table 6.1. Note that the integrated filter efficiency is not relevant for the signal calculation.

In cases where the width of the line approaches that of the filter, it will be necessary to convolve the line shape and filter bandpass using either the SYNPHOT or XCAL programs.

For example, H_α emission at 6563Å, with total source flux F=10^{-16} erg s^{-1} cm^{-2}, observed through the F656N filter (total system throughput T=0.104 from "F656N, F658N, F673N, F675W, F702W, F785LP" on page 217), will produce a target count rate R_{object}=0.155 e^- s^{-1} integrated over the entire source.

6.4 Sky Background

The sky background can contribute significant Poisson noise in broad and medium band filters, and must be taken into account during noise calculations. The actual sky brightness depends on the heliocentric ecliptic coordinates (latitude and longitude) in a manner summarized in Table 6.3. The appropriate AB_V can be taken from Table 6.2. To convert mag arcsec^{-2} to mag pixel^{-1} one needs to add 5 magnitudes (WFC) or 6.7 magnitudes (PC1). These values are actually lower limits on the effective sky-brightness that will be seen, because light from the bright Earth limb can scatter into the aperture.

If your observations are sky background limited, and signal-to-noise is a driver, consider the use of the special requirement LOW-SKY as described in the *Call for Proposals* or the *Phase II Proposal Instructions*. LOW-SKY has two effects:

- It causes the observation to be scheduled at the time of year when the zodiacal background light is within 30% of the minimum possible background value for the target, and
- It requires that the observation be made when the bright Earth limb is more than 40° from the OTA axis, which greatly reduces scattered light.

For many targets LOW-SKY will have minimal impact on the observing efficiency. Note, however, that targets in the Continuous Viewing Zone (CVZ) cannot be observed if LOW-SKY is specified. See "Observing Faint Targets" on page 143 for more information.

Table 6.3: Sky Brightness (V mag arcsec^{-2}) as a Function of Heliocentric Ecliptic Latitude and Longitude. "SA" denotes that the target is unobservable due to solar avoidance.

Heliocentric Ecliptic Longitude	Ecliptic Latitude						
	0°	15°	30°	45°	60°	75°	90°
180°	22.1	22.4	22.7	23.0	23.2	23.4	23.3
165°	22.3	22.5	22.8	23.0	23.2	23.4	23.3
150°	22.4	22.6	22.9	23.1	23.3	23.4	23.3
135°	22.4	22.6	22.9	23.2	23.3	23.4	23.3
120°	22.4	22.6	22.9	23.2	23.3	23.3	23.3
105°	22.2	22.5	22.9	23.1	23.3	23.3	23.3
90°	22.0	22.3	22.7	23.0	23.2	23.3	23.3
75°	21.7	22.2	22.6	22.9	23.1	23.2	23.3
60°	21.3	21.9	22.4	22.7	23.0	23.2	23.3
45°	SA	SA	22.1	22.5	22.9	23.1	23.3
30°	SA	SA	SA	22.3	22.7	23.1	23.3
15°	SA	SA	SA	SA	22.6	23.0	23.3
0°	SA	SA	SA	SA	22.6	23.0	23.3

Another option for reducing the sky brightness, is the special requirement SHADOW, which forces the observation to be made when HST is in the Earth's shadow. This usually has a large negative impact on the observing efficiency, and is recommended only when attempting to avoid geocoronal lines when observing far-UV emission lines (e.g. Ly α and OI 1304Å). Moreover, it does not attempt to minimize zodiacal emission, which dominates at visible wavelengths.

Table 6.4 shows approximate sky count rates for the WFC and PC1 for filters with significant sky count rates. An average sky brightness of V=22.9 mag arcsec^{-2} is assumed. Filters not listed in the table have sky count rates below that of the dark current, so the sky contribution will generally be unimportant. Values for other filters or sky brightnesses can be computed from Table 6.2, Table 6.1, Table 6.3, and Equation 6.2.

Table 6.4: Sky Count Rate per Pixel (P_{sky}). An average sky brightness of V = 22.9 mag arcsec^{-2} is assumed. Filters not listed have sky rate significantly below the dark current.

Filter	**Sky Count Rate (P_{sky}) (e^{-} s^{-1} $pixel^{-1}$)**	
	WFC	PC1
F336W	0.0009	0.0002
F380W	0.005	0.001
F439W	0.005	0.0011
F450W	0.018	0.004
F467M	0.003	0.0006
F547M	0.021	0.0045
F555W	0.052	0.010
F588N	0.002	0.0006
F569W	0.040	0.0081
F606W	0.090	0.020
F622W	0.060	0.012
F673N	0.002	0.0006
F675W	0.056	0.012
F702W	0.082	0.0016
F785LP	0.024	0.0050
F791W	0.048	0.010
F814W	0.054	0.011
F850LP	0.012	0.0024

6.5 Signal-to-Noise Ratio Estimation

The signal-to-noise ratio (SNR) for a point source depends on both the Poisson noise of the object, and on noises associated with the background. Sources of background noise include “read noise” of the CCDs, and Poisson noise in the dark current, sky background, and any smooth galaxy light superposed on the target.

The SNR obtained for photometry of a point source will depend on the analysis technique used. The optimum SNR will be obtained when the pixels of the point source PSF are weighted in proportion to their expected intensity by PSF fitting. Aperture photometry will tend to give lower SNR, especially for sources where the background is important, but nonetheless is widely used. We now consider both methods.

6.5.1 Point Sources -- PSF Fitting

In the bright target limit, Poisson noise sets the SNR and

$$SNR = (S)^{1/2} = (R_{object} \cdot t)^{1/2}$$

where S is the number of detected photons, and R_{object} is given by the above equations 6.2 through 6.4, and t is the exposure time.

In the background limited case (e.g. read noise, dark current, or sky noise limited) the SNR is a function not only of the expected number of detected photons S from the source but also of the average effective background count rate in each pixel B, the point spread function $(PSF)_{i,j}$, and the weights used to average the signal in the pixels affected by the source. It is easy to show that the signal-to-noise ratio for optimal weights (which are proportional to the point spread function) is given by:

$$SNR = \frac{S}{\sqrt{B}} \cdot \left(\sum (PSF)_{i,j}{}^2\right)^{1/2} = \frac{S}{\sqrt{B}} \cdot (sharpness)^{1/2} \qquad (6.5)$$

Where *sharpness* is effectively the reciprocal of the number of pixels contributing background noise. The summation is tabulated for a few representative cases in Table 6.5. To estimate the signal-to-noise, multiply the signal-to-noise obtained, assuming all the flux is in one pixel, by the square root of the value in the Table.

Table 6.5: Sharpness as a Function of Wavelength, Camera, and Location of the Star Center with Respect to the Pixel Grid. The "Obs." columns represent the values for the real OTA, WFPC2 optics, and CCD MTF function. The "Diff." column represents values for the theoretical diffraction limit with perfect optics and detectors. Target location refers to both the camera used (PC or WFC), and the location of the star center on the pixel grid.

Target Location	2000 Å		4000 Å		6000 Å		8000 Å	
	Obs.	Diff.	Obs.	Diff.	Obs.	Diff.	Obs.	Diff.
PC Pixel Center	0.084	0.409	0.095	0.259	0.066	0.115	0.046	0.073
PC Pixel Corner	0.063	0. 186	0.065	0.107	0.054	0.072	0.045	0.068
WFC Pixel Center	0.120	0.745	0.145	0.482	0.128	0.318	0.124	0.285
WFC Pixel Corner	0.102	0.228	0.105	0.193	0.098	0.178	0.081	0.126

We note that PSF fitting is equivalent to convolving the image with the PSF, and then measuring the peak counts for stellar objects. Also, the location of the star on the pixel grid will be impossible to know in advance of the observation (i.e. pixel center vs. pixel corner in Table 6.5). In general, the lower "pixel corner" values should be used, so as to insure adequate SNR.

The average effective background counts per exposure and per pixel can be expanded to include various sources:

$$B = readnoise^2 + P_{dark} \cdot (t + 46) + P_{sky} \cdot t + P_{background} \cdot t$$

where terms include the read out noise of the CCD (*readnoise*), the dark current (P_{dark}), sky background count rate (P_{sky}), and the count rate of any diffuse background light from astrophysical sources ($P_{background}$). Herein we will use "*P*" to represent count rates **per pixel**, and "*R*" to represent the **total** counts for an object. The exposure time is represented by *t*.

For example, Table 2.2 lists the faintest V magnitude star, V=28.14, measurable with a signal-to-noise ratio of 3 in a 3000s integration in F569W in the Wide Field Cameras. The calculation to check this goes as follows. The efficiency of the filter is 0.02139 from Table 6.1. The sky background in each pixel is 23.3+5=28.3, assuming an ecliptic latitude of 90° from Table 6.3, and the pixel area correction for the WFC given in that section. The total sky background collected per pixel in 3000 seconds is given by Equation 6.1 as 76.8 electrons. Note that the AB_ν color correction required for the sky in the wavelength range of the filter is 0.0 from Table 6.2. From Table 4.3, the read noise is 5.2 electrons. From Table 4.2, the median dark current at -88 ˚C is 0.004. Therefore the total dark current (on which there will be shot noise) is only 12 electrons. The equivalent background per pixel is then given as B=76.8+5.2^2+12=116. The total number of detected electrons from a star with V=28.14 is S=89 electrons, again using Equation 6.1. The expected peak count is 27 detected electrons using Table

5.4, which is much less than *B*, requiring the use of Equation 6.5 for the background limited case. The sharpness for the WF camera in the best case, when the star is centered on a pixel, is given in Table 6.5 as 0.128. Then Equation 6.5 above gives the signal-to-noise as 3.0:

$$SNR = \left(\frac{89}{\sqrt{116}} \cdot \sqrt{0.128}\right) = 3.0$$

If, instead, the peak count rate comes out much greater than the background, the observation is photon noise limited, and the signal-to-noise should be computed as the square root of the signal *S* in electrons.

In principle, one should also include contributions in the signal-to-noise for flat fielding uncertainties, noise in the bias and dark calibration files, and quantization noise. Flat fielding errors will be of order 1%, and will limit SNR in the large-signal limit. Noise in the bias and dark calibration files will be unimportant in most pixels, although these could become important if many (>10) non-dithered frames of the same field are combined.

Quantization noise can be estimated as $gain/\sqrt{12}$ (i.e., $\sqrt{4.1}$ in the 7 $e^- DN^{-1}$ channel, and $\sqrt{16.3}$ in the 14 $e^- DN^{-1}$ channel). In nearly all situations it can be ignored. In the weak signal case, the quantization noise is effectively included in the read noise values given throughout this Handbook; in the strong signal case it is very small compared to the Poisson noise and can be ignored.

A generalized equation for estimating point source signal-to-noise ratio per exposure is given below (Equation 6.6). It is exact in both the bright and faint object limits, and is a reasonable approximation to the intermediate case. $P_{background}$ represents any generalized source of diffuse background light (e.g. galaxy on which target is superposed). Table 6.6 gives rough values for some of the parameters, along with references for more accurate values.

$$SNR = \frac{R_{object} \cdot t}{\sqrt{R_{object} \cdot t + \dfrac{readnoise^2 + P_{dark} \cdot (t + 46) + P_{sky} \cdot t + P_{background} \cdot t}{sharpness}}} \qquad (6.6)$$

Note that in this formulation, $sharpness^{-1}$ is the equivalent number of pixels the weighted signal is integrated over. In the event that multiple exposures are taken (e.g. to remove cosmic rays), the signal-to-noise ratio for the final averaged image is approximately given by:

$$SNR_{total} = SNR \cdot \sqrt{N}$$

where *N* is the number of images averaged.

Table 6.6: Parameters for Point Source SNR Estimation - PSF Fitting

Parameter	Description	Units	Approx. Value	Better Value
R_{object}	object count rate	$e^{-} s^{-1}$		Equation 6.1, 6.2, or 6.3
P_{dark}	dark count rate	$e^{-} s^{-1} pixel^{-1}$	0.004	Table 4.2
P_{sky}	sky count rate	$e^{-} s^{-1} pixel^{-1}$	Table 6.4	Tables 6.2, 6.1, 6.3; Eqn 6.1
$P_{background}$	count rate from back-ground light (if any)	$e^{-} s^{-1} pixel^{-1}$		Tables 6.2, 6.1; Eqn 6.1
read noise		e^{-}	ATD-GAIN=7 use 5.3[a] ATD-GAIN=15 use 7.5	Table 4.3
sharpness			WFC use 0.11 PC1 use 0.06	Table 6.5
t	exposure time	s		

a. ATD-GAIN defaults to 7 unless otherwise specified on Phase 2 proposal.

6.5.2 Point Sources -- Aperture Photometry

When aperture photometry is used, one must consider the fraction of the object counts encircled by the aperture, as well the background noise in the aperture. In the bright target limit the SNR is given by

$$SNR = (S \cdot f(r))^{1/2} = (R_{object} \cdot f(r) \cdot t)^{1/2}$$

where S is the number of detected photons, $f(r)$ is the fraction of the total counts encircled by the aperture with radius r, and R_{object} is target count rate. Representative values of $f(r)$ are given in Table 6.7; values for other aperture sizes and filters can be estimated from Figure 5.3 on page 88, or Figure 5.4 on page 89.

In the faint target limit the noise contributed by background counts determines the SNR

$$SNR = \frac{S \cdot f(r)}{\sqrt{B \cdot \pi r^2}}$$

where B represents the effective background counts per pixel, and r is the aperture radius in pixels.

In the generalized case the SNR per exposure for aperture photometry is given approximately by:

$$SNR = \frac{f(r) \cdot R_{object} \cdot t}{\sqrt{(f(r) \cdot R_{object} \cdot t) + [readnoise^2 + P_{dark} \cdot (t + 46) + P_{sky} \cdot t + P_{background} \cdot t] \cdot \pi r^2}} \qquad (6.7)$$

where the parameters are summarized in Table 6.8.

Table 6.7: Encircled Energy for Representative Filters. Encircled energy values are normalized to unity at large radius.

CCD	Aperture Radius (r)	Encircled Energy f(r)		
		F218W	F555W	F814W
PC1	0.1″	0.60	0.67	0.53
	0.2″	0.73	0.85	0.78
	0.5″	0.84	0.96	0.87
	1.0″	0.92	1.00	0.92
WF3	0.1″	0.40	0.46	0.44
	0.2″	0.69	0.76	0.74
	0.5″	0.85	0.90	0.91
	1.0″	0.94	0.94	0.96

Table 6.8: Parameters for Point Source SNR Estimation - Aperture Photometry.

Parameter	Description	Units	Approx. Value	Better Value
R_{object}	object count rate	$e^{-} s^{-1}$		Equation 6.1, 6.2, or 6.3
P_{dark}	dark count rate	$e^{-} s^{-1}$ $pixel^{-1}$	0.004	Table 4.2
P_{sky}	sky count rate	$e^{-} s^{-1}$ $pixel^{-1}$	Table 6.4	Tables 6.2, 6.1, 6.3; Eqn 6.1
$P_{background}$	count rate from back-ground light (if any)	$e^{-} s^{-1}$ $pixel^{-1}$		Tables 6.2, 6.1; Eqn 6.1
readnoise		e^{-}	ATD-GAIN=7 use 5.3[a] ATD-GAIN=15 use 7.5	Table 4.3
$f(r)$	encircled energy		Table 6.7	Figure 5.3 or 5.4
r	aperture radius	pixels		
t	exposure time	s		

a. ATD-GAIN defaults to 7 unless otherwise specified on Phase 2 proposal.

6.5.3 Extended Sources

The calculations for extended sources are nearly identical to those for point sources. The easiest procedure is to compute the SNR per detector pixel, and then adjust this value if the total SNR is required for an area encompassing many pixels.

In general, one will have the target magnitude or flux per square arcsecond. To compute the flux per pixel for the PC one merely multiplies the flux per square arcsecond by 0.00207, or instead, adds the value 6.7 to the magnitude per square arcsecond to get the necessary magnitude per PC pixel. For the WFC, one either multiplies the flux per square arcsecond by 0.00993, or adds 5.0 to the magnitude per square arcsecond. Equations 6.2, 6.3, and 6.4 can be rewritten including these factors as below.

PC Camera

For the PC camera, sources with stellar spectra, and V surface brightness per square arcsecond σ_V we have a count rate in e^- s^{-1} $pixel^{-1}$ of

$$P_{object} = 2.5 \times 10^{11} \cdot [\int Q(\lambda)T(\lambda)d\lambda/\lambda] \cdot 10^{-0.4(\sigma_V + AB_\nu + 6.7)} \qquad (6.8)$$

For power law sources where B_ν is the target flux in units of ergs cm^{-2} s^{-1} Hz^{-1} $arcsec^{-2}$ we have

$$P_{object} = 1.4 \times 10^{28} \cdot [\int Q(\lambda)T(\lambda)d\lambda/\lambda] \cdot B_\nu\left(\bar{\lambda} + \alpha\frac{d\bar{\lambda}}{d\alpha}\right) \qquad (6.9)$$

And finally for emission line sources where I_ν is the flux in ergs cm^{-2} s^{-1} $arcsec^{-2}$ we have

$$P_{object} = 4.8 \times 10^{9} \cdot (QT) \cdot I_\nu \cdot \lambda \qquad (6.10)$$

where the emission line wavelength λ is in Angstroms.

WFC Camera

For the WFC camera and stellar sources with V surface brightness per square arcsecond σ_V we have a count rate in e^- s^{-1} $pixel^{-1}$ of

$$P_{object} = 2.5 \times 10^{11} \cdot [\int Q(\lambda)T(\lambda)d\lambda/\lambda] \cdot 10^{-0.4(\sigma_V + AB_\nu + 5)} \qquad (6.11)$$

For power law sources where B_ν is the target flux in units of ergs cm^{-2} s^{-1} Hz^{-1} $arcsec^{-2}$ we have

$$P_{object} = 6.9 \times 10^{28} \cdot [\int Q(\lambda)T(\lambda)d\lambda/\lambda] \cdot B_\nu\left(\bar{\lambda} + \alpha\frac{d\bar{\lambda}}{d\alpha}\right) \qquad (6.12)$$

And finally for emission line sources where I_ν is the flux in ergs cm^{-2} s^{-1} $arcsec^{-2}$ we have

$$P_{object} = 2.3 \times 10^{10} \cdot (QT) \cdot I_\nu \cdot \lambda \qquad (6.13)$$

where the emission line wavelength λ is in Angstroms.

SNR

The generalized SNR per pixel per exposure for an extended source is then obtained simply by setting the sharpness to unity in equation 6.5:

$$SNR = \frac{P_{object} \cdot t}{\sqrt{P_{object} \cdot t + (readnoise^2 + P_{dark} \cdot (t + 46) + P_{sky} \cdot t + P_{background} \cdot t)}} \quad (6.14)$$

Table 6.9: Parameters for Extended Source SNR Estimation.

Parameter	Description	Units	Approx. Value	Better Value
P_{object}	object count rate	$e^{-}\ s^{-1}\ pixel^{-1}$		Equations 6.9 to 6.12
P_{dark}	dark count rate	$e^{-}\ s^{-1}\ pixel^{-1}$	0.004	Table 4.2
P_{sky}	sky count rate	$e^{-}\ s^{-1}\ pixel^{-1}$	Table 6.4	Tables 6.2, 6.1, 6.3; Eqn 6.7 (PC) or 6.10 (WFC)
$P_{background}$	count rate from background light (if any)	$e^{-}\ s^{-1}\ pixel^{-1}$		Tables 6.2, 6.1; Eqn 6.7 (PC) or 6.10 (WFC)
readnoise		e^{-}	ATD-GAIN=7 use 5.3[a] ATD-GAIN=15 use 7.5	Table 4.3
t	exposure time	s		

a. Default value is ATD-GAIN=7.

Since many observations of extended sources are for galaxies in broad-band filters, a few rules of thumb can be useful. Saturation is seldom a concern, except in very bright spots such as the inner core of ellipticals and of some bulges. Count rates for spiral galaxies range typically from 2 to 0.01 e^{-} $pixel^{-1}$ s^{-1} (and lower) for filters such as F555W, F606W, F702W, and F814W; the lower end of the range corresponds roughly to the de Vaucouleurs D_{25}. Count rates are significantly lower in blue and UV filters. Spiral structure can typically be traced reasonably well with total exposures of 3000 seconds or longer in the above filters.

For galaxies of very small angular size at red-shifts of cosmological interest, the image may cover a small number of pixels; thus the detection of such objects follows rules similar to those of point sources. However, the fraction of light falling in the central pixel is smaller for most galaxies than it is for true point sources. The approximate magnitude difference between the light falling in the central pixel and the entire galaxy is plotted in Figure 6.1 for a typical giant elliptical galaxy, as a function of redshift. For other types of galaxies, a morphological term can be added to the values (for example, 0.6 magnitudes for lenticulars, 0.7 for S, 0.8 for Sab, 0.9 for Sbc, 1.2 for Scd, and 1.8 for Irr). These values must be increased by an additional 1.7 magnitudes for the PC.

Figure 6.1: Giant Elliptical Galaxy

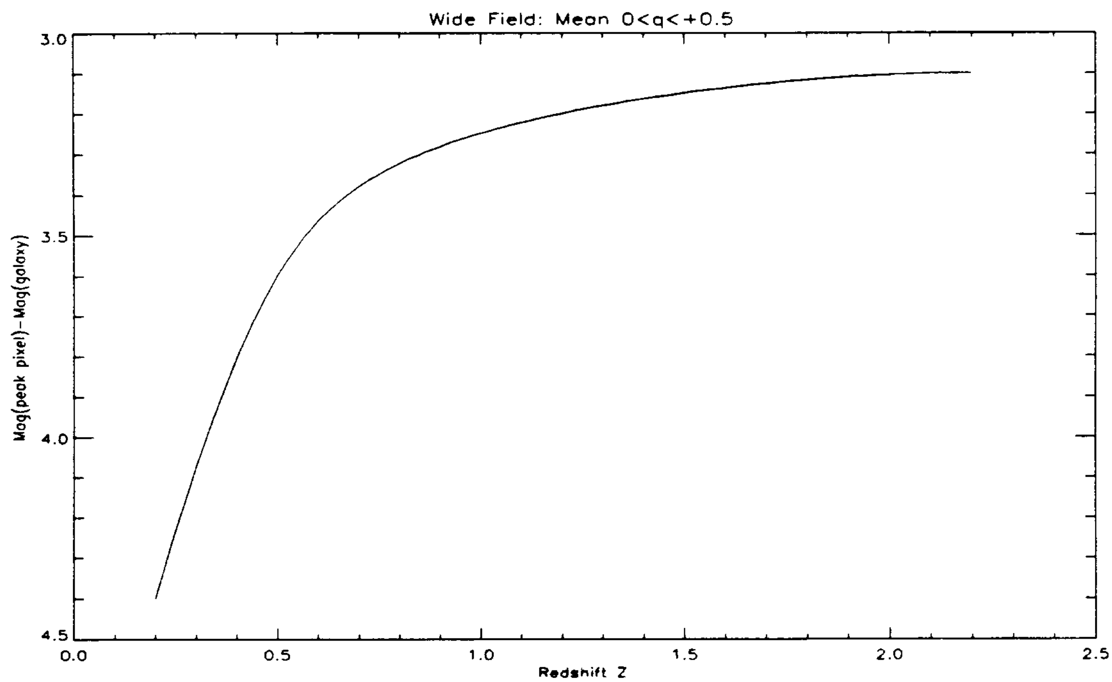

6.6 Exposure Time Estimation

In many instances one desires a certain SNR, and wishes to solve for the corresponding exposure time. Given the SNR, Equations 6.6, 6.7, or 6.14 can be solved for the exposure time, *t*. Since there are time-dependent and time-independent noise sources, quadratic equations are obtained. For example, we may solve equation 6.6 for the point source exposure time:

$$t = \frac{1}{2Y} \cdot (b + \sqrt{b^2 + 4aY})$$

where the term *A* contains the time-independent noise sources

$$a = \frac{readnoise^2 + 46P_{dark}}{sharpness}$$

and *B* contains the time-dependent noise sources

$$b = \frac{P_{dark} + P_{sky} + P_{background}}{sharpness} + R_{object}$$

and

$$Y = \left(\frac{R_{object}}{SNR}\right)^2$$

Equations for aperture photometry (6.7) and extended sources (6.12) can be solved with similar results. Parameters are as described in Tables 6.6, 6.8, and 6.9. We again note that the on-line WFPC2 Exposure Time Calculator program provides an easy method for these calculations.

6.7 Sample SNR Calculations

Below we give further examples of SNR calculations. The Appendix also gives tables of SNR values for a wide range of representative cases.

6.7.1 Point Sources

Simple Star, Manual Calculation, PSF Fitting

We begin with the simple example of V=20 star of spectral class G0. We want to observe with the PC using filter F555W. The star is somewhere near the ecliptic pole. We want to know the SNR for a 1200s CR-SPLIT exposure. Default ATD-GAIN=7 is used. We plan to use PSF fitting to analyze the data.

First we estimate the count rate for our target. Consulting Equation 6.2, Table 6.1, and Table 6.2 we have:

$$R_{object} = 2.5 \times 10^{11} \cdot \left[\int Q(\lambda)T(\lambda)d\lambda/\lambda\right] \cdot 10^{-0.4(V + AB_\nu)}$$

$$= 2.5 \times 10^{11} \cdot [0.027] \cdot 10^{-0.4(20 + 0.02)} = 66$$

in units of $e^- s^{-1}$. Next we fill out Equation 6.6. To keep things simple we just use values from Table 6.6, and get the sky count rate from Table 6.4. There is no background light (i.e. no superposed galaxy), so $P_{background}$=0. The exposure time t=600 for each exposure of the CR-SPLIT:

$$SNR = \frac{R_{object} \cdot t}{\sqrt{R_{object} \cdot t + \frac{readnoise^2 + P_{dark} \cdot (t + 46) + P_{sky} \cdot t + P_{background} \cdot t}{sharpness}}}$$

$$= \frac{66 \cdot 600}{\sqrt{66 \cdot 600 + \frac{(5.3)^2 + 0.004 \cdot (600 + 46) + (0.01 \cdot 600) + (0 \cdot 600)}{0.06}}}$$

$$= \frac{39600}{\sqrt{39600 + 611}} = 197$$

The SNR for the total 1200s exposure, i.e. both halves of the CR-SPLIT, would simply be:

$$SNR_{total} = SNR \cdot \sqrt{N} = 197 \cdot \sqrt{2} = 279$$

At these high SNR levels, it is likely that flat fielding would limit the photometric accuracy, rather than the noise. If we have a look at the terms in the SNR equation, we can see that the Poisson noise dominates; the term containing the sharpness and background noise sources is unimportant.

Just for fun, let us see what happens if we keep everything the same, but give the target V=25. Now we have R_{object}=0.66 $e^- s^{-1}$, and:

$$SNR = \frac{0.66 \cdot 600}{\sqrt{0.66 \cdot 600 + \frac{(5.3)^2 + 0.004 \cdot (600 + 46) + (0.01 \cdot 600) + (0 \cdot 600)}{0.06}}}$$

$$= \frac{396}{\sqrt{396 + 611}} = 12.5$$

We see that now the term with the background noise (in particular, the read noise) limits the SNR. For the full 1200s exposure the SNR_{total}=17.6.

Simple Star, Manual Calculation, Aperture Photometry

What if we now want to observe this same V=25 star, but we plan to reduce the data by measuring counts in a 0.5″ radius aperture? We now use Equation 6.7

instead, consult Table 6.7 for the encircled energy *f(r),* and note that 0.5″ corresponds to *r*=11.6 PC pixels:

$$SNR = \frac{f(r) \cdot R_{object} \cdot t}{\sqrt{(f(r) \cdot R_{object} \cdot t) + [readnoise^2 + P_{dark} \cdot (t+46) + P_{sky} \cdot t + P_{background} \cdot t] \cdot \pi r^2}}$$

$$= \frac{0.96 \cdot 0.66 \cdot 600}{\sqrt{(0.96 \cdot 0.66 \cdot 600) + ((5.3)^2 + 0.004(600+46) + 0.01 \cdot 600 + 0 \cdot 600) \cdot \pi (11.6)^2}}$$

$$= \frac{380}{\sqrt{380 + 15500}} = 3.0$$

Apparently using aperture photometry with a 0.5″ radius aperture reduces the SNR by a factor ~4 as compared to PSF fitting, for this background limited case.

Simple Star, SNR Tables, PSF Fitting

We now repeat the first calculation above for the V=20 star using the SNR tables in Appendix B. We look up the G0 spectral class and F555W filter (5500Å) in Table B.1, and obtain AB_V=0.02. For the V=20 star, we thus have V+AB_V=20.02. We look at Figure B.10 on page 234 and find this value on the horizontal axis. We locate exposure time 600s (one-half of the total 1200s CR-SPLIT exposure), and find SNR~200. For the total 1200s exposure the SNR would be $200\sqrt{2} = 280$.

Simple Star, On-Line Calculator, PSF Fitting

The above calculation for a V=20 GO star may also be performed using the WFPC2 Exposure Time Calculator program, which is available on the WFPC2 WWW pages at:

`http://www.stsci.edu/ftp/instrument_news/WFPC2/wfpc2_top.html`

To use this program, access the above address with NCSA Mosaic, Netscape, or a similar program. Once in the WFPC2 area, select the "Software Tools" page, and then the "ETC" page. For the first example above, choose the "Point Source" form and complete it as shown in Figure 6.2 for the 600s sub-exposure. Then clicks the "calculate" button and after a few seconds the result is displayed (Figure 6.3). The answer, SNR=198, is comparable to that obtained by the manual calculation above for the 600s sub-exposure (SNR=197). Alternatively, one can input the total exposure time (1200s), and then use the result farther down the output page for "No. Sub-Exposures = 2" (see Figure 6.4), thereby obtaining SNR=277 for the total 1200s CR-SPLIT exposure.

Figure 6.2: Sample Fill-out Form for WFPC2 On-Line Exposure Time Calculator.

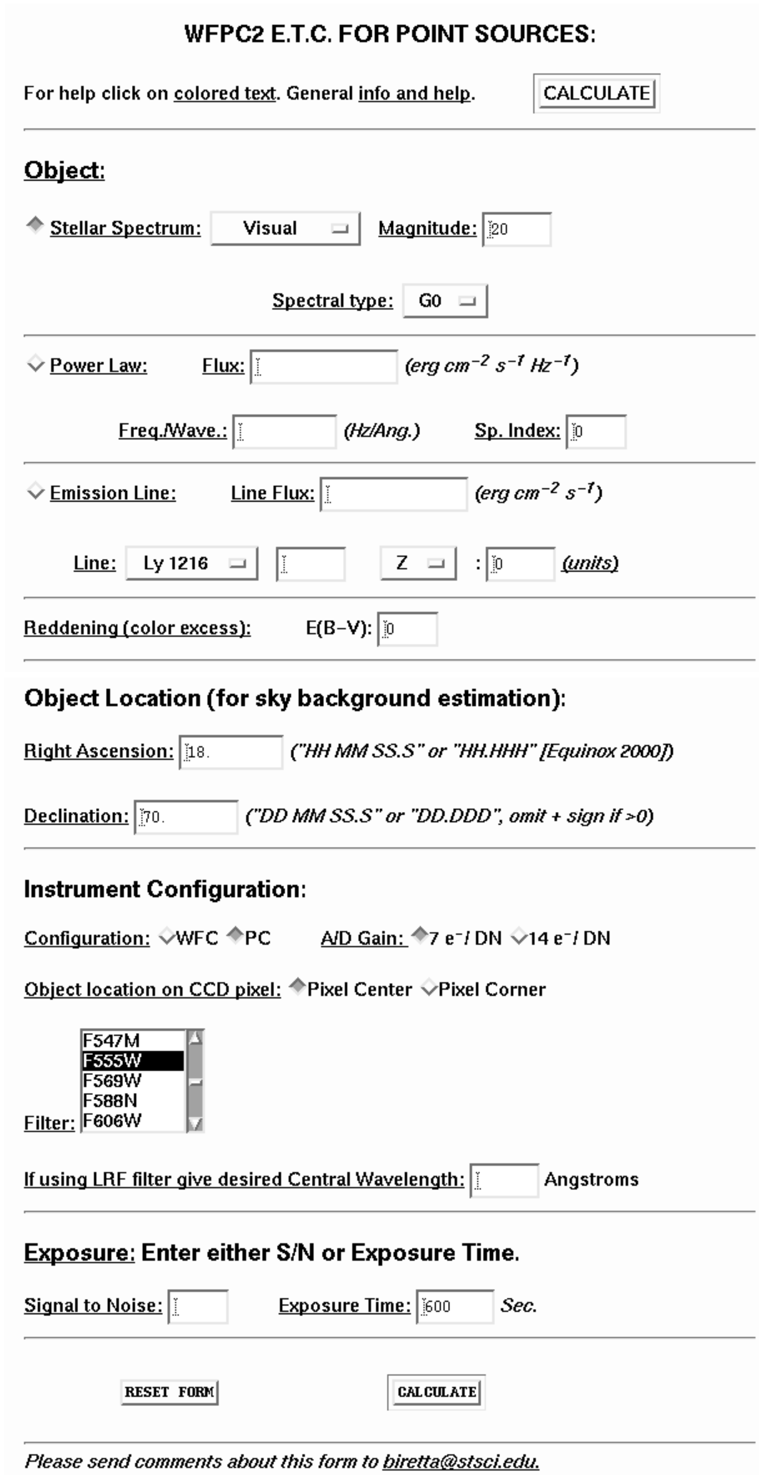

WFPC2 E.T.C. FOR POINT SOURCES:

For help click on colored text. General info and help. CALCULATE

Object:

Stellar Spectrum: Visual Magnitude: 20

Spectral type: G0

Power Law: Flux: (erg cm^{-2} s^{-1} Hz^{-1})

Freq./Wave.: (Hz/Ang.) Sp. Index: 0

Emission Line: Line Flux: (erg cm^{-2} s^{-1})

Line: Ly 1216 Z : 0 (units)

Reddening (color excess): E(B−V): 0

Object Location (for sky background estimation):

Right Ascension: 18. ("HH MM SS.S" or "HH.HHH" [Equinox 2000])

Declination: 70. ("DD MM SS.S" or "DD.DDD", omit + sign if >0)

Instrument Configuration:

Configuration: WFC PC A/D Gain: 7 e⁻/ DN 14 e⁻/ DN

Object location on CCD pixel: Pixel Center Pixel Corner

Filter: F547M F555W F569W F588N F606W

If using LRF filter give desired Central Wavelength: Angstroms

Exposure: Enter either S/N or Exposure Time.

Signal to Noise: Exposure Time: 600 Sec.

RESET FORM CALCULATE

Please send comments about this form to biretta@stsci.edu.

Figure 6.3: Sample Results from WFPC2 On-Line Exposure Time Calculator.

WFPC2 ETC results

Final Result

Signal-to-Noise Ratio = 198.1

Exposure Time Quantization

Figure 6.4: Sample Results on CR-SPLITing from WFPC2 On-Line Exposure Time Calculator Results Page.

No. Sub-Exposures	Total SNR	Pixels Lost
(No Split)	280.8	3.981250%
2	277.4	0.039626%
3	277.7	0.000234%
4	277.6	0.000001%
6	276.8	0.000000%
8	275.8	0.000000%
12	273.6	0.000000%
16	271.4	0.000000%
32	262.8	0.000000%

Star Superposed on Galaxy, Manual Calculation

We now consider a B=25 point source of spectral class B0, which is superposed on an elliptical galaxy with σ_V=22 mag arcsecond^{-2}. We want to compute the SNR obtained from a one-orbit (40 min.) non-CR-SPLIT observation in filter F300W on the WFC. PSF fitting will be used for the photometry.

We begin by computing the total count rate for the target. Using Table 6.2 we see that this target will have V=25.31. From Table 6.1 we obtain the filter efficiency and mean wavelength. Interpolating by mean wavelength in Table 6.2 we obtain AB_V=-0.83 for the B0 star. Using Equation 6.2 we have:

$$R_{object} = 2.5\times 10^{11}\cdot\left[\int Q(\lambda)T(\lambda)d\lambda/\lambda\right]\cdot 10^{-0.4(V+AB_V)}$$

$$= 2.5\times 10^{11}\cdot[0.00519]\cdot 10^{-0.4(25.31-0.83)} = 0.21$$

in units of e^{-} s^{-1}. Next we consider the background light from the superposed galaxy. We set σ_V=22 mag arcsecond^{-2} in Equation 6.11, and AB_ν=3.63 for a gE galaxy at λ=3000Å (filter F300W) from Table 6.2. Hence the count rate per pixel due to the background light is:

$$P_{background} = 2.5 \times 10^{11} \cdot \left[\int Q(\lambda) T(\lambda) d\lambda/\lambda\right] \cdot 10^{-0.4(\sigma_V + AB_\nu + 5)}$$

$$= 2.5 \times 10^{11} \cdot [0.00519] \cdot 10^{-0.4(22 + 3.63 + 5)} = 0.00073$$

For the sky background, we note that Table 6.4 has no entry for F300W, so that the sky must be unimportant. If we wanted to calculate it anyway, as a check, we would use Table 6.3 for the sky brightness, Table 6.2 for the sky's AB_ν, and again Equation 6.11. We will assume the target is near the ecliptic pole.

$$P_{sky} = 2.5 \times 10^{11} \cdot \left[\int Q(\lambda) T(\lambda) d\lambda/\lambda\right] \cdot 10^{-0.4(\sigma_V + AB_\nu + 5)}$$

$$= 2.5 \times 10^{11} \cdot [0.00519] \cdot 10^{-0.4(23.3 + 3.12 + 5)} = 0.00035$$

For the sharpness function we will use "pixel corner" values (least optimistic choice) from Table 6.5. Using read noise and dark current from Table 6.6, and Equation 6.6 for point source SNR:

$$SNR = \frac{R_{object} \cdot t}{\sqrt{R_{object} \cdot t + \frac{readnoise^2 + P_{dark} \cdot (t + 46) + P_{sky} \cdot t + P_{background} \cdot t}{sharpness}}}$$

$$= \frac{0.21 \cdot 2400}{\sqrt{0.21 \cdot 2400 + \frac{(5.3)^2 + 0.004 \cdot (2400 + 46) + (0.00035 \cdot 2400) + (0.00073 \cdot 2400)}{0.103}}}$$

$$= \frac{504}{\sqrt{504 + 393}} = 16.8$$

for this single exposure. The SNR for multiple 40 min. exposures would be simply $16.8(N^{1/2})$, where N is the number of exposures.

Star Superposed on Galaxy, On-Line Calculator

The above calculation could also be performed with the on-line WFPC2 Exposure Time Calculator. One would select the "Point source + stellar background" form, and complete it as in Figure 6.5, and then click on "calculate." Figure 6.6 shows some of the results.

6.7.2 Extended Sources

In general, the signal-to-noise level for extended sources can be computed by comparing the expected signal, S, in each pixel, determined from Equations 6.8 through 6.13, to the noise $N=(S+B)^{1/2}$, where B is the equivalent background, determined in a manner similar to that for point sources. Unlike for point sources, the calculation does not, in a first approximation, involve the sharpness of the point spread function. For example, let us consider the observation of a source with a V surface brightness of 24 mag arcsec^{-2}, assuming the F569W filter F569W, WFC camera, and sky background V=23.3 mag arcsec^{-2}. The signal-to-noise estimate goes as follows. The signal in each WFC pixel is 24.0+5.0 = 29.0 magnitude. By Equation 6.11, the total signal collected from the source in a 3000 second integration is S = 41.8 electrons, neglecting the small AB color correction. The sky signal per pixel is 76.8 electrons. The dark current is ~12 electrons. The total equivalent background is thus $B = 76.8+5.3^2+12 = 116.9$ electrons, larger than the signal detected, thus the noise is background-dominated. The noise is $N=(S+B)^{1/2}= 12.6$ electrons, and the signal-to-noise *per pixel* expected in this case is 3.3. Similar calculations can be carried out for other filters; for observations in narrow-band filters and in the UV, the sky background signal will usually be unimportant. For very long observations of faint objects, other noise terms, such as flat field uncertainty, and errors in dark (and possibly bias) subtraction, must be considered more carefully.

If the scale of features in the target is larger than one pixel, the signal-to-noise can sometimes be improved by smoothing the observed image or - if read noise is a significant contributor - by reading the image out in AREA mode (see section 2.8, "CCD Orientation and Readout", on page 31).

6.7.3 Emission Line Sources

The signal-to-noise ratio calculation for point-like or extended emission-line sources is similar to that for continuum sources. However, the details of the calculation are different, because of the units used for the line flux, and because the flux is in a narrow line. The integrated filter efficiency is not relevant for the signal calculation; what matters is the total system throughput QT at the wavelength of the line, which can be determined from inspection of the Figures in section A.2, "Passbands including the System Response", on page 211. For lines near the center of the filter bandpasses the QT_{max} values from Table 6.1 can be used. The total signal expected for a point source of line strength F, expressed in erg s^{-1} cm^{-2}, is $S=2.28\mathrm{x}10^{12}\ \lambda\ t\ QT\ F$, where t is the exposure time in seconds, and λ the wavelength of the line in Angstroms. Thus, H_{α} emission at 6563Å, with flux $F=10^{-16}$ erg s^{-1} cm^{-2}, observed for 1000 seconds through the F656N filter (total system throughput QT=0.104 from "F656N, F658N, F673N, F675W, F702W, F785LP" on page 217), will produce a total signal of S=155 electrons. The equivalent background per pixel is read-noise dominated: $B=1+5.3^2+4=33$, for a

Figure 6.5: Point Source + Stellar Background Fill-out Form for WFPC2 On-Line Exposure Time Calculator. SNR is calculated for B=25 star (class B0) superposed on an elliptical galaxy (gE) with σ_V=22. WFC is used with F300W.

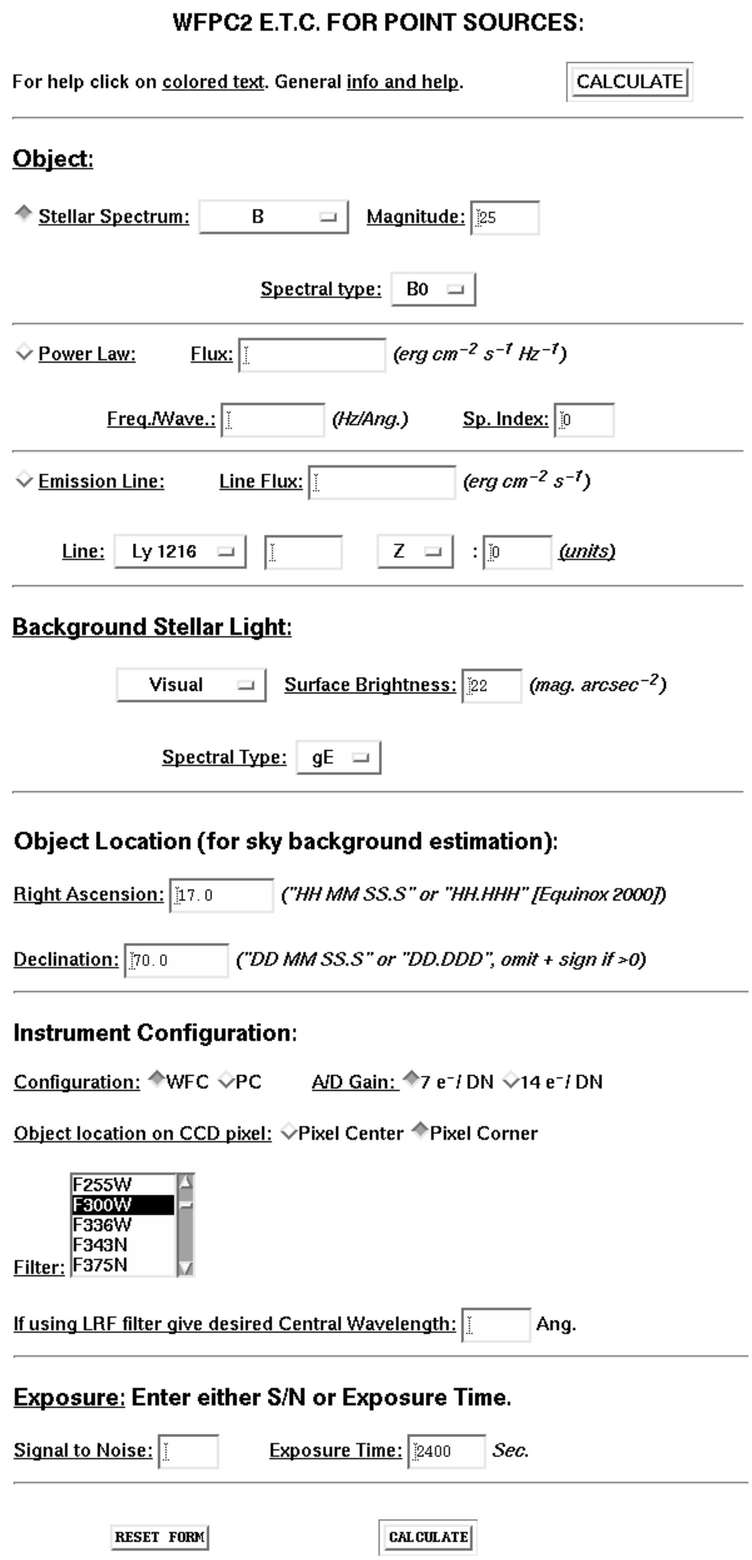

WFPC2 E.T.C. FOR POINT SOURCES:

For help click on colored text. General info and help. CALCULATE

Object:

Stellar Spectrum: B Magnitude: 25

Spectral type: B0

Power Law: Flux: (erg cm^{-2} s^{-1} Hz^{-1})

Freq./Wave.: (Hz/Ang.) Sp. Index: 0

Emission Line: Line Flux: (erg cm^{-2} s^{-1})

Line: Ly 1216 Z : 0 (units)

Background Stellar Light:

Visual Surface Brightness: 22 (mag. $arcsec^{-2}$)

Spectral Type: gE

Object Location (for sky background estimation):

Right Ascension: 17.0 ("HH MM SS.S" or "HH.HHH" [Equinox 2000])

Declination: 70.0 ("DD MM SS.S" or "DD.DDD", omit + sign if >0)

Instrument Configuration:

Configuration: WFC PC A/D Gain: 7 e^-/ DN 14 e^-/ DN

Object location on CCD pixel: Pixel Center Pixel Corner

Filter: F255W F300W F336W F343N F375N

If using LRF filter give desired Central Wavelength: Ang.

Exposure: Enter either S/N or Exposure Time.

Signal to Noise: Exposure Time: 2400 Sec.

RESET FORM CALCULATE

Figure 6.6: Sample Output from WFPC2 On-Line Exposure Time Calculator.

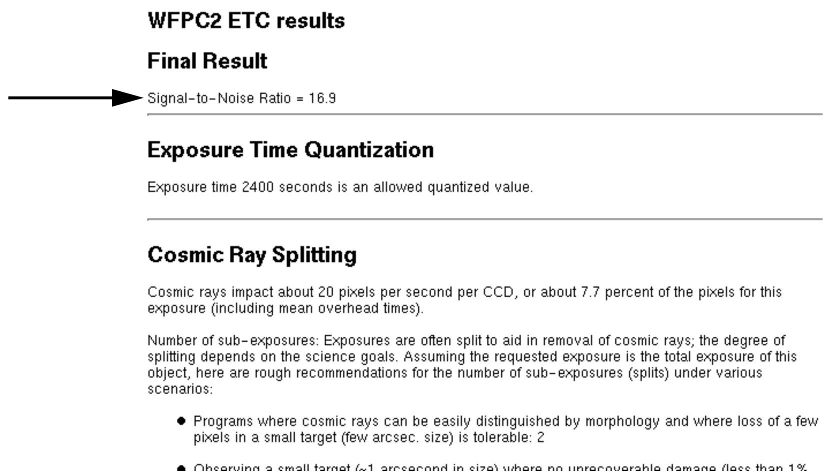

WFPC2 ETC results

Final Result

Signal-to-Noise Ratio = 16.9

Exposure Time Quantization

Exposure time 2400 seconds is an allowed quantized value.

Cosmic Ray Splitting

Cosmic rays impact about 20 pixels per second per CCD, or about 7.7 percent of the pixels for this exposure (including mean overhead times).

Number of sub-exposures: Exposures are often split to aid in removal of cosmic rays; the degree of splitting depends on the science goals. Assuming the requested exposure is the total exposure of this object, here are rough recommendations for the number of sub-exposures (splits) under various scenarios:

- Programs where cosmic rays can be easily distinguished by morphology and where loss of a few pixels in a small target (few arcsec. size) is tolerable: 2

background noise of ~6 electrons. The total noise is dominated by photon noise from the signal itself, and the signal-to-noise ratio achieved in this observation is over 10.

If the source is extended, the expected signal *per arcsecond* must be multiplied by the effective pixel area: 0.0099 arcsec^2 for the WF, 0.0021 for the PC. For a line flux of, say, F = 10^{-15} erg s^{-1} cm^{-2} arcsec^{-2}, this corresponds to 15 electrons in 1000 seconds for a WFC pixel. The noise is now dominated by the background, and the single-pixel signal-to-noise ratio is $15/(33 + 15)^{1/2} \sim 2.1$.

Extended Line Emission Source, Manual Calculation

We now consider a detailed example of a planetary nebula observed on the PC with the F502N filter. The nebula has a diameter of 5″ and a total flux F=4x10^{-13} erg s^{-1} cm^{-2} in the [OIII] 5007Å line. We want to estimate the SNR for an 1800s exposure, which will be CR-SPLIT.

First we must estimate the flux per square arcsecond. Using the nebula diameter, the average brightness is I_ν = 2.0x10^{-14} erg s^{-1} cm^{-2} arcsec^{-2}. From the plots in section A.2, "Passbands including the System Response", on page 211, we see that QT=0.053. Using Equation 6.10 for the target count rate per pixel:

$$P_{object} = 4.8 \times 10^9 \cdot (QT) \cdot I_\nu \cdot \lambda$$

$$= 4.8 \times 10^9 \cdot (0.053) \cdot 2.0 \times 10^{-14} \cdot 5007 = 0.025$$

Next we estimate the SNR for each 900s sub-exposure using Equation 6.14 and Table 6.9. For this narrow filter the sky background can be ignored. We presume there is no background light from astrophysical sources:

$$SNR = \frac{P_{object} \cdot t}{\sqrt{P_{object} \cdot t + (readnoise^2 + P_{dark} \cdot (t + 46) + P_{sky} \cdot t + P_{background} \cdot t)}}$$

$$= \frac{0.025 \cdot 900}{\sqrt{0.025 \cdot 900 + (5.3^2 + 0.004 \cdot (900 + 46) + 0 \cdot 900 + 0 \cdot 900)}} = 3.1$$

Hence SNR=3.1 per pixel for each 900s sub-exposure. The SNR per pixel for the total 1800s is

$$SNR_{total} = SNR\sqrt{N} = 3.1 \cdot \sqrt{2} = 4.3$$

The SNR for the entire nebula is this SNR per pixel times the square root of the number of pixels in the image, or ~420. In actuality, uncertainties in the photometric calibration and flat fields, would limit the SNR to ~100.

Extended Line Emission Source, On-Line Calculator

The above example could be calculated with the “Extended Source” form of the ETC program. The fill-out form would be completed as shown in Figure 6.7. We have selected “[OIII] 5007” on the emission line menu, and have left the redshift (z) set to zero. The PC and F502N filter are selected. Note we have entered the exposure time as 1800s. Scrolling down through the output page we find a table of SNR for various CR-SPLITings of the exposure (See Figure 6.8). “No. Sub-Exposures = 2” gives the answer we want, SNR=4.5 per pixel.

Figure 6.7: Extended Source Form for WFPC2 On-Line Exposure Time Calculator. Here target is galactic [OIII] 5007 line emission source and is observed on PC with filter F502N. SNR is computed for 1800s exposure.

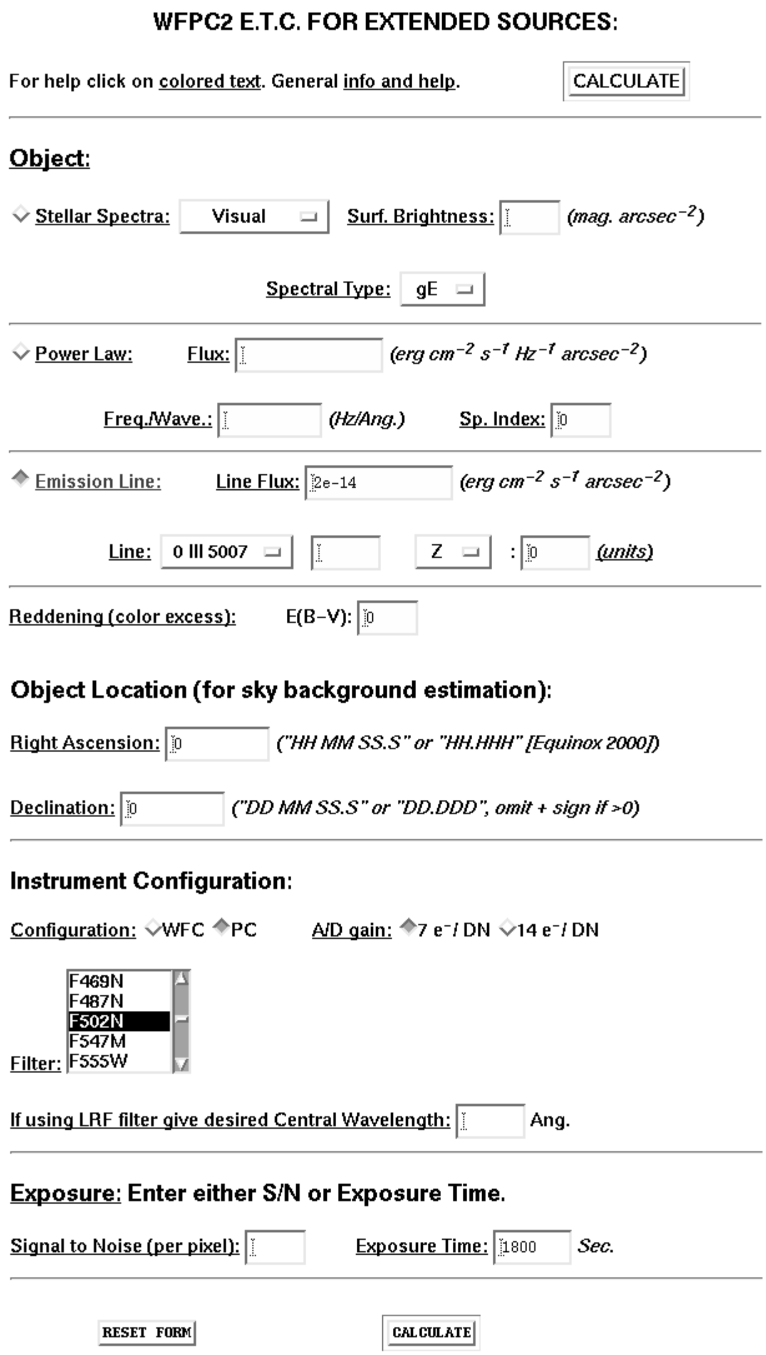

WFPC2 E.T.C. FOR EXTENDED SOURCES:

For help click on colored text. General info and help. CALCULATE

Object:

Stellar Spectra: Visual Surf. Brightness: (mag. arcsec^{-2})

Spectral Type: gE

Power Law: Flux: (erg cm^{-2} s^{-1} Hz^{-1} arcsec^{-2})

Freq./Wave.: (Hz/Ang.) Sp. Index: 0

Emission Line: Line Flux: 2e-14 (erg cm^{-2} s^{-1} arcsec^{-2})

Line: 0 III 5007 Z : 0 (units)

Reddening (color excess): E(B−V): 0

Object Location (for sky background estimation):

Right Ascension: 0 ("HH MM SS.S" or "HH.HHH" [Equinox 2000])

Declination: 0 ("DD MM SS.S" or "DD.DDD", omit + sign if >0)

Instrument Configuration:

Configuration: WFC PC A/D gain: 7 e$^-$/ DN 14 e$^-$/ DN

Filter: F469N F487N F502N F547M F555W

If using LRF filter give desired Central Wavelength: Ang.

Exposure: Enter either S/N or Exposure Time.

Signal to Noise (per pixel): Exposure Time: 1800 Sec.

RESET FORM CALCULATE

Figure 6.8: Sample Output from WFPC2 On-Line Exposure Time Calculator.

No. Sub-Exposures	Total SNR	Pixels Lost
(No Split)	5.3	5.856250%
2	4.5	0.085739%
3	4.1	0.000744%
4	3.8	0.000005%
6	3.3	0.000000%
8	2.9	0.000000%
12	2.5	0.000000%
16	2.2	0.000000%
32	1.6	0.000000%

Line Emission Point Source w/ LRF, Manual Calculation

In this example we consider an unresolved source of H_{α} emission in a galaxy at redshift z=0.22 with flux F=1.5x10^{-16} erg s^{-1} cm^{-2}. We want the SNR for a 2400s exposure without CR-SPLITing.

Since the redshift is significant, we cannot observe with the F656N filter. Instead we will use the Linear Ramp Filter (LRF). The observed wavelength will be 8007Å. From Table 3.7 on page 48 we see that this will be observed using the FR868N filter on CCD WF3. Combining the LRF transmission from Figure 3.2 and the "WFPC2 + OTA System Throughput" from Figure 2.4 we estimate QT=0.054. We compute the count rate using Equation 6.4: To estimate the SNR

$$R_{object} = 2.3 \times 10^{12} \cdot (QT) \cdot F \cdot \lambda$$

$$= 2.3 \times 10^{12} \cdot (0.054) \cdot (1.5 \times 10^{-16}) \cdot 8007 = 0.15$$

we use Equation 6.6, which assumes that PSF fitting will be used to analyze the image. Since the filter is narrow, we will ignore the sky emission. We use Table 6.6 for the WFC sharpness and also the read noise.

$$SNR = \frac{R_{object} \cdot t}{\sqrt{R_{object} \cdot t + \frac{readnoise^2 + P_{dark} \cdot (t + 46) + P_{sky} \cdot t + P_{background} \cdot t}{sharpness}}}$$

$$= \frac{0.15 \cdot 2400}{\sqrt{0.15 \cdot 2400 + \frac{5.3^2 + 0.004(2400 + 46) + 0 \cdot 2400 + 0 \cdot 2400}{0.11}}}$$

$$= \frac{360}{\sqrt{360 + 344}} = 14$$

which is for an un-split 2400s exposure. The Poisson noise and background noises contribute nearly equally. For three such exposures over three orbits

$$SNR_{total} = SNR\sqrt{N} = 14\sqrt{3} = 23.$$

Line Emission Point Source w/ LRF, On-Line Calculator

The above calculation can be performed using the ETC program. The “Point Source” form is used. “Emission Line” source and the “H 6563” line are selected; the redshift is set to 0.22. The program will automatically choose between PC and WFC, depending on the LRF setting. The least optimistic case of placing the object on a “pixel corner” is selected. The filter “LRF” is selected from the filter menu, and 8007Å is given for the central wavelength. The exposure time is specified as 2400s. (See Figure 6.9 for example of completed form.) The result is SNR=13.1 for the un-split 2400s exposure (Figure 6.10), which is comparable to the manual calculation of SNR=14.

Figure 6.9: Point Source Form for WFPC2 On-Line Exposure Time Calculator. Target is unresolved galaxy (z=0.22) nucleus with Hα line emission which is observed with LRF. SNR is computed for 2400s exposure.

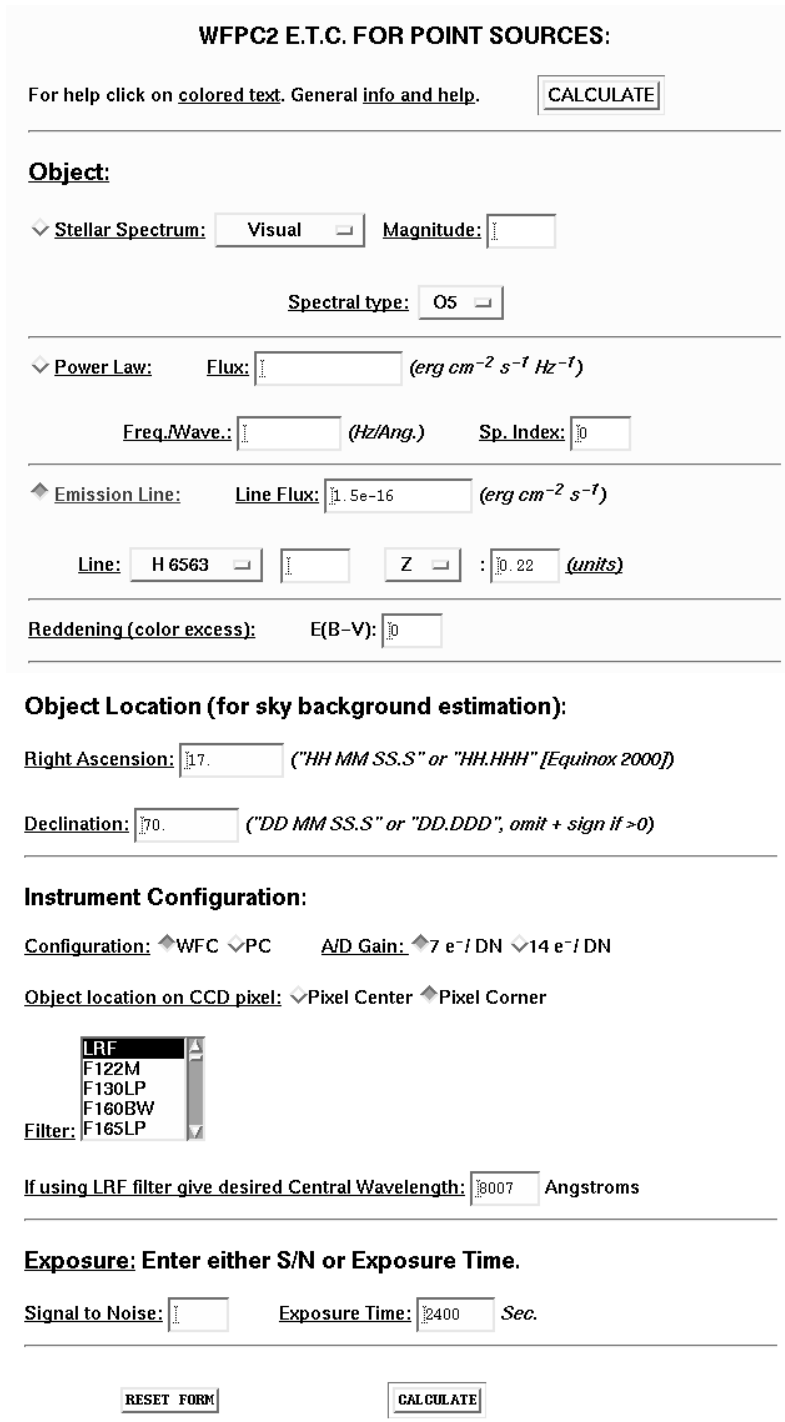

WFPC2 E.T.C. FOR POINT SOURCES:

For help click on colored text. General info and help. CALCULATE

Object:

Stellar Spectrum: Visual Magnitude:

Spectral type: O5

Power Law: Flux: (erg cm^{-2} s^{-1} Hz^{-1})

Freq./Wave.: (Hz/Ang.) Sp. Index: 0

Emission Line: Line Flux: 1.5e-16 (erg cm^{-2} s^{-1})

Line: H 6563 Z : 0.22 (units)

Reddening (color excess): E(B−V): 0

Object Location (for sky background estimation):

Right Ascension: 17. ("HH MM SS.S" or "HH.HHH" [Equinox 2000])

Declination: 70. ("DD MM SS.S" or "DD.DDD", omit + sign if >0)

Instrument Configuration:

Configuration: WFC PC A/D Gain: 7 e$^-$/ DN 14 e$^-$/ DN

Object location on CCD pixel: Pixel Center Pixel Corner

Filter: LRF F122M F130LP F160BW F165LP

If using LRF filter give desired Central Wavelength: 8007 Angstroms

Exposure: Enter either S/N or Exposure Time.

Signal to Noise: Exposure Time: 2400 Sec.

RESET FORM CALCULATE

Figure 6.10: Sample Output for WFPC2 On-Line Exposure Time Calculator.

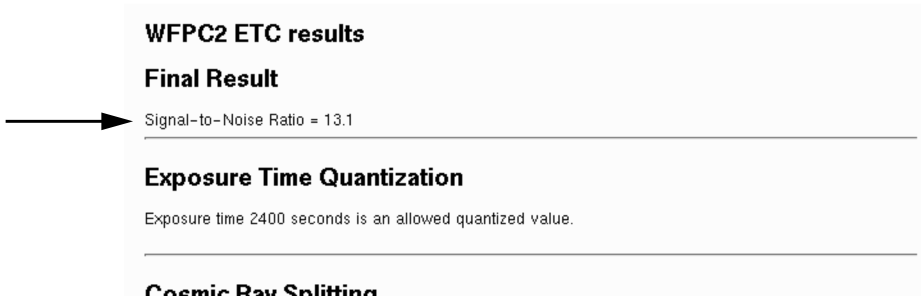

6.8 Red Leaks in UV Filters

The presence of significant red leaks in the UV filters, together with the much greater sensitivity and wavelength coverage in the red part of the spectrum, can make UV observation and calibration difficult. Observers must sometimes be prepared to take additional frames at red wavelengths, in order to estimate the contribution of red leak to the UV counts. The counts contributed by red leak can be a significant noise source, and must also be taken into account during SNR and exposure time estimation. See section 3.7 on page 57 for detailed information. Note that the SYNPHOT synthetic photometry package can be used to estimate counts due to red leak for particular filter / target combinations.

6.9 Time Dependence of UV Response

The UV throughput of the WFPC2 degrades in a predictable way after each monthly decontamination. The photometric calibration given in Section 6.1 is applicable at the start of each cycle, and measurements taken at other times must be corrected to account for the change in sensitivity since the last decontamination. In addition, a long-term change in sensitivity is present for the F160BW and F170W filter observations on the PC, and may be present to a lesser degree at other wavelengths.

Figure 6.11 shows the photometric monitoring data for the standard star GRW+70D5824 (a white dwarf classified DA3; B-V = -0.09) in the WF3 and PC1 for the set of filters which are routinely monitored. The dotted vertical lines mark the dates of the decontaminations. The solid vertical lines labeled "-88" mark the date the operating temperature was changed from -76˚C to -88˚C (April 24, 1994). The following information is for the period following the cooldown date. Figure 6.11 shows that the effect of contamination on the F675W and F814W filter observations is essentially negligible, but it rises toward the UV until it reaches values of 30% - 40% per month for the F160BW filter. Table 6.10 shows

Table 6.10: Change in WFPC2 Throughput Over 30 Days[a].

Filter	PC1	WF2	WF3	WF4
F160BW	-0.263 ± 0.030		-0.393 ± 0.051	
F170W	-0.160 ± 0.011	-0.284 ± 0.005	-0.285 ± 0.006	-0.232 ± 0.006
F218W	-0.138 ± 0.009		-0.255 ± 0.010	
F255W	-0.070 ± 0.007		-0.143 ± 0.009	
F336W	-0.016 ± 0.008 (-0.038 ± 0.018)	(-0.043 ± 0.010)	-0.057 ± 0.011 (-0.046 ± 0.008)	(-0.047 ± 0.007)
F439W	-0.002 ± 0.007 (0.002 ± 0.014)	(-0.022 ± 0.007)	-0.021 ± 0.010 (-0.023 ± 0.009)	(-0.023 ± 0.007)
F555W	-0.014 ± 0.006 (0.007 ± 0.013)	(-0.007 ± 0.007)	-0.016 ± 0.008 (-0.009 ± 0.009)	(-0.008 ± 0.008)
F675W	-0.001 ± 0.006 (-0.020 ± 0.020)	(0.001 ± 0.011)	-0.001 ± 0.006 (0.002 ± 0.011)	(0.004 ± 0.011)
F814W	0.007 ± 0.007 (0.013 ± 0.019)	(-0.002 ± 0.009)	0.003 ± 0.008 (-0.000 ± 0.009)	(-0.002 ± 0.010)

a. Values in parentheses are from the ω Cen observations.

the monthly decline in throughput based on this data. The values in parentheses are based on similar observations of the globular cluster ω Cen (NGC 5139; mean B-V ~ 0.7 mag). In general the values derived from the ω Cen data are in good agreement with the values derived from GRW+70D5824 data.

A slight difference between the throughput declines for GRW+70D5824 and ω Cen might be expected due to differences in spectral shape, especially for filters like F336W which have a substantial red leak. However, even in the case of F336W the effect should be less than 0.01 mag based on SYNPHOT simulations.

Figure 6.12 shows the throughput decline in all four chips as a function of days since the last decontamination for the F170W filter. The contamination rate is remarkably constant during each decontamination cycle, and can be accurately modeled by a simple linear decline in throughput following the decontaminations, which appear to return the throughput to roughly the nominal value each month. While the contamination rates are similar for the three WF chips, the values for the PC are much lower.

In addition to the monthly changes in throughput there is now evidence for a long-term variation in the F170W data on the PC, where the throughput has *increased* at the rate of 4.8% $\pm$ 0.3% per year. This is evident in Figure 6.11, but is much clearer in Figure 6.12 where the data before and after Jan. 1, 1995 are compared, and in Figure 6.13 where the effect of the monthly decontamination is removed. The F160BW filter shows an even stronger trend but with larger uncertainties (i.e., an increase of 9.0% $\pm$ 1.7% per year). The WF chips do NOT show this effect, nor do the observations on the PC at longer wavelengths. One possible explanation of the throughput increase is that WFPC2 was flown with some initial contaminant on the PC1 optics which is slowly evaporating on-orbit. The pre-launch thermal vacuum test gave evidence of elevated contamination in PC1, which is consistent with this hypothesis.

ISR 96-4 will describe detailed results of this monitoring (available from our WWW site). Observers are advised to consult the STScI WFPC2 WWW page for the latest information at the following address:

```
http://www.stsci.edu/ftp/instrument_news/WFPC2/wfpc2_top.html
```

Figure 6.11: Photometric Monitoring Data for WFPC2.

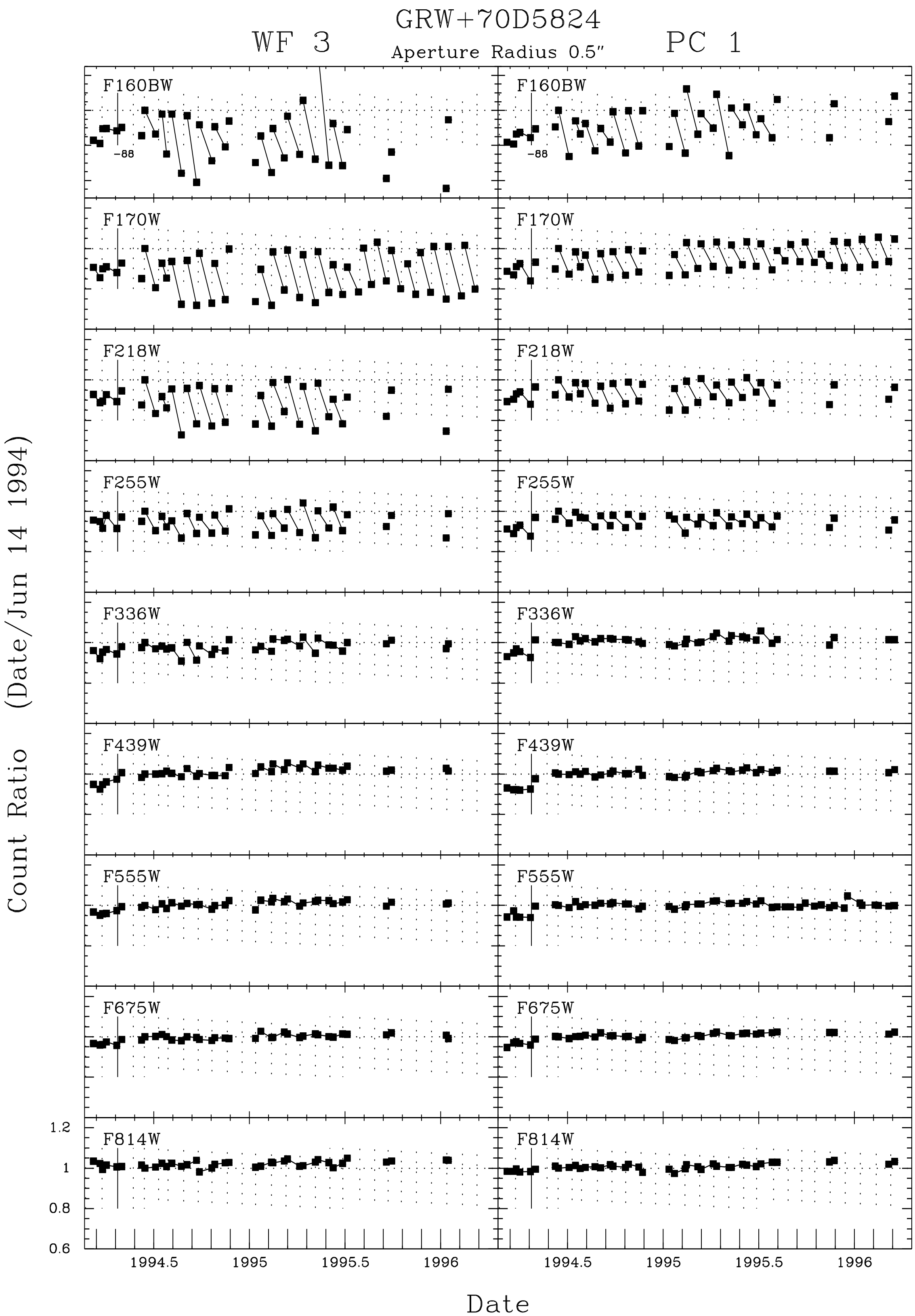

Figure 6.12: Throughput for the F170W Filter Following Decontaminations.

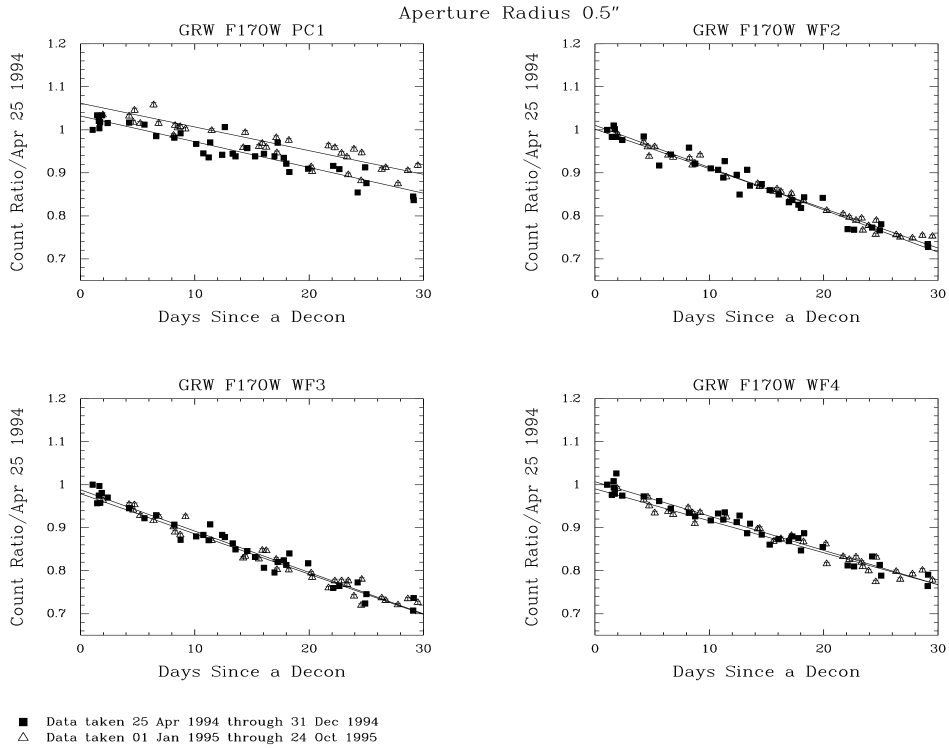

Figure 6.13: Change in Throughput vs. Time.[1]

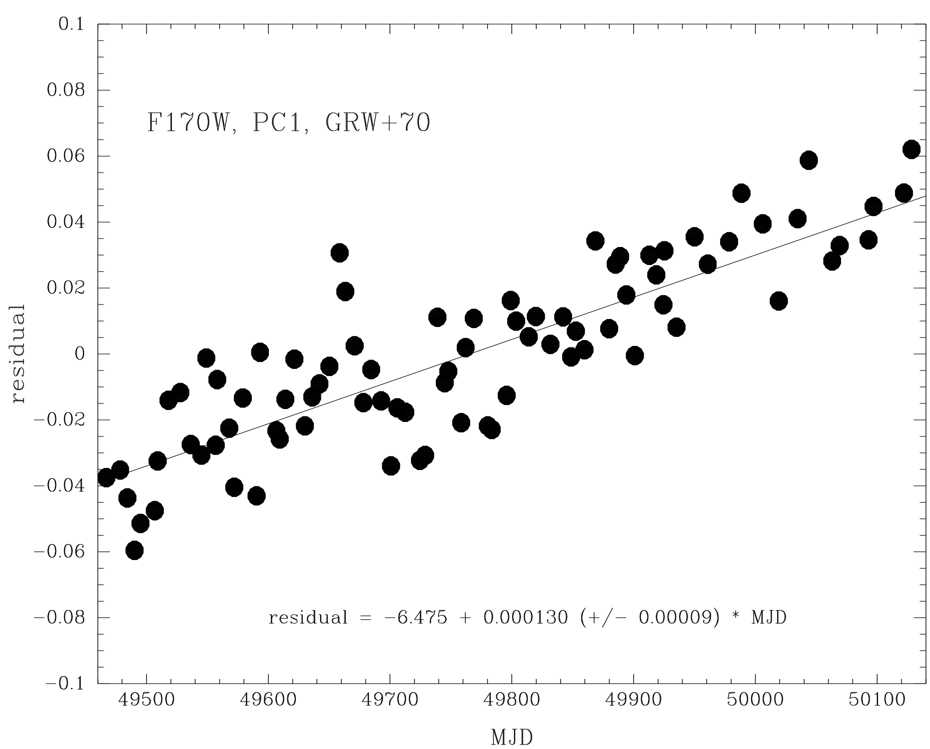

1. Determined after removing the effects of the monthly decontamination

CHAPTER 7: Observation Strategies

In This Chapter...

7.1 Observing Faint Targets

For broad band filters the sky background will limit the detection of faint targets. For example, an 8 orbit observation in F555W gives a 5σ detection limit at V=28.6 for an average sky level 23 mag arcsec^{-2} in V. Note that the sky background is a strong function of position, especially for targets near the ecliptic; the sky level can vary from V=23.3 mag arcsec^{-2} at the ecliptic pole to about V=20.9 mag arcsec^{-2} on the ecliptic near the solar avoidance limit. (See Table 6.3 on page 113 for sky level as function of ecliptic coordinates.)

If these higher sky levels would severely impact the science data, observers should consider specifying the special requirement LOW-SKY on the Phase II proposal. This parameter forces the observation to be made when the sky background is within 30% of the minimum value for the target. Note, however, that this will also reduce the number of HST calendar windows available to the observation, and so could result in scheduling delays or may even make the observation infeasible if there are other constraints such as ORIENTs. A minor decrease in the per-orbit visibility period also results from LOW-SKY, but for background limited programs this is a minor price to pay for the guarantee of a much lower background. In summary, LOW-SKY will reduce the sky background, but should only be used if the science goals *require* it.

Note that LOW-SKY cannot be used for CVZ targets, as they imply mutually exclusive pointing constraints.

Scattering of bright Earth light in the OTA can produce non-uniformities in the background which may hamper analysis of faint target images. Most often these take the form of diagonal bars of suppressed background light in several of the CCDs. These effects tend to occur for broad band filters when the OTA axis is about 25° from the bright Earth. This effect is most often seen in observations of targets in the CVZ (continuous viewing zone), since the Earth limb is never very far from the OTA axis when observing in the CVZ. Figure 7.1 shows a typical case. LOW-SKY will eliminate this effect for non-CVZ targets, as it places the OTA axis more than 40° from the bright Earth. Alternatively, one can place the target away from the CCD center to avoid these artifacts.

Another option for reducing the sky brightness, is the special requirement SHADOW, which forces the observation to be made when HST is in the Earth's shadow. This usually has a large negative impact on the observing efficiency, and is recommended only when observing far-UV emission lines (e.g. Ly α and OI 1304Å). Its primary goal is only to reduce geocoronal emission lines. Moreover, it does not attempt to minimize zodiacal emission, which dominates at visible wavelengths.

7.2 Observing Bright Targets

Saturation is the primary concern when observing bright targets. The analog-to-digital converter will run out of bit codes at ~28,000 e^- $pixel^{-1}$ in the ATD-GAIN=7 (default) setting, and at ~53,000 e^- $pixel^{-1}$ in the ATD-GAIN=15 setting. Count levels above these are merely reported as 4095 DN in the data. Hence ATD-GAIN=15 is recommended for targets approaching 28,000 e^- $pixel^{-1}$. The disadvantage of this setting is that the read noise is poorly sampled by this coarse digitization, and hence the read noise is slightly increased.

At count levels above ~90,000 e^- $pixel^{-1}$ charge will overflow the potential well of each pixel, and begin to bloom up and down the CCD columns. For example, this occurs in the F555W filter at about V=13.5 for a 10s exposure on the WFC, and at about V=13.0 on PC1.

At very high count levels, above ~10^8 e^- per CCD column, the charge bloom will reach the top and bottom of the CCD and flow into the serial registers. CLOCKS=YES will dispose of this charge as it reaches the ends of the CCD, and thus prevent it from leaking back into adjacent CCD columns. This exposure level corresponds roughly to a 10s exposure of a V=7 star in F555W. Note that CLOCKS=YES offers no benefit unless the bloom reaches the ends of the CCD, and that it may slightly compromise the bias and dark calibration. Moreover, CLOCKS=YES will result in anomalous exposure times; exposure times are rounded to the nearest integral second, minus a delay time of up to 0.25s for the

Figure 7.1: Example of Scattered Earth Light. Scattered light contributes ~100 e^- of background throughout this image. The camera spiders block some of this scattered light along CCD diagonals, hence forming “X” patterns and bars where the background is reduced by ~40% in this image.

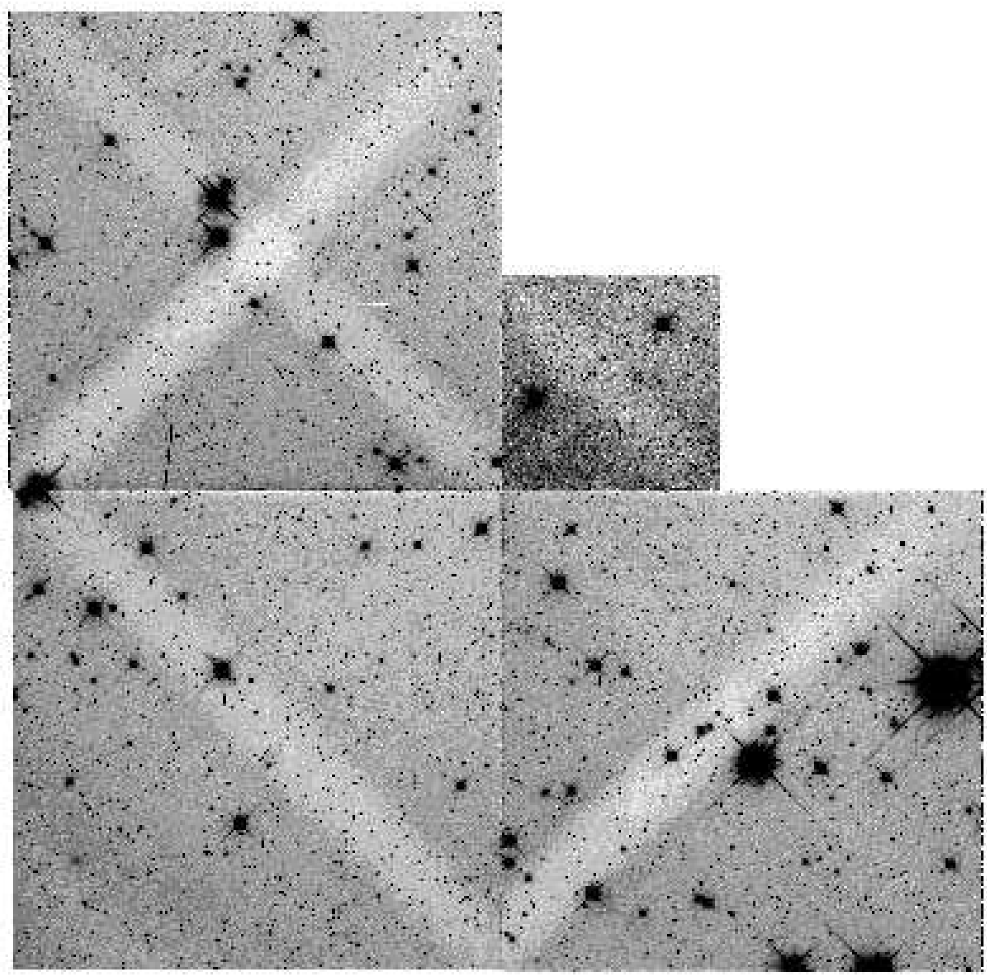

shutter to open. (See “Serial Clocks” on page 27 for further discussion of exposure time anomalies caused by CLOCKS=YES.)

Besides setting ATD-GAIN=15, the PC CCD can be used to reduce saturation effects for stellar objects. The peak of the PSF will be spread over more pixels on the PC (vs. WFC), so stars can be exposed about 50% longer on the PC before saturation sets in.

Note that the narrow band filters may be useful when observing very bright targets. For example, stars as bright as V~4.4 can be observed without saturation in F502N using the PC at ATD-GAIN=15 with a 0.11s exposure time.

7.3 Observing Faint Targets Near Bright Objects

The concerns here are similar to those for observing bright targets; saturation and blooming of the bright companion PSF must not impact the faint target. Also, one may need to consider subtracting the PSF of the bright object, and effects which limit the accuracy of that subtraction.

If the bright companion will saturate and bloom, it will be necessary to rotate the CCD so that blooming along the CCD columns does not obliterate the faint target. See Figure 7.8 on page 161 for an illustration of the bloom directions. It may also be useful to orient the field so that the OTA diffraction spikes from the bright companion (along diagonal lines on the CCDs) avoid the faint target. Table 7.1 summarizes ORIENTs which can be used to avoid CCD blooming tracks and OTA diffraction spikes caused by bright objects. For example, if a faint companion is at PA 60˚ on the sky relative to a bright companion, it would be advantageous to observe on PC1 with ORIENT= PA + 45˚ = 105˚. Ideally, some range in ORIENT would be specified to ease scheduling, hence “ORIENT=90D TO 120D” might be specified on the Phase II proposal. Note that “ORIENT=270D TO 300D” is also feasible, and should be indicated in the visit level comments.

Table 7.1: ORIENTs for Avoiding Bloom Tracks and Diffraction Spikes. “PA” is the position angle of the faint target relative to the bright object. Note that ORIENT should be between 0D and 360D, so subtract 360˚, if necessary. On proposal these are specified as, e.g., “ORIENT=231D TO 261D”.

CCD	ORIENT
PC1	PA+30˚ to PA+60˚, PA+210˚ to PA+240˚
WF2	PA+120˚ to PA+150˚, PA+300˚ to PA+330˚
WF3	PA+30˚ to PA+60˚, PA+210˚ to PA+240˚
WF4	PA+120˚ to PA+150˚, PA+300˚ to PA+330˚

If instead of observing a known companion, one is *searching* for companions, it is advisable to observe at several ORIENTs so that the CCD bloom track and OTA diffraction spikes will not hide possible companions. For example, three ORIENTs, each separated by 60˚, would give good data at all possible companion position angles.

If PSF subtraction will be needed during data analysis, then the PC CCD may have some advantage, since it provides better sampling of fine undulations in the PSF. It may also be useful to obtain observations of a second bright star for PSF calibration, though these may be of limited utility since thermal effects and OTA “breathing” can modify the telescope focus, and hence the PSF, on timescales of less than one hour. Any such PSF star should be similar in color to the target, and should be observed at the same CCD position (within 1″) and with the same filter. Sub-pixel dithering may also be useful, so as to improve sampling of the PSF (see “Dither Strategies” on page 155).

Figure 7.2 illustrates the effect of OTA breathing, and periodic focus adjustments, on PSF subtraction. It shows the difference between an “in focus” PSF and one where the OTA secondary mirror has been moved by 5µm. This amount of focus change is comparable to the range of OTA “breathing” effects (timescale <1 hour), and the periodic (semi-annual) focus adjustments of the OTA. Each panel shows a different contrast setting; the percentages indicate the energy per pixel which is plotted as white, expressed as a fraction of the total (un-subtracted) PSF energy. For example, features which are just white in the “0.003%” panel contain 0.003% of the total PSF energy in each pixel. In other words, the feature labeled “a” is, in effect, ~10 magnitudes fainter than the PSF of the bright object, so that it may be very difficult to detect a “real” companion object ~10 magnitudes fainter than the bright object, at this distance from the bright object. In a real PSF subtraction situation, other effects including PSF sampling, noise, and pointing instability would further degrade the subtraction. (The elongated appearance of the residuals in the PSF core is due to astigmatism in PC1.)

Table 7.2 gives some quantitative indication of the performance expected for PSF subtractions in the high signal-to-noise limit. It gives the magnitude of “star-like” artifacts remaining in the subtracted image, as a function of distance from the bright object, and magnitude m_{bright} for the bright object. The right-most column gives an effective magnitude limit imposed by artifacts from the PSF subtraction. These results are derived for the 5µm focus shift described above, and are for PC1 and filter F555W. It may be possible to do somewhat better than these limits by subtracting accurate model PSFs, or by finding an observed PSF with matching focus.

Table 7.2: Approx. PSF Subtraction Artifact Magnitudes and Magnitude Limits.

Distance from Bright Object	Effective Magnitude of Subtraction Artifacts	Effective Faint Object Detection Limit (3σ)
0.1″	m_{bright}+4.7	m_{bright}+3.5
0.3″	m_{bright}+8.6	m_{bright}+7.4
1″	m_{bright}+11.4	m_{bright}+10.2
3″	m_{bright}+13.2	m_{bright}+12.0

Large angle scattering may also impact identification of very faint objects near very bright ones. This scattering appears to occur primarily in the camera relay optics, or in the CCD. Hence, if a faint target is more than ~10″ from a bright object (i.e. very highly saturated object), it would be advisable to place the bright object on a different CCD, so as to minimize large angle scattering in the camera

Figure 7.2: Impact of OTA Focus Shift on PSF Subtraction. Each image shows the difference between an "in focus" and a 5 micron defocused PSF at different contrast settings. Numbers indicate the energy per pixel which is plotted as white, as a percentage of total energy in the un-subtracted PSF. Based on Tiny-TIM models for PC1 in F555W filter.

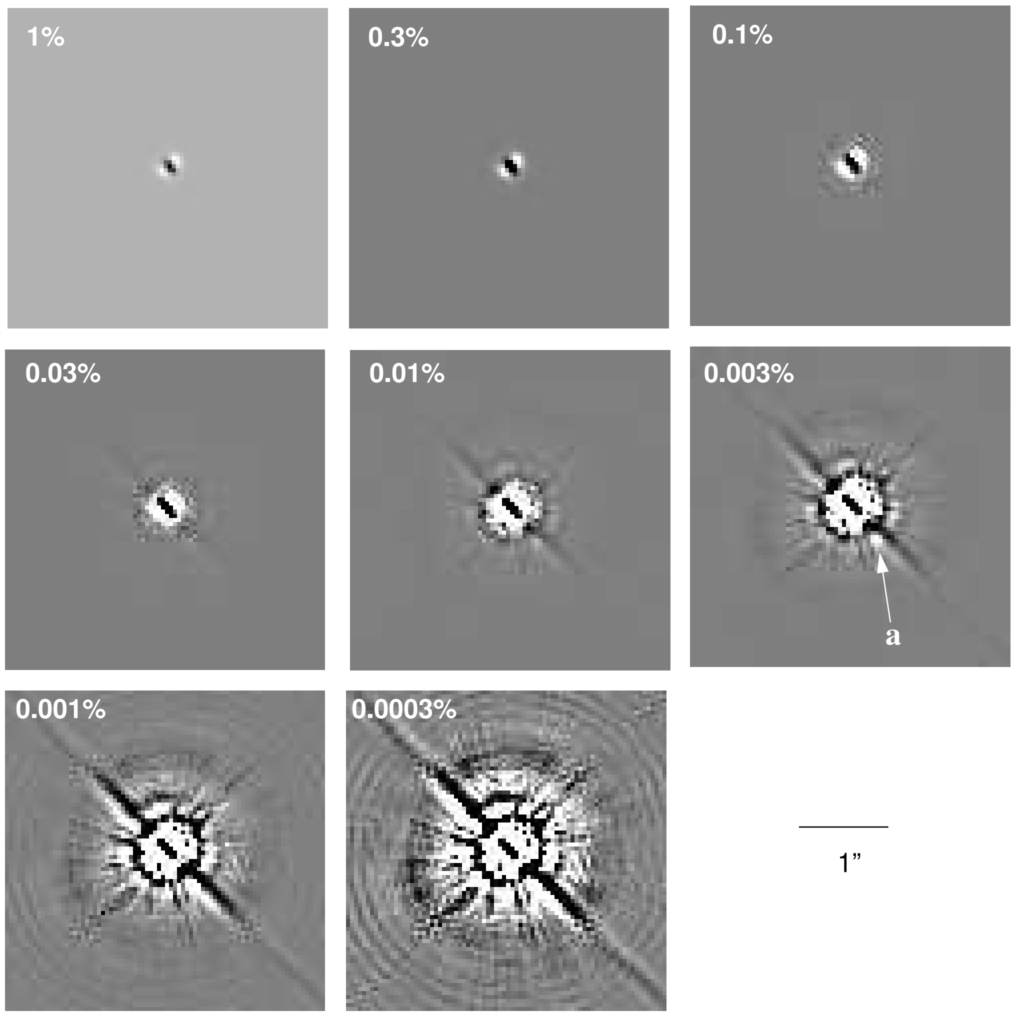

containing the faint target. See section on "Large Angle Scattering" on page 99. Note also that highly saturated PSFs exist for PC1 in filters F439W, F555W, F675W, and F814W, and for F606W on WF3; these may be useful when attempting to subtract the large-angle scattered light. As of this writing TinyTIM does not accurately model the large angle scattering, and should be used with caution when analyzing highly saturated images (Krist 1996).

It is generally unwise to place bright companions or other bright objects just outside the area imaged by the CCDs. The region of the focal plane just outside the CCDs (within about 6″ of the CCDs) contains a number of surfaces which can reflect light back onto the CCDs, hence placing bright targets there can have undesired results. Also, the un-imaged “L” shaped region surrounding PC1 should be avoided, since incomplete baffling of the relay optics allows out-of-focus images of objects in this region to fall on the CCDs. Figure 7.3 illustrates various bright object avoidance regions near the WFPC2 field-of-view; the indicated avoidance magnitudes will produce 0.0016 e^{-} s^{-1} $pixel^{-1}$ in the stray light pattern for F555W. Figures 7.4 and 7.5 show examples of artifacts which can result from bright stars near the PC1 CCD. The report “A Field Guide to WFPC2 Image Anomalies” (WFPC2 ISR 95-06, available on the WFPC2 WWW pages and from `help@stsci.edu`) gives more detailed discussions of artifacts associated with bright objects, and their avoidance.

Figure 7.3: Bright Object Avoidance Regions Near WFPC2 FOV.

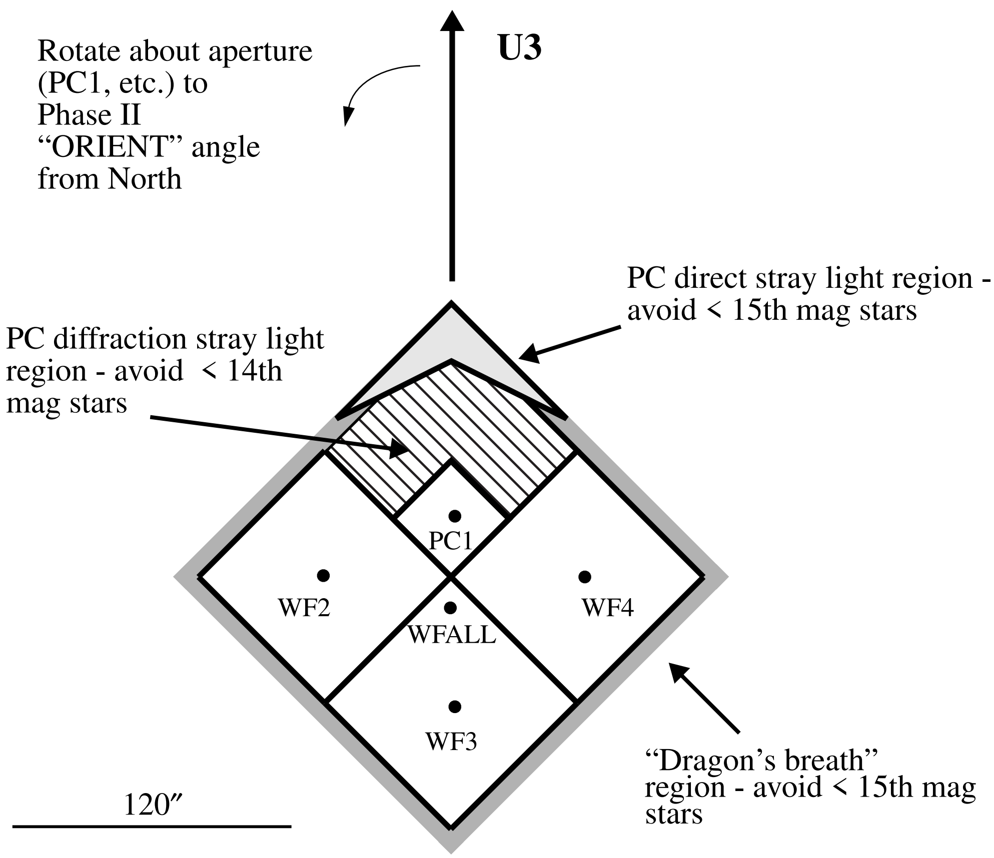

Figure 7.4: Example of PC1 “Direct” Stray Light Ghost.

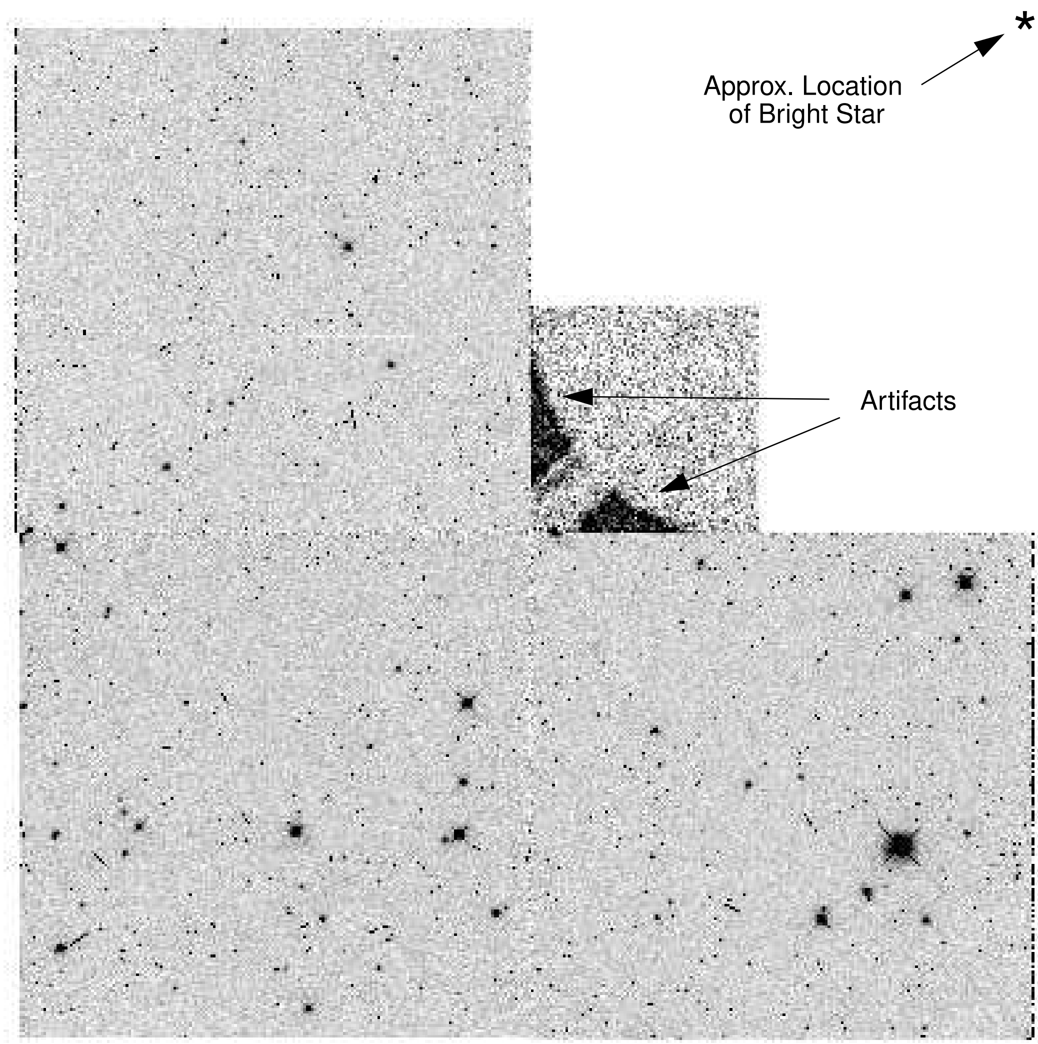

Figure 7.5: Example of PC1 “Diffraction” Stray Light Ghost.

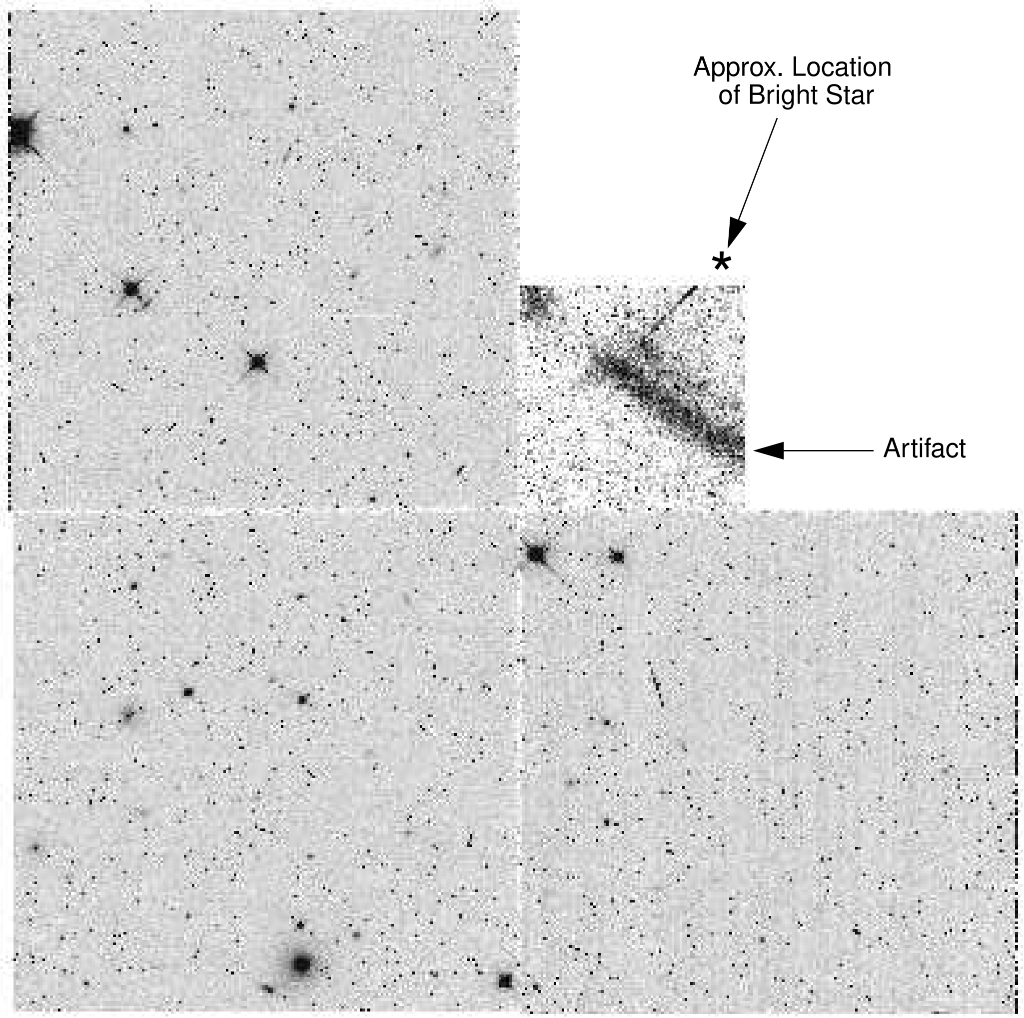

7.4 Cosmic Rays

Cosmic rays will obliterate ~20 pixels per second per CCD. It is imperative that two or more images be obtained at each pointing position, if these artifacts are to be removed from the data. The default action by the Phase II proposal processing software is to split exposures longer than 600s into two near equal parts, so as to allow removal of the cosmic ray tracks. The CR-SPLIT and CR-TOLERANCE optional parameters on the Phase II proposal allow observers to adjust this behavior. CR-SPLIT can be set to either DEF (default), NO, or a numeric value (0.0 to 1.0) giving the fraction of the total exposure allotted to the first sub-exposure of the pair. CR-TOLERANCE indicates the spread allowed in dividing the exposure, as a fraction of the total exposure time. For example, the default CR-TOLERANCE=0.2 allows the first sub-exposure to range from 0.3 to 0.7 of the total exposure. Setting CR-TOLERANCE=0 will force equal-length sub-exposures.

The required degree of cosmic-ray avoidance will depend on the science goals of the proposal; observations of a single small target will usually suffer much less impact from cosmic rays than programs needing very "clean" data over a large area. Table 7.3 gives very rough recommendations for the number of sub-exposures for a given total exposure time. Note that splitting into *many* sub-exposures introduces additional overhead time and will increase the noise for "read noise" limited exposures (usually exposures in UV or narrow band filters), and hence one should not use more sub-exposures than are truly required by the science goals.

Table 7.3: Recommended Exposure Splittings.

Total Exposure Time (s)	Rough Recommended Number of Sub-exposures	
	Programs with Single Small Target	Wide-area Search Programs
<300	1	3
300 - 600	1 or 2	4
600 - 1600	2 or 3	4
1600 - 5000	3	5
5000 - 10000	4	6
>10000	One exposure per orbit (2400s each)	

7.5 Choosing Exposure Times

The choice of exposure time generally depends on the signal-to-noise ratio required to meet the science goals. This can be assessed using information in Chapter 6 or Appendix B herein, or by using the on-line WWW Exposure Time Calculator tool.

However, when packing orbits, one must often compromise somewhat and decide which exposures to lengthen or shorten. Table 7.4 may be helpful in this regard. It shows the total time required to execute a single CR-SPLIT=NO exposure, *excluding* any time needed to change filters.

Note that the most efficient exposure times are those whose length approaches or equals, but does not exceed, an integral number of minutes *plus* 40s. Figure 7.6 illustrates event timings during a typical 60s WFPC2 exposure, similarly, Figure 7.7 illustrates events during a (more efficient) 100s exposure. (See "Overhead Times" on page 29 for more information about exposure timings.)

Figure 7.6: Event Timings During a 60s WFPC2 Exposure. All events, except shutter opening, start on 1 minute spacecraft clock pulses. Both the CCD clear and readout of each CCD require 13.6s. This 60s exposure, including the filter change, requires 4 minutes.

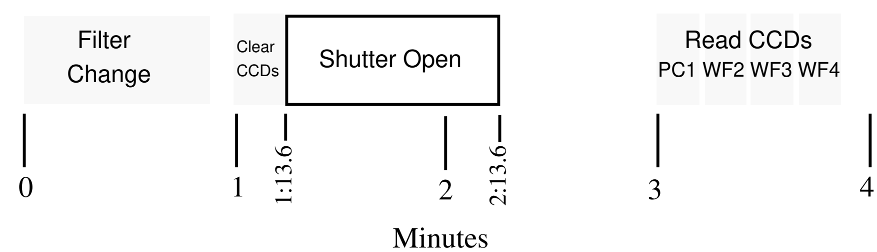

Figure 7.7: Event Timings During a 100s WFPC2 Exposure. This exposure, including the filter change, requires 4 minutes.

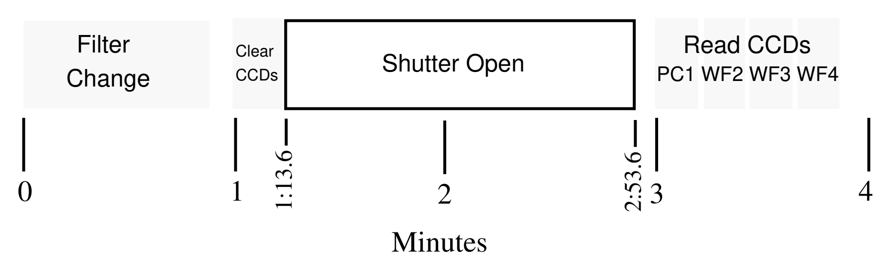

Due to the various overheads, shortening or lengthening an exposure can have unexpected effects on the orbit packing. For example, shortening an exposure from 400s to 350s has no effect on orbit packing; they both require 9 minutes to execute (CLOCKS=NO, the default setting). On the other hand, shortening an exposure from 180s to 160s trims the execution time by 2 minutes (again CLOCKS=NO, the default setting).

CLOCKS=YES may have some advantage in a long series of exposures whose lengths are 180s or somewhat greater. Each savings of 1 minute can add up to a few more exposures per orbit. The down side is that most calibrations are derived for exposures with CLOCKS=NO, so the calibration maybe slightly compromised. The largest calibration error is expected to occur on the dark current, where there may be a slight increase near the top and bottom of each CCD. In many situations this error may be acceptable, such as a small target near a CCD center, or broad band filter images where the sky completely dominates the dark current. CLOCKS=YES will have more impact on calibration of narrow filters, or situations requiring an extremely flat background. (Also, see "Serial Clocks" on page 27 for discussion of exposure time anomalies associated with CLOCKS=YES, though these are most important for exposures <30s.)

An exposure with CR-SPLIT=YES would simply require the total time for each sub-exposure as given by Table 7.4, again, plus any time needed to change filter before the first exposure. However, the default CR-SPLITting allows schedulers some latitude in dividing the exposures (CR-TOLERANCE=0.2 is the default) so the exact overheads are unpredictable. For example, a 700s exposure with CR-SPLIT=0.5 (the default) could be split into a pair of 350s exposures totaling 18 minutes, or a 300s and 400s exposure totaling 17 minutes.

Table 7.4: Basic Time to Execute Single Non-CR-SPLIT Exposure. This includes time to prep the CCD, execute the exposure, and readout the CCDs. Times needed to change filter (1 minute), or insert a second filter (1 minute), are *excluded*. See "Overhead Times" on page 29 for more discussion and other overheads.

Exposure Time (s)	Total Execution Time (min.)	
	CLOCKS=NO (default)	CLOCKS=YES
0.11 to 30	2	(not recommended)
35, 40	2	2
50,60,70,80,100	3	3
120,140,160	4	4
180,200	6	5
230,260	7	6
300	8	7
350,400	9	8
500	11	10
600	13	12
700	14	13
800	16	15
900	18	17
1000	19	18
1100	21	20
1200	23	22

7.6 Dither Strategies

There is no single observing strategy that is entirely satisfactory in all circumstances for WFPC2. One must consider cosmic rays, hot pixels (i.e. pixels with high, time variable dark count), spatial undersampling of the image, and large-scale irregularities such as the few arcsecond wide region where the CCDs adjoin. One strategy that can be used to minimize the effects of undersampling and to reduce the effects of hot pixels and imperfect flat fields is to dither, that is, to offset the telescope by either integer or sub-pixel steps. The best choice for the number and size of the dithers depends on the amount of time available and the goals of the project. In the following we will address a few issues related to dithering:

1. **Undersampling:** Individual images taken with ***sub-pixel*** offsets can be combined to form an image with higher spatial resolution than that of the original images. A single dither from the original pixel position -- call it (0,0) -- to one offset by half a pixel in both x and y, (0.5,0.5) will produce a substantial gain in spatial information. On the other hand very little extra information is gained from obtaining more than four positions, if the standard four point dither is used, and if the telescope has successfully executed the dither. Therefore the recommended number of sub-pixel dither positions is between 2 and 4.
2. **Hot Pixels:** There are three ways to deal with hot pixels: correct using "dark frames" that bracket the observation, dither by an ***integer*** amount of pixels, or use a task such as "WARMPIX" within STSDAS to filter out the known hot pixels. Note that the integer dither strategy would ideally use six images, i.e. two CR-SPLIT images at each of three different dither positions. This is because in addition to hot pixels, low or "cold" pixels[1] can be present and simple strategies selecting the minimum of two pixel values can fail. However, even four images (two each at two dither positions) will greatly aid in eliminating hot pixel artifacts.
3. **Cosmic Rays:** Although dithering naturally provides many images of the same field it is better to take several images at each single pointing in order to remove cosmic rays. In principle, it should be possible to remove cosmic rays using only sub-pixel dithered data. At present, however, no publicly released software is available for this task. *Hence we recommend obtaining two or more images (i.e. CR-SPLITing)* ***at each position*** *in the dithered sequence.* For very long integrations it is convenient to split the exposure into *more than two separate images.* As an example, for two 2000s exposures, about 1000 pixels per chip will be hit in both images and will therefore be unrecoverable. Moreover, since CR events typically affect 7 pixels per event, these pixels will not be independently placed, but rather will frequently be adjacent to other unrecoverable pixels.

1. Cold pixels usually result from hot pixels in the dark calibration file which do not actually appear in the science data.

4. **Accuracy of dithering**: We do not yet have good statistics on the accuracy of HST dither offsets. During the Hubble Deep Field, nearly all dithers were placed to within 10 mas (during ±1.3″ offsets and returns separated by multiple days), although in a few cases the dither was off by more than 25 mas, and on one occasion (out of 107 reacquisitions) the telescope locked on a secondary FGS peak causing the pointing to be off by approximately 1″ as well as a field rotation of about 4 arcminutes. The software which was developed for the Hubble Deep Field is able to reconstruct images even for these non-optimal dithers, still gaining in resolution over non-dithered data. This software will be available in STSDAS in mid 1996 and is based on the variable pixel linear reconstruction technique developed by Fruchter and Hook (this procedure is also known as "dripping and drizzling"). The Richardson-Lucy-Hook non-linear deconvolution technique (STSDAS task ACOADD) can also use non-optimal dithers.

The simplest way to schedule dithers is to use the options DITHER-TYPE=LINE (e.g. for two-point diagonal dithers) or DITHER-TYPE=BOX (for four-point dithers). Alternative approaches are to specify a spatial scan or to use POS TARGs. Note that when the WF3 is specified as an aperture, the POS TARG axes run exactly along the WF3 rows and columns. For the other chips, they only run approximately along the rows and columns due to the small amount of rotation between CCDs. For small dithers these rotations are not important.

Some specific offsets allow one to shift by convenient amounts both the PC and the WFC chips. For instance an offset of 0.5″ is equivalent to 5 WFC pixels and 11 PC pixels. The default DITHER-LINE spacing of 0.3535″ along the diagonal is equivalent to shifts of (2.5,2.5) pixels for the WFC and (5.5,5.5) pixels for the PC.

Note that large dithers will incur errors due to the camera geometric distortion which increases toward the CCD corners and alters the image scale by about 2% at the corners. Hence a 1.993″ offset will be 20.3 WF pixels at the field center, but suffer a 0.4 pixel error at the CCD corners. Large dithers may also occasionally require a different set of guide stars for each pointing, thus greatly reducing the expected pointing accuracy (accuracy only ~1″ due to guide star catalogue). One set of software presently available to handle the reduction of large dithers (which show the effects of geometric distortion) is the Fruchter-Hook code developed for reduction of the Hubble Deep Field images.

For related articles on dither strategies, see the January, 1995 issue of the WFPC2 Space Telescope Analysis Newsletter and the February, 1995 issue of the ST-ECF Newsletter. For more information on dithering, please see "Questions about Dithering WFPC2 Observations" on the "Frequently Asked Questions" page of the WFPC2 WWW area. For detailed information on POS TARGs, please see the report "Dithering: Relationship Between POS TARGs and CCD Rows/Columns" obtainable from the WFPC2 WWW pages or `help@stsci.edu`.

7.7 Pointing Accuracy

Some WFPC2 programs have critical target positioning constraints (i.e. the target must be as close as possible to a specified aperture). A sure way to meet such requirements is to include an interactive acquisition. However, INT ACQs are costly in terms of allotted orbits. The only alternative is to provide accurate target coordinates. This section provides some guidance in doing that, and indicates the level of residual error that can be expected.

7.7.1 Absolute Pointing Accuracy

We have looked carefully at a sequence of images to assess the absolute pointing performance that HST delivers to WFPC2. The apertures used in the observations studied were either PC1, PC1-FIX, or WF2. The observed positions of stars on WFPC2 images were measured and compared with the proposed coordinates and apertures. Where necessary, coordinate and proper motion errors were accounted for (with the assumption that SAO catalog coordinates are exact - they form the astrometric basis for the guide star coordinate system). The typical residual pointing error is 0.86″, with 1.84″ being the largest error seen. This study did bring out several easy-to-make target coordinate errors (which we corrected in the analysis, but which frequently dominated the pointing error), so we discuss these first.

In a number of cases studied, the proposal coordinates were from the printed version of the Yale Bright Star Catalog. One problem is that the equinox 2000 positions in the BSC are given in the FK4 (Besselian) reference system. The proposal system assumes that equinox 2000 and later coordinates are in the FK5 (Julian) reference frame, and that earlier ones are in the FK4 frame. This can be overridden by specifying B2000 instead of J2000 for the equinox in the proposal. The latest digital version of the BSC (BSC5) is in J2000. The 1950 edition of the SAO catalog is in B1950 (FK4), and a digital version is available for J2000 (FK5). An error of up to 1.5″ can result from assuming BSC positions are J2000 instead of B2000 in the proposal.

Another common problem with target coordinates is that they lack precision. For example, in the BSC, RA is given to the nearest 0.1^s and DEC to the nearest arcsecond. This can cause an error of up to 0.75″ in RA and 0.5″ in DEC. The SAO coordinates have higher precision, 0.001^s in RA and 0.01″ in DEC, and should be used when possible.

A common error source is not specifying proper motion or specifying it in the wrong units. It is critical to follow the latest version of the proposal instructions on this because the units have changed. Even small proper motions are significant at the resolution of HST images.

Residual pointing errors (after coordinate errors and aperture location changes) range from 0.26″ to 1.84″. The average is 0.93″ and the median is 0.86″. There are no obvious trends in any coordinate system. These are errors which cannot be accounted for by a proposer, being due to guide star position errors, FGS alignment uncertainties, and residual aperture location errors. Using Guide Star Catalog positions may help reduce the error between target and guide stars. Most of the targets used in this study were too bright to have true Guide Star Catalog positions.

In summary, a target with good coordinates (and proper motion) referenced to the SAO catalog can typically be placed within 0.9″ of a specified aperture. However, errors of around 1.5″ occasionally happen.

7.7.2 Updates to Aperture / Coordinate Systems

We note that on 11 April, 1994 an update was made to the spacecraft database which tells HST where to place targets relative to the FGSs. This impacted both the location of targets in the WFPC2 field-of-view, and the position reference frame in the image headers. The nominal (or intended) pixel locations of the apertures in the WFPC2 focal plane did not change. Only the (V2,V3) coordinates of the apertures changed, as their locations relative to the FGSs became better known. For example, PC1 and PC1-FIX are designated to be at pixel (420,424.5). Before April 1994, this aperture was thought to be at (V2,V3) =(4.95″,-30.77″), which using the most current information was actually located at pixel (X,Y) = (459.8,377.3). Since April 1994, the aperture in the spacecraft's database has been at (V2,V3) = (1.87″,-30.96″) or, assuming the current best estimate is exactly correct, at (X,Y) = (414.9,428.1). Thus, for the same coordinates and aperture, the pixel position of a target in an image taken before April 1994 could be nearly 3″ different from its position in later images, due to aperture updates. Similar corrections apply to all WFPC2 data taken before this date.

This update also affects the position information placed in the image headers, which maps sky coordinates onto each individual CCD. Observations taken before April 11, 1994 have preliminary plate scales, rotations, and reference pixel locations in their image headers. Thus, the sky coordinates associated with a given pixel will be different for otherwise identical images taken before and after April 11, 1994, due to improvements in the aperture locations. The change is primarily an approximate 3″ shift, as well as a small rotation. There is a 0.8° rotation for WF2, and smaller rotations for the other chips (0.28° in PC1, 0.46° in WF3, and 0.06° in WF4).

The STSDAS task METRIC, which is used to assemble the 4 CCDs into a single image, uses this header information. Hence images taken before 11 April 1994 will not properly assemble into a single image. A new STSDAS task UCHCOORD will be available in the next STSDAS release (early 1996) to update the header group parameters to reflect the improved plate scale, shift, and rotations. This task will supersede the task UCHSCALE in the current STSDAS release, which can update only the scale, *not* the rotation or shift.

We also note, that in April and May 1996 two updates were made to the (V2,V3) coordinate system. This update should be transparent to most observers. The purpose was to remove a slow drift in the position of WFPC2 in the HST focal plane; the largest change was 0.6″. (See Table 3.15 on page 61 for details.)

All the apertures are now thought to be correct to within 0.3″, and updates in the near future should be small.

7.7.3 Pointing Repeatability

The Hubble Deep Field (HDF) afforded an opportunity to study the repeatability of pointing over many images and acquisitions of the same field. The pointing appears to have been stable to better than 5 mas accuracy while taking many images of the same field without interruption over several orbits. The accuracy for full-up acquisition of the same field after slewing to other targets appeared to be ~10 mas typically, with occasional 20 mas errors seen. However, a few large errors were seen; in about 1 in 100 acquisitions the FGSs locked-up incorrectly resulting in a ~1″ error.

Other programs report similar 3 mas pointing accuracy if simple re-acquisitions are done between orbits. Approximately once per day a “full-up” acquisition is usually required (for engineering reasons) where the dominant FGS is fixed in position, but the sub-dominant FGS performs a spiral search for the guidestar and tracks wherever the star is found. On rare occasion these full-up acquisitions produce position errors of several hundred mas, and field rotations of up to ~0.1°, relative to previous images of the same field. This may impact long sequences of exposures requiring half a day or more to execute.

7.7.4 Tracking Modes

Three guiding modes are available: (1) Gyro Hold, (2) Coarse Track, and (3) Fine Lock. Fine Lock (PCS MODE FINE) is used by default, since use of Coarse Track may be harmful to the Fine Guidance Sensors. Use of Gyro Hold (PCS MODE GYRO) is not generally recommended, even for snapshot (SNAP) observations, since the pointing accuracy is only 14″. Also the drift rate is 0.0014″ s^{-1} so exposures >100s can result in smeared images. However, if the reduced pointing accuracy can be tolerated, and the exposures are only a few seconds or less, Gyro Hold can give a significant savings in the target acquisition overhead time.

7.8 CCD Position and Orientation on Sky

During observation the target is placed at the aperture (PC1, WF2, WFALL, etc.) specified on the Phase II proposal. Locations of the principal apertures are shown in Figure 7.8 (Table 3.14 on page 61 gives a complete list of apertures; the (V2,V3) system here is post 1996 day 127).

The POS TARG special requirement can be used when a position offset is needed. The target is positioned with offset “POS TARG x,y”, measured in arcseconds, from the specified aperture. The approximate directions (within 1°) of the POS TARG offsets are shown in Figure 7.8. The exact directions of the offsets are parallel to the rows and columns of the CCD on which the aperture is specified. There are small rotations (few tenths of a degree) between the CCDs. (For detailed information see "Dithering: Relationship Between POS TARGs and CCD Rows/Columns" obtainable from the WFPC2 WWW pages or `help@stsci.edu`.)

It is often useful to explicitly specify the desired rotation of the WFPC2 field-of-view on the sky. This is specified in the Phase II proposal using the ORIENT special requirement. It is defined as the PA (measured from North through East) of the +U3 axis on the sky. Figure 7.8 shows the CCD orientation and aperture locations relative to the U3 axis. In effect, the sequence of events is to first move the target to the desired aperture, then offset by any specified POS TARG from the aperture, and finally to rotate the target "in place" on the CCDs to the desired ORIENT.

Observers should try to specify all possible ORIENTs which would give the desired data, since having a range of values, or several ranges, will make the observation much easier to schedule. Often two ORIENTs separated by 180° will both give useful data. Sometimes ORIENTs separated by 90° will also give similar data.

The ORIENT for any observation can be computed as follows:

1. Obtain the Position Angle (PA) of the source axis on the sky, measured in the standard way, North through East.
2. Look at Figure 7.8 and decide what angle you want, measured clockwise, from the +U3 axis to the source axis.
3. Sum the angles in steps 1 and 2.
4. ORIENT must be between 0° and 360°, so subtract 360°, if necessary. The result is the ORIENT you should specify on the proposal.

Another way to select the ORIENT, is to place Figure 7.8 on an image of the target, shift and rotate to get the desired alignment, and then simply measure the position angle of the +U3 axis relative to North.

Note that the +V3 axis is quite different from the +U3 axis. They are exactly parallel, but oppositely directed. The +U3 axis is used for specifying orientation (ORIENT) in the proposal, while the +V3 axis is used in the data headers to indicate field orientation. Data header keyword PA_V3 gives the position angle of the +V3 axis on the sky.

We now give two examples of how the POS TARG and ORIENT special requirements might be used. The first example (Figure 7.9) shows placement of a 100″ long jet along the CCD diagonals in PC1 and WF3 (i.e. along the -U3 direction). The coordinates of the nucleus are given on the proposal. Aperture PC1 together with POS TARG +10, +10 are used to place the nucleus near the outer corner of PC1. We want to rotate the WFPC2 field-of-view about the nucleus so the jet is diagonal on PC1 and WF3. We can thus compute the desired orientation as

Figure 7.8: ORIENT Definition, Aperture Positions, and CCD Alignments. “FIX” apertures are in same locations, unless otherwise indicated. Dashed lines show vignetted regions along CCD boundaries. Short lines and “X”s in outer CCD corners indicate directions of bloom and OTA diffraction spikes, respectively. Origin of the (V2, V3) system is at the origin of the plot axes, with V2 and V3 exactly along diagonal lines as marked. POS TARGs are offsets measured from the aperture specified on the proposal (PC1, WF2, WFALL, etc.); their directions are as indicated. CCDs have pixel (1,1) where the four CCDs overlap.

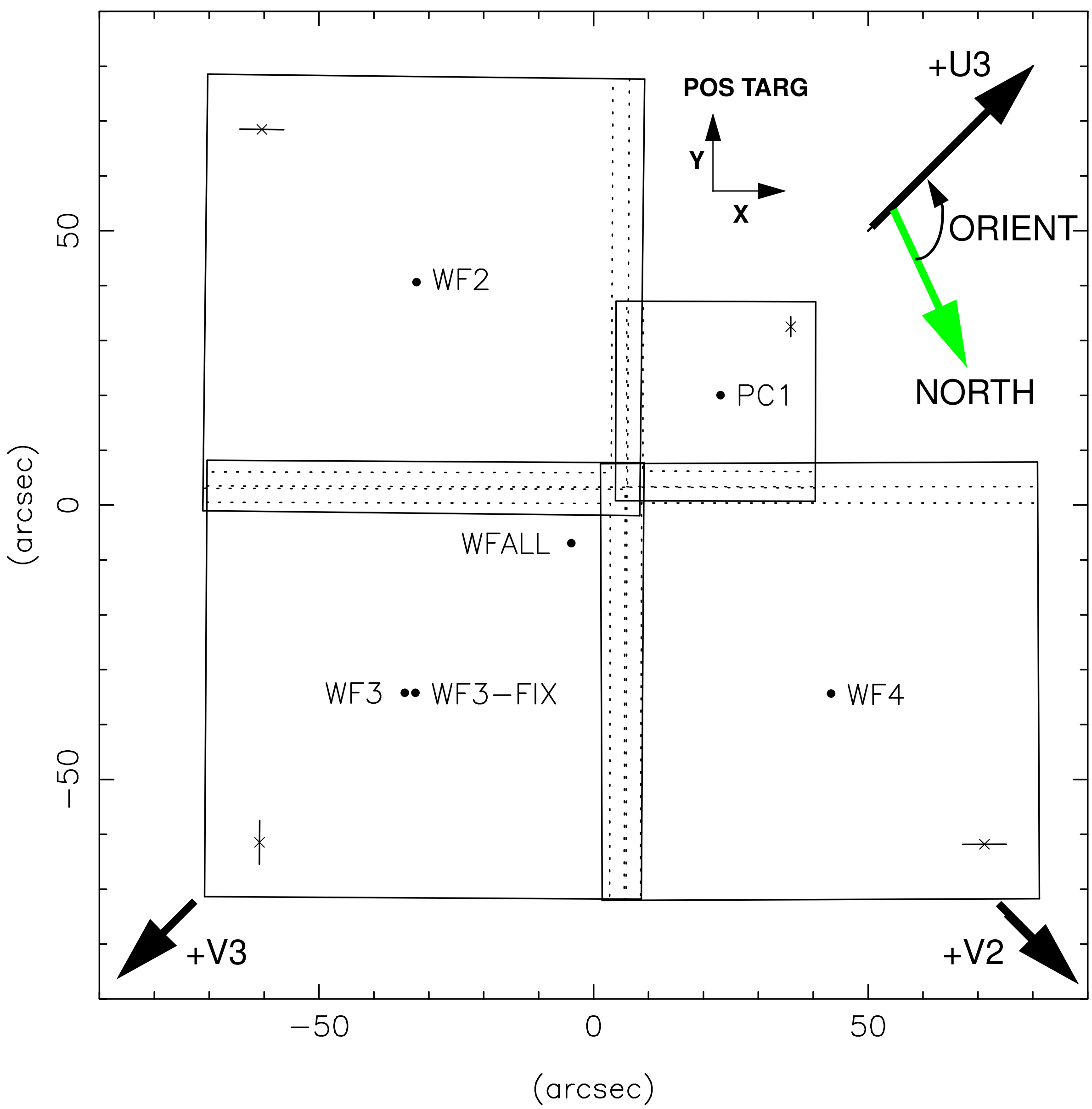

ORIENT is defined as the Position Angle of the +U3 Axis on the Sky.

ORIENT = (source PA on sky)

+ (desired source angle in field-of-view measured CW from +U3 axis)

$= 290^\circ + 180^\circ = 470^\circ - 360^\circ = 110^\circ$

On the Phase II proposal we would allow some range in the angle (to ease scheduling), hence "ORIENT 105D TO 115D" might be specified.

The second example (Figure 7.10) shows placement of a galaxy across WF2 and WF3, with the nucleus on WF3 safely away from the vignetted region. Aperture WF3 together with POS TARG +20, 0 is used to place the nucleus near the outer edge of WF3. We want to rotate the WFPC2 field-of-view about the nucleus so the galaxy major axis is across WF2 and WF3. We can thus compute the desired orientation as

ORIENT = (source PA on sky)

+ (desired source angle in field-of-view measured CW from +U3 axis)

$= 60^\circ + 315^\circ = 375^\circ - 360^\circ = 15^\circ$

On the Phase II proposal we would again allow some range in the angle (to ease scheduling), hence "ORIENT 5D TO 25D" would be specified. Note that "ORIENT 185D TO 205D" is also feasible, and should be indicated in the visit level comments. Note also, that WF3 and WF4 could be used with either "ORIENT 95D TO 115D" or "ORIENT 275D TO 295D"

7.9 Polarization Observations

Polarization observations require three or more images with the polarizing filter spanning a large range of position angles on the sky. For WFPC2, this may be achieved by using different quads of the polarizing filter (each quad being oriented 45° to the others), by rotating the spacecraft though different angles, or by a combination of these methods. Rotating the spacecraft through use of ORIENTs provides the simplest calibration, as a single polaroid can be used for all images. However, in practice, it will be the most difficult method to schedule. For further information see Biretta and Sparks (1995, WFPC2 ISR 95-01).

We note that WFPC2 has significant instrumental polarizations which will make measurements on targets with less than 3% polarization difficult. The pick-off mirror introduces about 6% instrumental polarization. Furthermore, the pair of mirrors in the calibration channel, which is used to generate the polarizer flat fields, introduces ~12% polarization. In principle these effects can be calibrated out, but this has yet to be demonstrated.

The polarizers are most effective in the range from 3000Å to 6500Å; this corresponds roughly to filters in the range F255W to F675W. At shorter wavelengths the transmission decreases sharply, and at longer wavelengths they cease to polarize the incoming light.

Figure 7.9: Example of ORIENT and POS TARG Selection. (A) A jet at PA=290° is observed using PC1 and WF3; the position of the nucleus is used for the target position. (B) The aperture is specified as “PC1” and the nucleus is placed near the outer corner of PC1 using “POS TARG +10,+10.” To place the jet across PC1 and WF3 “ORIENT 105D TO 115D” is specified.

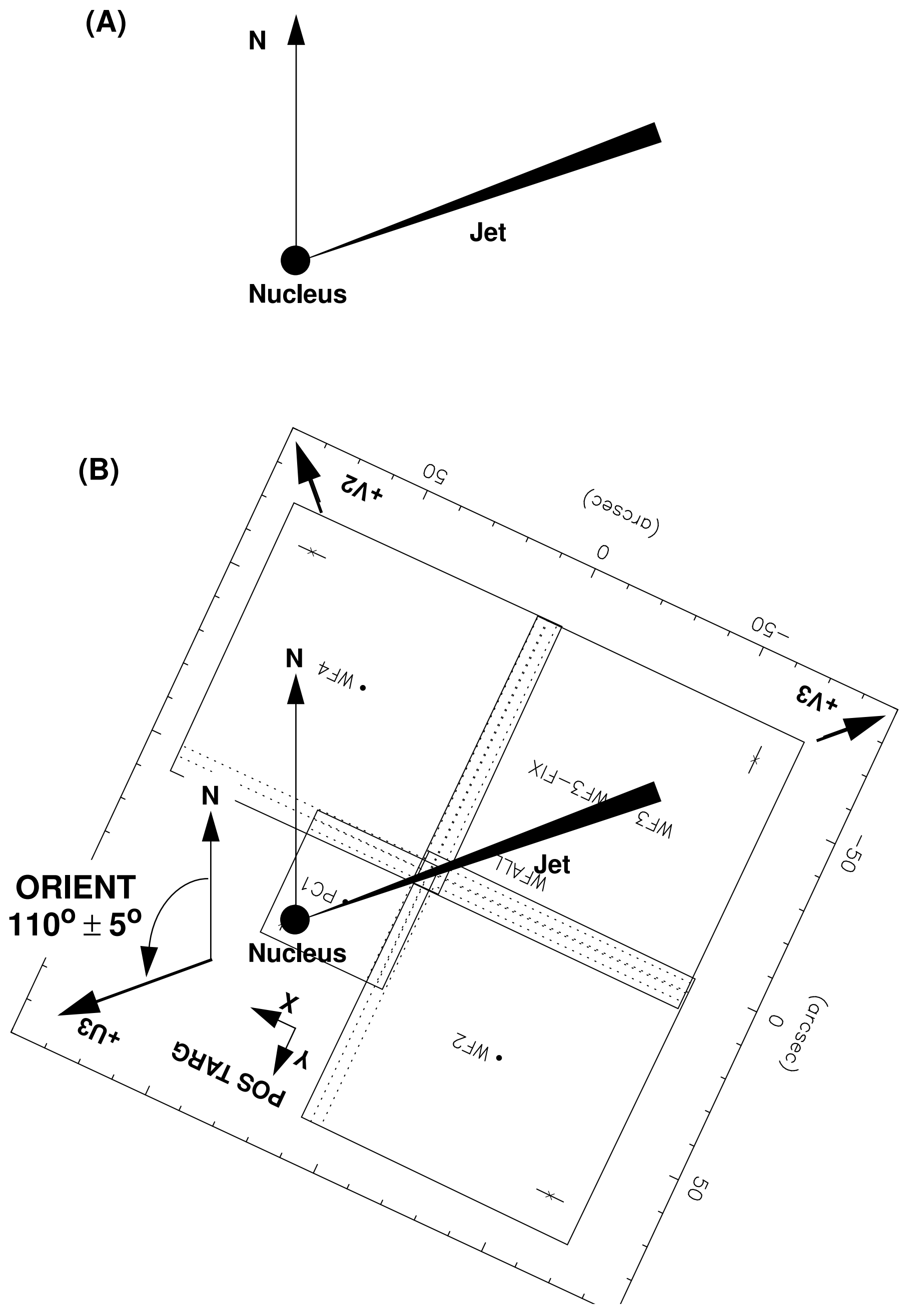

Figure 7.10: Example of ORIENT and POS TARG Selection. (A) A galaxy with major axis at PA=60° is to be placed across WF2 and WF3. (B) The aperture is specified as “WF3” and the nucleus is placed near the outer edge of WF3 using “POS TARG +20,0.” To place major axis across WF2 and WF3 “ORIENT 5D TO 25D” is specified. Note that “ORIENT 185D TO 205D” is also feasible.

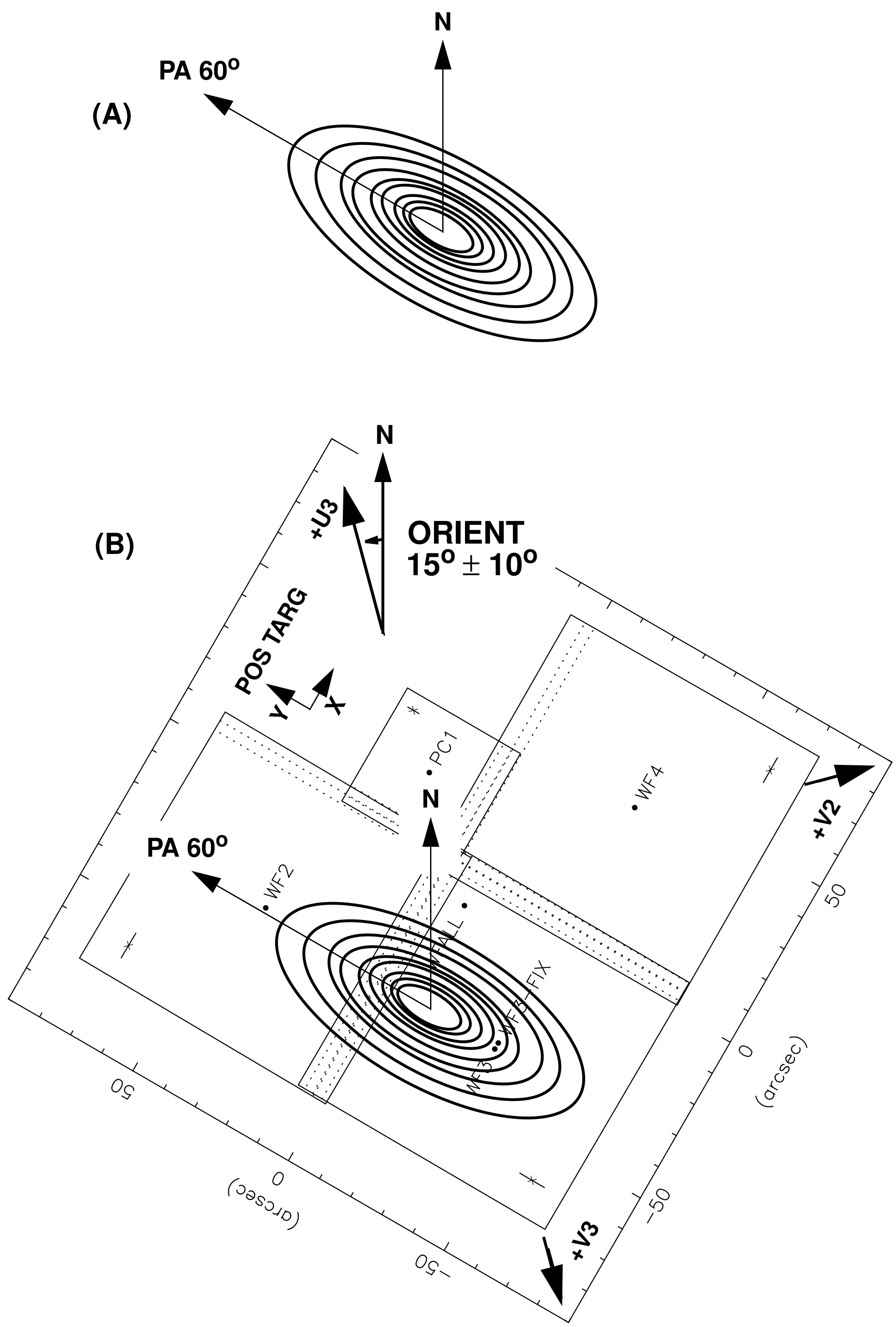

7.10 Observing with Linear Ramp Filters

The Linear Ramp Filters provide a narrow band ($\Delta\lambda/\lambda = 0.013$) imaging capability which is continuously tunable from 3710Å to 9762Å. These are essentially a collection of narrow band interference filters whose central wavelength varies with position on the filter glass. The filter and aperture should be specified as LRF on the Phase II proposal, and the desired central wavelength should also be specified. The HST scheduling software will then select the target position so as to provide the desired wavelength.

Note that it is not possible to choose between PC1 and WFC for the LRFs; one must use whatever CCD is automatically assigned by the scheduling software. If it is necessary to know which CCD will be used, observers can consult Table 3.7 on page 48 or Table 3.8 on page 49, or use the on-line LRF calculator tool on the WFPC2 WWW pages.

It is possible to use POS TARGs with LRF observations; the offsets are made from the default pointing for the specified wavelength. Observers should be mindful that the unvignetted field-of-view has a minimum size of ~10″ in diameter, so that only small POS TARGs (<4″) should be used.

While it is recommended that observers assume a 10″ diameter field-of-view when using the LRFs, larger elongated (e.g. 15″ x 10″) targets can be sometimes be accommodated by placing the target major axis along the direction of the wavelength variation on the filter. This will result in a small reduction in throughput (i.e. small central wavelength offset) at the outer edges of the target. However, placing targets outside the central 10″ of each ramp is strongly discouraged; outside the central 10″ width the light will pass through more than one ramp segment, hence mixing light from different wavelengths, and making the data very difficult to calibrate. (See page 40 for further details on LRFs.)

A common situation is one in which observers desire to make observations through an LRF filter, and then repeat the observation in a standard broad or narrow band filter at the same position on the CCD. The LRF Calculator Tool, available on the WFPC2 WWW pages, will tell observers the aperture (PC1-FIX, WF2-FIX, etc.) and POS TARG for any wavelength setting of the LRFs. Observers merely need to use this same aperture and POS TARG for the exposure through the other filter. If it is necessary to calculate the POS TARG manually, one can do this using the information in Table 3.7, Table 3.8, Table 3.14, and Figure 7.8. For example an LRF observation at 5034Å would be made on WF2 at pixel (673.4, 235.7) (from interpolation by wavelength between X1 and X2, and between Y1 and Y2 in Table 3.7). These offsets are referred to the WF2-FIX aperture which is located (Table 3.14) at pixel (423.5,414). From Figure 7.8 we can deduce that pixel X direction is parallel to POS TARG "+Y" on WF2, and that pixel Y direction runs in the POS TARG "-X" direction. Using the pixel scale in section 5.10, "Optical Distortion", on page 103, we have

POS TARG "X" = -0.09961 (235.7-414) = 17.76″, and

POS TARG "Y" = 0.09961 (673.4-423.5) = 24.89″, hence POS TARG=+17.76,+24.89 would be requested for the non-LRF exposure.

7.11 Emission Line Observations of Galaxy Nuclei

Saturation is a common problem for narrow band filter images of galaxy nuclei. Often the surface brightness of the emission line is estimated from ground-based images with 1″ resolution; sometimes line fluxes are quoted for apertures several arcseconds in radius. However, at HST resolution, much of this flux may occur in a single unresolved spot at the galaxy nucleus, thus leading to saturated images. Observers should be cautious and consider this possibility when estimating exposure times.

CHAPTER 8: Calibration and Data Reduction

In This Chapter...

8.1 Calibration Observations and Reference Data

Standard calibration observations are obtained and maintained in the HST archive at the STScI, and can be obtained by external users using StarView. This includes those flat field, dark, and bias frames needed to operate the Post Observation Data Processing System (PODPS; sometimes called OPUS, and usually just called the "pipeline"), photometric calibration derived from standard star observations and the measured filter profiles, and derived determinations of the plate scale, distortion, and so on. The first set of these calibrations was provided to the STScI by the WFPC2 IDT from the Servicing Mission Observatory Verification (SMOV) and System Level Thermal Vacuum (SLTV) testing periods, and has been maintained and updated thereafter by the STScI with assistance from the IDT as part of the long term calibration program. For measurements requiring more precise calibrations, special calibration observations may need to be obtained as part of the observing proposal. Please consult the STScI WFPC2 Instrument Scientists for guidance if the routine calibration appears unlikely to support the requirements of a proposed observation. Individual GO programs requiring special calibrations must directly request these observations as part of their Phase I proposal.

A database of laboratory characterizations of optical components, CCD sensors, filters, and the flat field channel has been collected to support the instrument calibration. On-orbit pointed calibrations require large HST resources, taking time that could otherwise be used for direct scientific observations. They can also be unsatisfactory due to the limitations of the available astronomical reference sources. For WFPC2, the inherent stability and uniformity of the CCD sensors, the well calibrated filters, the internal flat field calibration system, and an archive populated with flat field images obtained in SLTV prior to launch improve the scientific data analysis and productivity. Hence the need for on-orbit calibrations has been minimized.

8.2 Flat Fields

The process of correcting for the effect of the variation in the sensitivity of the WFPC2 with field position is usually known as flat-fielding, or flattening. A "flat field" (an exposure of a spatially uniform source) needs to be observed through the telescope and desired filter. Real flat fields are always external; however, the WFPC2 has an internal calibration channel which produces a reasonably flat illumination pattern down to about 1800Å. This channel is used to monitor and correct for changes in the flat fields. The instrument flat field is also coarsely monitored using the internal flat channel, using exposures called INTFLATS. Flat fields in narrow bandpass filters are obtained using the sunlit Earth (Target = EARTH-CALIB) as part of routine calibration in order to provide an absolute reference for the internal calibrations (and remove the low frequency effects of variations in the OTA illumination pattern).

The Earth is an imperfect flat field target because it is too bright for the WFPC2 in the broad-band green and red filters. The rapid motion of the HST also creates streaks across the flat field images. The removal of the streaks requires the combination of multiple Earth observations with the streaks at different angles on the CCDs. An extensive discussion of the generation of Earth flat fields is available in Chapter 6 of the WF/PC-1 IDT OV/SV Report.

The flat field calibration system works by imaging an illuminated diffuser plate onto the WFPC2 exit pupil (relay secondary) by means of an MgF_2 lens. Two lamps provide optical and FUV illumination, providing a flat field which resembles the input beam from the OTA between 1600Å and 10000Å. During SLTV, flat fields were obtained using both the flat field calibration module and the WFPC2 optical stimulus (HST simulator), to generate a database of ratio images which link the internal flats to external flats.

The external stimulus flats have been updated by comparison against on-orbit streak flats, obtained for a small subset of narrow band filters (F375N, F502N and F953N). These were obtained during the initial in-flight calibration of the instrument, to effectively calibrate low frequencies in the internal flat-fielding source. Eventually, sky flats for the broad photometric filters will be made by combining many frames.

Flat fields have been obtained for all filters by combining information from SLTV test flats (which are good for all but the lowest spatial frequencies), and Earth flats in a limited number of filters (which fix the low frequency terms). The calibration channel monitors for time dependent changes in the flat fields, and none have been seen to date in the visible filters. Some redundancy is provided by the internal flat channel, but it does not form a part of the baseline calibration.

During early 1996 flat fields for many filters were updated using an improved illumination pattern derived from large numbers of streak flats. Corrections were typically ≤1%, though the outermost corner of WF2 showed a 7% correction. The improved flats compared very favorably with sky flats.

Note that the flat fields presently used in the pipeline are based on gain 14 data. The gain ratios are not constant from chip to chip, and therefore a small correction to photometric results derived from gain 7 data should be applied (see Table 4.3 on page 82). (See Biretta 1995 for further discussion of WFPC2 flat fields; also see the *HST Data Handbook*.)

8.3 Dark Frames

Dark frames are long exposures that are taken with no light incident on the CCDs. They are used to detect CCD counts (the dark current) caused by thermal generation (at the interfaces between the silicon and oxide layers), and the rate of charged particle and secondary radiation events. Estimated dark current and cosmic ray event rates are given in section 4.8, “Dark Backgrounds”, on page 71 and section 4.9, “Cosmic Rays”, on page 75, respectively. Observers are cautioned that the calibration provided by the pipeline may not use the most up-to-date dark frames (partly because constructing these may involve data taken after the observation). This matters because new hot pixels are being generated all the time. Data to construct improved super-darks is available in the archive with at least 5 long dark exposures being taken weekly.

8.4 Bias Frames

Bias frames are readouts of the CCDs without an exposure (so the dark current is negligible). They are used to measure the DC offset built into the signal chain which ensures that the ADC input is above zero. They fix the constant that is subtracted from the raw data prior to dark subtraction and flat fielding in Routine Science Data Processing (RSDP).

8.5 Data Reduction and Data Products

The routine processing of WFPC2 science data consists of the pipeline functions described below. The resulting images will be available on magnetic tape in FITS format, and as greyscale printouts. The reformatted raw data will also be available, along with the relevant calibration data. The *STSDAS Calibration Guide* should be consulted for a more complete description than the summary presented here.

The following data are supplied to observers on FITS tapes:

- Edited Image and DQF (uncalibrated): `d0h`,`.q0h`
- Standard Header Packet: `.shh`
- Extracted Engineering Data and DQF: `.x0h`,`.q1h`
- Trailer File (ASCII file): `.trl`
- Calibrated Image and DQF: `.c0h`,`.c1h`

In addition, a histogram file used for monitoring of the signal chain (`.c2h` file), and a calibration file which gives the throughput curve used in populating the photometric keywords (`.c3t` file) are included.

Further data reduction and analysis can be performed under the STScI's science data analysis software system (STSDAS). Standard routines are available, operating under IRAF, for the analysis of data for image photometry, spectral analysis, astrometry, and the generation of the calibration data files.

8.6 Pipeline Processing

The pipeline processing of WFPC2 data sets reformats the telemetry received from HST into group FITS format images, generates headers containing a large number of keywords taken from both the HST and WFPC2 telemetry streams, in addition to various STScI ground system databases, and applies the calibration described below. This calibration is done with a module known as "CALWP2" which is written in the IRAF SPP language and is available, in identical form, to users of the STSDAS system. Therefore, off-line recalibration of observations is fairly easy, and will use the same program as the PODPS system. Documentation is available in the *HST Data Handbook*, and the *STSDAS User's Guide*.

CALWP2 performs the following operations if required by the observation:

- ADC correction
- Bias level removal
- Bias image subtraction (depending on the gain channel in use)
- Dark image scaling and subtraction
- Shutter shading correction

- Flat field image correction
- Population of various photometric calibration keywords

In addition, the following conditions are flagged in the Data Quality File (DQF):

- Transmission failures and other possible failures
- Known bad pixels (e.g. blocked columns)
- Pixels at or above the maximum A/D converter level (i.e. saturated)
- Bad pixels in reference images

8.7 Fluxes and Standard Magnitudes

The pipeline calibrated data are not flux calibrated and the data are in units of Data Numbers (DN). However a flux calibration is implicit in the header. To get flux density, multiply DN by the value of the keyword PHOTFLAM in the calibrated (`.c0h`) science header file, and divide by the value of the keyword EXPTIME.

The magnitude of an object can be determined using the photometric zero-point keyword PHOTZPT as .

$$m = -2.5\log_{10}\left(PHOTFLAM \times \frac{DN}{EXPTIME}\right) + PHOTZPT$$

where m is in the STMAG system which is based on a spectrum with constant flux per unit wavelength set to roughly match the Johnson system at V. The more conventional systems are based on Vega's spectrum. Table 8.1 was generated using SYNPHOT to provide rough conversions to the Johnson UBVRI and Cousins RI systems. Typical uncertainties are 5%, and probably much worse for the U filter. The correction depends on the spectrum of the object, hence the table was generated using a wide range of Bruzual models.

For example, to convert to the Cousins I band for an object on WF4, get PHOTZPT=-21.1 and PHOTFLAM=2.6044 x 10^{-18} from the header. Then convert from WFPC2 counts to magnitudes in Cousins I using:

$$I_c = -2.5\log_{10}\left(2.6044 \times 10^{-18}\frac{DN}{EXPTIME}\right) - 21.2 - 1.21$$

Note that the Cousins I filter is much closer to the F814W filter than Johnson I, as shown by the nearly constant correction as a function of spectral type (i.e. color term).

Table 8.1: Conversion from STMAG to Johnson UBVRI and Cousins RI.

	U-F336W	B-F439W	V-F555W	R_J-F675W	I_J-F814W	R_C-F675W	I_C-F814W
O5V	0.53	0.67	0.05	-0.67	-1.11	-0.71	-1.22
B0V	0.46	0.66	0.05	-0.67	-1.13	-0.70	-1.22
A0V	-0.08	0.67	0.02	-0.68	-1.22	-0.67	-1.21
F2V	-0.03	0.62	-0.00	-0.69	-1.28	-0.63	-1.22
G0V	-0.02	0.58	-0.01	-0.70	-1.31	-0.60	-1.23
K0V	-0.10	0.53	-0.01	-0.69	-1.32	-0.58	-1.23
M0V	-0.04	0.43	-0.00	-0.78	-1.48	-0.54	-1.22
M6V	0.05	0.29	-0.03	-1.05	-1.67	-0.56	-1.21

This procedure will provide typical accuracies of about 0.05 mag (worse in the UV). More accurate photometry will require a variety of corrections (e.g., CTE effect, contamination and red leaks for the UV filters, variable gains on different chips, color terms, geometric distortions) which are discussed in detail in Holtzman et al. (P.A.S.P., 1995b).

8.8 Color Transformations of Primary Photometric Filters

The WFPC2 UBVRI system is fairly close as regards effective wavelengths to the Johnson UBVRI system, but cross-calibration is necessary to convert to Johnson magnitudes. See the IDT OV/SV Report and Harris et al., A.J. 101, 677 (1991) for examples in the case of WF/PC-1. Figures 8.1 through 8.5 show the results of regression fits between these two systems on the main sequence stars in the Bruzual, Persson, Gunn, Stryker atlas that is installed in the calibration database system (CDBS).

These fits should be used with caution for quantitative work. The zero-points in all cases are defined so that Vega's spectrum integrated over the bandpass is exactly magnitude zero (VEGAMAG in XCAL). The zero-points of the canonical Johnson-Cousins system differ from this by up to 0.02 magnitudes. The zero-points thus defined for the HST filters do not coincide with the STMAG definition used in the previous section. In addition, the ground based filter curves used, which are taken from Bessel (P.A.S.P. 102, 1181), give a good approximation to the standard Johnson-Cousins system, but are not as accurate as taking Landolt's curves and applying his color corrections to transform to the standard system. The latter procedure was used to derive the transformations

Figure 8.1: F336W-F439W against Johnson U-B for the BPGS atlas of MS dwarf spectra. The change in slope in the transformation for U-B greater than about 0.1 is due to red leak in the F336W filter. For hotter stars, the transformation is quite linear.

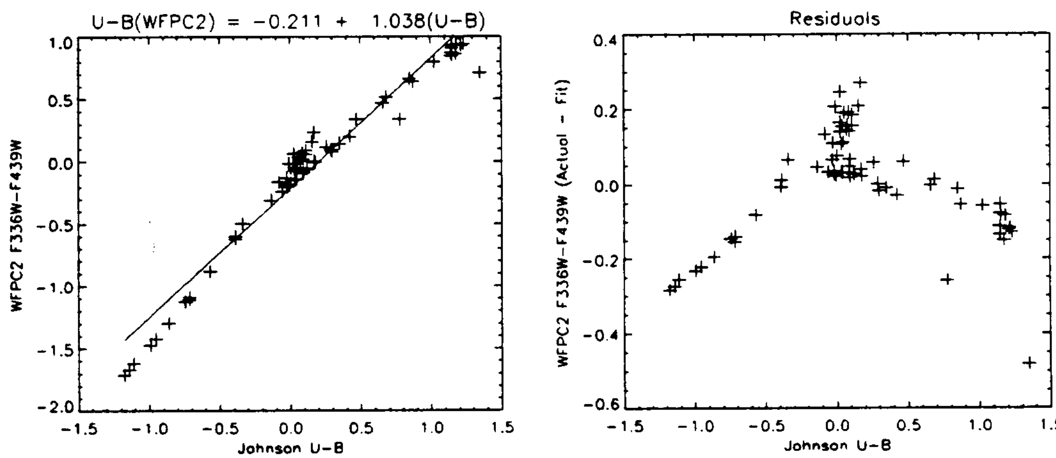

Figure 8.2: F439W-F555W against Johnson B-V. The residuals from the best linear fit are quite similar to those that apply if F569W (instead of the preferred F555W) is chosen for a WFPC2 passband.

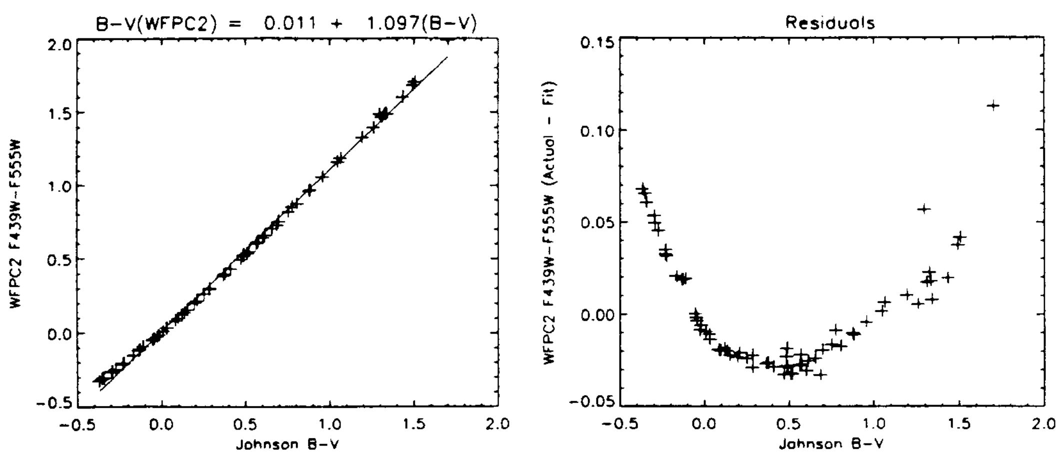

Figure 8.3: F555W-F814W against Johnson V-I_C. The residuals from the best linear fit are generally very small. This particular color combination is widely used.

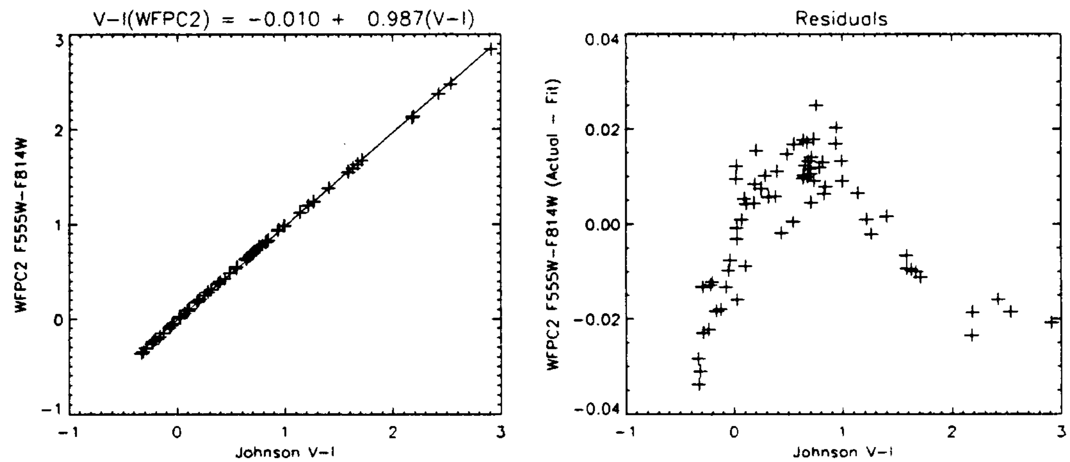

Figure 8.4: F555W-F675W against Johnson V-R_C. The residuals from the best linear fit are somewhat larger for blue stars than those that apply if F569W is chosen.

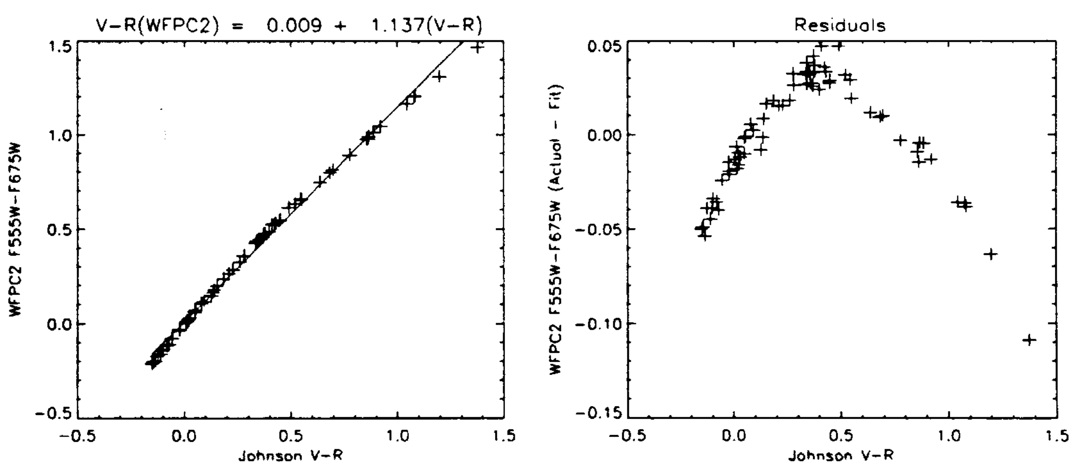

given in Holtzman et al. (P.A.S.P., 1995b), which also discusses the changes in the transformations that result from source spectrum variations (such as metallicity and gravity effects).

Figure 8.5: F675W-F814W against Cousins R_C-I_C. The residuals from the best linear fit are similar to those that apply if F791W is chosen for a WFPC2 I passband. For spectral type M8V and later (not shown) the transformation will not work as well.

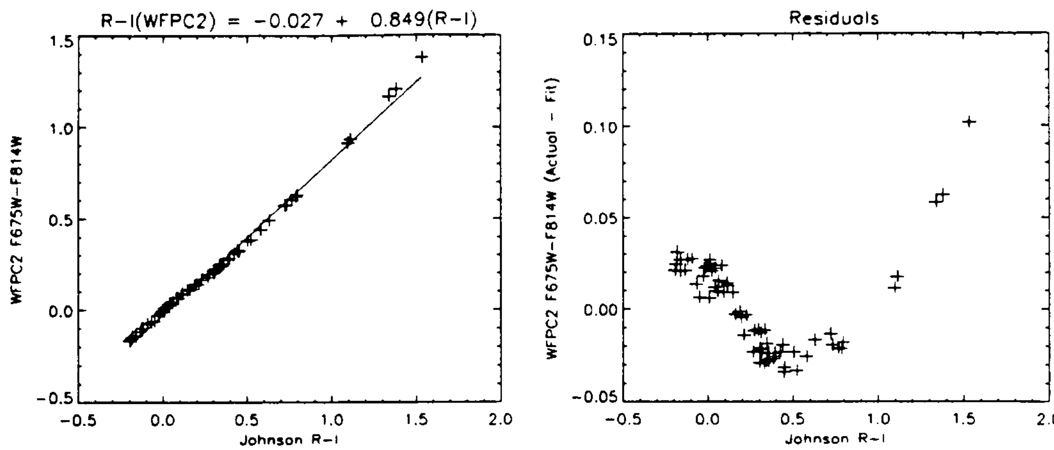

8.9 Cycle 5 Calibration Plan

A summary of the Cycle 5 calibration plan follows as a general guide to the calibration and monitoring program in place for WFPC2. The full proposals are available through STScI's proposal status web page.

`http://presto.stsci.edu/public/propinfo.html`

The data that the calibration and monitoring program produces has no proprietary period and is available through the HST archive. In each case the proposal ID is given followed by its title, purpose, description, accuracy goals and products produced.

Calibration information obtained to date consists primarily of the System Level Thermal Vacuum (SLTV) tests, the initial on-orbit tests conducted in SMOV, and the Cycle 4 calibration. These tests have shown that the instrument is stable with some important exceptions and have provided an initial calibration sufficient for routine processing of most data.

The Cycle 5 calibration is designed to enable users to maximize the scientific usefulness of their data, while at the same time minimizing the use of spacecraft time. This is done by designing efficient proposals that:

- A) Improve the existing calibration - in particular towards the goal of 1% absolute photometric accuracy.
- B) Assess the accuracy of the existing and new calibrations.
- C) Recalibrate important known time variable features of the instrument.
- D) Calibrate some important instrumental effects that are not well understood.
- E) Monitor the instrument and telescope to ensure that no new problems or variability in their performance are missed.
- F) Maintain the instrument in a healthy state and ensure that in the event of partial instrumental failures, the calibration can be maintained when possible.

The calibration of the instrument must be seen in a larger context than simply preparing reference files for a pipeline reduction and assessing the errors in them. Several calibrations (such as geometric distortion, CTE correction, PSF calibration, chip-to-chip alignments, polarization calibration) are very important to some observers. Yet they are not included in the pipeline. Other things frequently need to be done to the data after it is ADC, bias, dark, and flat field corrected, with a photometric calibration included in the header. These other calibrations are made available to users through this Instrument Handbook, journal publications, instrument science reports, and postings linked to the Institute's WFPC2 WWW home page. The address is:

`http://www.stsci.edu/ftp/instrument_news/WFPC2/wfpc2_top.html`

A list of the most important calibrations consists of the following items:

1. Photometric zero-point. This involves converting DN values to flux units.
2. Photometric transformations. This involves converting DN values to magnitudes in standard systems. Two separate photometric calibrations can be used for this, a direct approach and a synthetic approach.
3. Photometric temporal variations. This is particularly important in the UV where significant variability is seen.
4. Photometric spatial variation (flat fields and CTE).
5. Dark current. This includes its time variability (hot pixels).
6. Bias.
7. Analog-to-Digital converter errors.
8. PSF. This is crucial for PSF fitting photometry, PSF subtraction, PSF modeling, and deconvolution efforts. Because PSF subtraction of very saturated sources is specialized to a few very diverse programs, PSF calibration in the image halo (beyond about 0.5 arcsecond) is not supported and must be requested with the program as a special calibration.
9. Polarization calibration.
10. Geometric calibration.

The program consists of 15 proposals which use a total of 63 orbits of spacecraft time (to be compared to a total of about 1550 orbits of approved GO time). The proposal summaries and their associated RPS2 files largely speak for themselves. Table 8.2 lists all of the proposal numbers, titles, the schedule for the calibration execution, an indication of whether the output forms part of the pipeline data reduction (CDBS) or provides other information, usually documented in Instrument Science Reports (ISR), the approximate calibration accuracy expected (see the summary forms for the interpretation of these numbers, because they are almost meaningless without a context), and the primary areas from the above 10 calibration types they address and in what ways (A-F from the above list). Therefore, if you are interested in a particular calibration, look for its number in the last column of the table, and then refer to the subsequent proposal summaries for more details.

Table 8.2: Summary of Cycle 5 Calibration Plans.

ID	Proposal Title	Schedule	Results	Accuracy	External Time (orbits)	Notes[a]
6179	Photomet. Zero.	Late 95	CDBS	1%	8	1ABE, 2AB
6182	Photomet. Trans.	9/95, 3/96	CDBS	2%	6	2ABE
6183	Decontamination	1x per 4 wks.	ISR	N/A	0	F
6184	Photometric Mon.	2x per 4 weeks	ISR	1%	24	3E
6186	UV Throughput	Early in Cyc. 5	CDBS	10%	6	1AB, 3C
6187	Earth Flats	Continuous	CDBS	1%	0	4ABE
6188	Darks	Weekly	CDBS	6%	0	5ABC
6189	Visflat Monitor	2x per 4 weeks	ISR	0.6%	0	4E
6190	Internal Flats	Early Cyc. 5	CDBS	0.6%	0	4F,7E
6191	UV flats	2x in Cyc. 5	ISR	2%	0	4ABE
6192	CTE Calibration	Early Cyc. 5	TIPS	<1%	4	4ABD
6193	PSF	CTE+2m	TIM	10%	5	8ABD
6194	Polarizers+Ramps	TBD	CDBS	3%+2%	8	9DE, 1AB
6195	Flat field Check	Late 95	CDBS	1%	2	4B
6250	Internal Monitor	2x per week	ISR	N/A	0	5,6,10F
	TOTALS				63	

a. Letters and numbers are keyed to lists in text.

6179: Photometric Zero-point

- **Purpose**: Set synthetic zero points of all WFPC2 filters.

- **Description**: GRW+70D5824 is observed through all filters not in the photometric calibration monitors and longward of F336W (inclusive). It is observed in both PC1 and WF3. This data-set is directly comparable to the corresponding results for Cycle 4 (program 5572). Because of possible errors in the spectrophotometry for this target, and in order to check synthetic color transformations over a reasonably wide range of colors, the observations are repeated with 3 red standards, and 2 other blue standards in WF3 only. This time, most of the 18 broad and medium bandpass filters longward of F336W are included (restricted to 1 orbit/target). If CTE calibration fails, this proposal may need to be run with preflash (and take more time or do less targets). This proposal is needed by all GO proposals that want to do quantitative photometry at the few percent level.
- **Accuracy**: Overall discrepancies between the synthetic photometric products and the results of this test should be reduced to 1% rms. Part of the point of the test is to measure this accuracy, which will largely depend on the accuracy of the spectrophotometric calibration sources.
- **Products**: After pipeline processing, each image will be reduced by aperture photometry to measure the throughput of each filter. These numbers can be directly compared to SYNPHOT predictions. Systematic differences will be corrected in the throughput database by tweaking the filter normalizations (already done for the primary target in Cycle 4), overall system response (which is quite uncertain particularly longward of 8000Å), and finally bandpass shapes. Residual differences will give an idea of the intrinsic accuracy of the calibration.

6182: Photometric Transformation

- **Purpose**: Update photometric transformations to Johnson-Cousins system.
- **Description**: A photometric standard star field in ω Cen is observed twice, once at the September 1994 orientation and once rotated by 180˚ degrees (to correct to first order for residual CTE effects). All broad and medium bandpass filters are used. Based on Cycle 4 program 5663, this proposal also gives a check on the long term full field photometric stability of the instrument.
- **Accuracy**: Independent of the synthetic photometry results this test gives direct transformations to the Johnson-Cousins system for a wide range of source colors (but excluding very blue stars). These transformations should be accurate to 2%. The stability of these transformations will be measured to the sub-percent level (because then errors in the ground based photometry do not enter significantly).
- **Products**: A comparison with the corresponding Cycle 4 monitor (which ran monthly) will verify the photometric stability of the camera. Direct transformations to the Johnson-Cousins photometry system can be derived for all filters. The observations also provide a check of the astrometric and PSF stability of the instrument over its full field of view.

6183: Decontamination

- **Purpose**: Remove UV blocking contaminants from CCD windows.
- **Description**: A sequence of observations is defined that is run twice - once before and once after a DECON when the CCDs are heated to +20˚C for 6 hours. The sequence consists of 2 bias frames at each gain setting, 5 1800 second darks, 2 INTFLATS through F555W at each gain, and two K-spot images. The observations are arranged so that the first sequence occurs about 33 hours before the DECON, and the second follows it by 12 hours. The proposal is run every 4 weeks. This is based on Cycle 4 program 5568 with bias frames added.
- **Accuracy**: This proposal is mainly designed to test aliveness, and monitor the instrument to ensure that no untoward effects from the DECON have occurred. It will identify all hot pixels that are annealed by the DECON.
- **Products**: The data is examined and checked for anomalies. The dark frames are processed to yield plots showing the growth and annealing of hot pixels.

6184: Photometric Monitor

- **Purpose**: Monthly external check of instrumental stability.
- **Description**: GRW+70D5824 is observed through F170W in all four chips. It is then observed in one chip for filters F160BW, F185W, F218W, F255W, F300W, F336W, F439W, F555W, F675W, F814W to fill out the orbit. The chip chosen is changed each month, so each chip is used three times during the year. One extra F555W exposure is taken through the PC to allow for focus monitoring. The proposal is run once before and once after each monthly decontamination, with the same chip selected. Based on Cycle 4 programs 5629 + 6143 + (5563) + 5564.
- **Accuracy**: Overall discrepancies between the results of this test should be less than 1% rms. The point of the test is to measure this variation.
- **Products**: After pipeline processing, each image will be reduced by aperture photometry to measure the throughput of the filters. These numbers can be directly compared to results for previous months. This will allow the long term performance of the instrument to be checked for changes, and verify that the decontaminations are satisfactory. This proposal will be run every 4 weeks in association with the DECON. Results reported in Baggett et al., WFPC2 ISR 96-02 and Whitmore, et al., WFPC2 ISR 96-04

6186: UV Throughput

- **Purpose**: Update SYNPHOT database for UV throughput.
- **Description**: GRW+70D5824 is observed shortly before and after a DECON through all of the UV filters in each chip and through F160BW crossed with F130LP, F185LP and F165LP (where applicable) to determine the wavelength dependence of the throughput across the bandpass (hence

color terms). Based on no particular Cycle 4 program, this program is designed to characterize better the spectral response curve in the UV, and the spectral shape introduced by the contamination.

- **Accuracy**: Overall discrepancies between the updated synthetic photometric products and the results of this test should be 1-2% rms. This does not mean that the UV throughput will be known to this accuracy, primarily because of uncertainties in the flux calibration of the standard used (5%), uncertainties in the UV flat fields (maybe 3% near the chip center), and time dependent contamination corrections (3% error), and uncertainties in the CTE correction (2%). The derived UV absolute photometric accuracy at the center of the chips should therefore be about 10%.
- **Products**: After pipeline processing, each image will be reduced by aperture photometry. The throughput curves and their normalizations can be updated by trial and error.

6187: Earth Flats

- **Purpose**: Generate flat fields.
- **Description**: 4 sets of 200 Earth streak-flats are taken to construct high quality narrow-band flat fields with the filters F375N, F502N, F656N, and F953N. Of these 200 perhaps 50 will be at a suitable exposure level for de-streaking. The resulting Earth superflats map the OTA illumination pattern, and will be combined with SLTV data (and calibration channel data in case of variation) for the WFPC2 filter set, to generate a set of superflats capable of removing both the OTA illumination and pixel-to-pixel variations in the flat field. In addition, more limited observations are made in F160BW and the broad bandpass photometric filters.

  The Cycle 4 plan is being largely repeated except: (1) UV filters are dropped because the measurement is generally only of the red leak. (2) F160BW is retained in order to check for developing pinholes. (3) Crossed filters used as neutral densities are eliminated (illumination pattern is wrong). (4) An attempt will be made to schedule some broad bandpass measurements on the dark Earth. This is based on Cycle 4 programs 5570 + 5571 + 6142.
- **Accuracy**: Overall accuracy of the flats derived from this test and the corresponding Cycle 4 observations should be below 1% RMS. Discrepancies between the results of this test and those from Cycle 4 should be 1% RMS. Differences between the two datasets analyzed separately will measure the flat field variability to this level. This data, together with the flat field check proposal should enable similar accuracy in the broad bandpass flats.
- **Products**: This proposal provides medium and narrow bandpass streak flats which can be combined with the high frequency information in the TV flats to yield accurate flat fields. The ratio of the TV and derived flats provides a correction that can also be applied to the TV broad bandpass data. We may also get broad band flat fields directly for comparison from the sky or from this proposal's exposures on the Earth's shadow.

6188: Darks

- **Purpose**: Provide dark frames for pipeline reduction, and hot pixel lists.
- **Description**: 5 dark frames are taken every week to provide ongoing calibration of the CCD dark current rate and to monitor the characteristics and the evolution of hot pixels. Over an extended period, these data provide a monitor of radiation damage to the CCDs. The dark frames will be obtained with the CLOCKS=OFF. In addition, 4 darks are taken per month with CLOCKS=ON (although there is no effect such as amplifier glow expected from running the serial register for these CCDs).

  Changes from the Cycle 4 program 5562 are that each group of 5 darks is constrained to be taken within a 2-day period, in order to simplify the data analysis (because fewer new hot pixels are involved), and the CLOCKS=ON exposures have been added.
- **Accuracy**: The accuracy of the super-dark computed from these data depends on the number of frames combined. The present practice is to combine them in groups of 10 frames for pipeline super-darks. This gives a median signal-to-noise of 16 and higher signal-to-noise on hotter pixels than the median (with the somewhat shaky assumption that the dark noise is Poisson). This means that the residual systematic error after super-dark subtraction on an 1800-second exposure is about 3 electrons - much less than the read noise. In principle, this residual can be further reduced to 0.4 electrons if a super-dark is generated from all of the dark frames, with suitable masking based on hot pixel lists.
- **Products**: The data is grouped into sets of 10 frames every two weeks. These are combined into super-darks for use in the pipeline. In addition, hot pixel lists can be generated with a time resolution of one week.

6189: VISFLAT Monitor

- **Purpose**: Monitor internal flat fields of instrument.
- **Description**: All use of the VISFLAT channel is concentrated in this proposal. It is based on Cycle 4 programs 5568 and 5655. The program takes one complete set of exposures using the visible calibration channel lamp (VISFLATS) at the start of the cycle through all visible filters. Monthly, VISFLATS will be obtained with the photometric filter set (F336W, F439W, F555W, F675W, and F814W) both before and after the DECON. A monthly VISFLAT exposure with the Wood's filter, F160BW, allows its visible transmission to be monitored. Two monthly VISFLAT exposures obtained through the LRF (FR533N), one at each gain, provide a monitor of the ADC's performance. The VISFLAT exposures should be packed together to optimize use of each lamp-on cycle.
- **Accuracy**: The internal flats, when well exposed, are each accurate to 0.6% in terms of the pixel-to-pixel (high frequency) variations in the CCDs. Thus, high frequency flat field stability can be verified to 1%. When the results from several filters are combined it will be possible to check that the CCDs are indeed relatively stable to much better than 1%.

- **Products**: The complete filter-set sweep will be compared to the corresponding Cycle 4 data-set primarily to verify that none of the filters are developing problems. Ratios of these flats will primarily indicate the stability of the channel itself, unless there are strong variations from filter to filter. Unless time dependence in the filters is seen, it is likely that flat fields for pipeline calibration will continue to be made by combining Earth-flat, SLTV-flats, and eventually sky-flats.

  The bi-monthly photometric filter-set observations will be used to monitor WFPC2's flat field response and to build a high S/N flat field database (primarily useful in tracking any changes in the pixel-to-pixel response of the instrument and any possible long term contamination induced changes). Histograms generated from the ramp filter flats will be used to trace the ADC transfer curve. F160BW can be checked monthly for pinholes. Results reported in Stiavelli and Baggett, WFPC2 ISR 96-01.

6190: Internal Flats

- **Purpose**: Provide backup database of INTFLATS, in case VISFLAT channel fails.
- **Description**: Based on Cycle 4 program 5568. A complete set of illuminated shutter blade flats (INTFLATS) is taken close to the complete set of VISFLATS. Each filter is exposed on each shutter blade (A or B) at each gain setting (7 or 15). Thus, there are 4 exposures per filter which should be uninterruptedly sequenced as (A7, A15, B15, B7). There is a possible concern on thermal control, where an out-of-limit condition was almost reached when 5568 was run. This will be avoided by spacing the exposures suitably.
- **Accuracy**: The signal-to-noise per pixel is similar to that obtained in the VISFLAT program (0.6%) but there are much larger spatial and wavelength variations in the illumination pattern. As a result, this data-set will not form any part of the pipeline calibration. This baseline is necessary in case the VISFLAT channel fails, and there are temporal variations in the camera flat fields at the 1% level. The test does give a good measurement of the gain ratios and their stability, which should be accurate to much better than 1%, when all of the data is analyzed.
- **Products**: INTFLAT/VISFLAT ratios can be generated if there is a failure in the calibration channel. Gain ratios and stability will be assessed. Results reported in Stiavelli and Baggett, WFPC2 ISR 96-01.

6191: UV Flats

- **Purpose**: Use UV calibration channel to monitor long term internal UV stability.
- **Description**: UV flat fields will be obtained with the calibration channel's ultraviolet lamp (UVFLAT) using the limited FUV filter set (F122M, F170W, F160BW, F185W, and F336W) twice in the cycle immediately after a DECON. The UV lamp is degrading with use, so its use must be minimized. The UV flats will be used to monitor the FUV flat field stability

and the stability of the Wood's filter, F160BW, by using F170W as a reference. The VISFLAT/UVFLAT ratio from the F336W filter will provide a diagnostic of the UV flat field stability, and tie the UVFLAT and VISFLAT flat field patterns together. This program represents the entire use of the UV lamp in Cycle 5. This proposal is based on the Cycle 4 program 5568, but with two extra filters (F122M and F185W).

- **Accuracy**: Should verify stability of the UV filters and flat field to 2%. The overall flatfield response is not measured because the lamp output is not uniform, and temporal variations in throughput are not measured because the lamp output varies.
- **Products**: Ratio images with the corresponding data-set from Cycle 4 and future cycles will verify the UV flat field stability.

6192: CTE Calibration

- **Purpose**: Calibrate CTE effect for a range of star brightness and background.
- **Description**: The crowded ω Cen field is observed for 40 seconds through F555W with gain 7 and preflashes of 0, 5, 10, 20, 40, 80 and 160 electrons. As a gain check and calibration, it is observed at the same orientation with gain 15 twice at preflash levels of 0 and 160 electrons. The whole sequence is repeated with filter F814W. Then a whole orbit is filled with 1 second exposures, in order to investigate the effect of CTE on low signal level stars (but with high accumulated signal-to-noise). This last orbit is repeated with a preflash of 40 electrons. This is based on Cycle 4 programs 5645 + 5646 + 5659.
- **Accuracy**: As this test is a differential measurement of the CTE slope, it should be very accurate (much better than 1%). As a large number of stars are involved, and the photon noise on each measurement is of order 1%, the slope derived should be much more accurate. The largest remaining uncertainty will be the absolute level of the slope, not differential effects caused by varying background.
- **Products**: After pipeline processing, each image will be reduced by aperture photometry to measure the stellar brightness and how it depends on the preflash level. This is a differential measurement and gives no direct information about the slope of the CTE effect at high background levels. The absolute CTE can be estimated from 5646 (already run once with a raster in this field).

6193: PSF Characterization

- **Purpose**: Provide a sub-sampled PSF over the full field to allow PSF fitting photometry.
- **Description**: This proposal measures the PSF over the full field in photometric filters in order to update the TIM and TinyTIM models and to allow accurate empirical PSFs to be derived for PSF fitting photometry. With one orbit per photometric filter, a spatial scan is performed over a 4x4 grid on the CCD. The step size is 0.025 arcseconds. This gives a critically sampled

PSF over most of the visible range. The crowded ω Cen field is used. 40 sec images are taken through each of the photometric filters (F336W, F439W, F555W, F675W, F814W). Data volume will be a problem, so special tape recorder management will be called for. This is based partially on Cycle 4 program 5575, which used the same field. The proposal also allows a check for sub-pixel phase effects on the integrated photometry.

- **Accuracy**: The chosen field will have hundreds of well exposed stars in each chip. Each star will be measured 16 times per filter at different pixel phases. In principle, the proposal therefore provides a high signal-to-noise critically sampled PSF. This would leave PSF fitting photometrists in a much better position than now where pixel undersampling clearly limits the results. The result will be largely limited by breathing variations in focus. It is hard to judge the PSF accuracy that will result. If breathing is less than 5 microns peak-to-peak, the resulting PSFs should be good to about 10% in each pixel. PSF fitting results using this calibration would, of course, be much more accurate. In addition, the test gives a direct measurement of sub-pixel phase effects on photometry, which should be measured to much better than 1%.
- **Products**: This program provides sub-sampled PSFs for photometry codes, data for comparison with PSF codes, and measurement of pixel phase effect on photometry (sub-pixel QE variations exist).

6194: Polarization and Ramps

- **Purpose**: Perform residual calibration and check for stability of polarizer and ramp filters.
- **Description**: This proposal does not duplicate the existing ramp wavelength calibration or polarization calibration (Cycle 4 programs 5574 and 6140). Instead, it provides a full polarization calibration for a filter that was not supported in Cycle 4 (F300W), a check for polarization stability, and a throughput calibration for the linear ramp filters, by scanning the spectrophotometric standard along the ramps.
- **Accuracy**: The proposal should support polarimetry at the 3% level and measure the ramp throughput at the 2% level.

6195: Flat field Check

- **Purpose**: Check quality of flat fields and estimate errors in them.
- **Description**: The crowded ω Cen field is positioned with a bright star at the center of each CCD in turn. 40 second images are taken through each of the photometric filters (F336W, F439W, F555W, F675W, F814W) and as many supplementary filters (from F450W, F606W, F702W and F547M) as can be fitted in. If data volume is a problem, single chip readout is acceptable, but should be avoided as much as possible. This is based on Cycle 4 programs 5659 and 5646.
- **Accuracy**: Overall discrepancies between the existing flat fields and the results of this test should be 1-2% rms. Part of the point of the test is to measure this accuracy.

- **Products**: After pipeline processing, each image will be reduced by aperture photometry to measure the RMS errors in the flat fields. The RMS error will be determined by the additional noise in the independent measurements over the expected variance of less than 1% from photon statistics. The single bright star at the center of each chip independently estimates the chip to chip normalization error.

6250: Internal Monitor

- **Purpose**: Check for short term stability of instrument.
- **Description**: The routine internal monitor, to be run twice weekly for WFPC2 during Cycle 5, obtains two bias frames at each gain, two INTFLATs with the F555W filter at each gain, and two Kelsall spot images with exposure times optimized for the WF and PC, respectively. It is identical to the Cycle 4 program 5560.
- **Accuracy**: This monitor is not involved in generating quantitative calibration information.
- **Products**: The test provides a biweekly monitor of the integrity of the CCD camera chain electronics both at gain 7 and 15, a test for quantum efficiency hysteresis in the CCDs, and an internal check on the alignment of the WFPC2 optical chain. Stiavelli and Baggett, WFPC2 ISR 96-01.

8.10 Cycle 6 Calibration Plan

The Cycle 6 calibration plan is similar to that for Cycle 5, and is summarized in Table 8.3. Important differences include the addition of programs to check the astrometric calibration (6941), more detailed checking of the camera electronics (6942), and measurements of narrow band filter throughputs (6943). Also, it is expected that there will be reduced usage of the calibration channel VISLAMP, so as to prolong the lamp lifetime. More detailed program descriptions are given below.

Table 8.3: Summary of Cycle 6 Calibration Plan.

ID	Proposal Title	Schedule	Results	Accuracy	External Time (orbits)	Notes
			Routine Monitoring Programs			
6902	Photometric Monitor	2x per 4 weeks	SYNPHOT	2%	26	
6903	Decontamination	1x per 4 weeks	CDBS	n/a	0	(darks, internals)
6904	Darks	Weekly	CDBS	1 e/hr	0	WWW hot pixel lists
6905	Internal Monitor	Weekly	CDBS	0.8 e	0	
6906	Visflat Monitor	2x per 4 weeks	ISR	0.3%	0	(monitor lamp health)
6907	Intflat Monitor	1x per 4 weeks	ISR	0.3%	0	
6908	UV Flat Field Monitor	2x in Cyc. 6	ISR	2-8%	0	
6909	Earth Flats	Continuous	CDBS	0.3%	0	
			Special Calibration Programs			
6934	Photometric Zeropoint	1x in Cyc. 6	SYNPHOT	2%	6	Add 2 new standards
6935	Photometric Trans.	2x in Cyc. 6	ISR	2-5%	9	Three targets
6936	UV Throughput & Ly α	2x in Cyc. 6	SYNPHOT	3-10%	12	Include BD+75D325
6937	CTE Calibration	1x in Cyc. 6	ISR	1%	2	
6938	PSF Characterization	1x in Cyc. 6	CDBS	10%	7	
6939	Linear Ramp Filters	1x in Cyc. 6	CDBS	3%	4	
6940	Polarizers	1x in Cyc. 6	CDBS	3%	4	
6941	Astrometry Verification	1x in Cyc. 6	STSDAS	0.01″	4	
6942	Camera Elect. Verification	1x in Cyc. 6	ISR	0.5%	1	
6943	Narrow Band Throughput	SNAP	SYNPHOT	3%	8	SNAP
	TOTALS				83	

6902: Photometric Monitor

- **Purpose:** Monthly external check of instrumental stability.
- **Description:** The standard star GRW+70D5824 is observed before and after each decontamination (thus twice in a four-week period). Each observation consists of three sequences: (1) F170W in all four chips to monitor contamination in the far UV; (2) F439W, F555W, F814W on the PC to monitor focus; and (3) F160W, F185W, F218W, F255W, F300W, F336W, F439W, F555W, F675W, F814W in a different chip each month. Some filters may be cut because of lack of time (F185W cut first, then F300W, then

F675W, then F218W). This proposal is based largely on Cycle 5 program 6184; focus monitoring in F439W and F814W is added at the expense of some UV filters.

- **Accuracy:** Overall discrepancies between the results of this test need to be measured to better than 2% and are expected to be less than 1% rms. The point of the test is to measure this variation.
- **Products:** Documents produced are Instrument Handbook, TIPS, WWW (sensitivity trends). Updates in UV sensitivity variation used in SYNPHOT are provided.

6903: Decontamination

- **Purpose:** UV blocking contaminants are removed by warming the CCDs.
- **Description:** The decon itself is implemented via use of the DECON mode, in which the TECs are turned off and the CCD and heatpipe heaters are turned on to warm the detectors and window surfaces. Keeping WFPC2 warm for ~6 hours has been shown in previous Cycles to be sufficient to remove the contaminants and anneal many hot pixels; continuation of 6-hour decons is anticipated for Cycle 6.

  The internal observations taken before and after each decontamination consist of: 4 biases (2 at each gain setting), 4 INTFLATs (2 at each gain setting), 2 kspots (both at gain 15, one short and one long exposure, optimized for PC and WF), and finally, 5 darks (gain 7, CLOCKS=NO). To minimize time-dependent effects, each set of internals will be grouped within 2 days and performed no more than 1 day before the DECON and no later than 12 hours after the DECON. To protect against residual images in the darks (which results in the irretrievable loss of the critical pre-DECON hotpixel status), the darks will be executed NON-INT and requested to be done at least 30 minutes after any WFPC2 activity.

  Special Requirements: This requires scheduling at 4 week intervals. It prevents WFPC2 from being used for several hours, although other instruments can be used most of that time. Dark frames taken before decontaminations need to be protected from possible residual images from overexposed sources.
- **Accuracy:** This proposal is mainly designed to maintain the health of the instrument. Biases, darks and other internals taken with this proposal are used in generating appropriate reference files.
- **Products:** They are obtained from use of darks, biases and other internals (see Proposals 6904 and 6905).

6904: Darks

- **Purpose:** Measure dark current on individual pixels and identify hot pixels at frequent intervals.
- **Description:** Every week, five 1800s exposures are taken with the shutter closed. The length of the exposures is chosen to fit nicely within an occultation period. The weekly frequency is required because of the high forma-

tion rate of new hot pixels (about 70/CCD/day). Five darks a week are required for cosmic ray rejection, to counterbalance losses due to residual images, and to improve the noise of individual measurements. Even with these measures, some weeks no usable darks will be available because of residual images. Normally this results only in a longer-than-usual gap in the hot pixel lists, but in a decontamination week, information on pixels that became hot and then annealed would be lost irretrievably. For this reason, pre-DECON darks are to be executed NON-INT and at least 30 minutes after any WFPC2 activity (see Proposal 6903). Normal darks do not need to be protected in this fashion.

- **Accuracy:** Superdarks should be accurate to better than 1 e/hour and are expected to reach errors of about 0.05 e/hour (single-pixel rms). Systematic errors due to dark glow (a spatially and temporally variable component of dark signal) and hot pixels may exceed these limits significantly.
- **Products:** Weekly dark frames are delivered to CDBS and monthly tables of hot pixels are posted on the Web.

6905: Internal Monitor

- **Purpose:** Verification of short-term instrument stability for both gain settings.
- **Description:** The internal observations will consist of 8 biases (4 at each gain, and 4 INTFLATs (2 at each gain). The entire set should be run once per week (except for DECON weeks) on a non-interference basis. This proposal is similar to the Cycle 5 Internal Monitor (6250), except that the K-spot images have been removed (these are being taken with the DECON Proposal). The execution frequency during Cycle 6 has also been reduced, from twice a week to once a week, although the total number of biases has been increased to continue to provide an adequate number of frames for pipeline reference file generation.
- **Accuracy:** Approximately 40 bias frames will be used for each pipeline reference file; accuracy is required to be better than 1.5 e/pixel, and is expected to be 0.8 e/pixel.
- **Products:** Superbiases are delivered every few months to CDBS. TIPS reports are made on possible buildup of contaminants on the CCD windows (worms) as well as gain ratio stability, based on INTFLATs. ISRs are prepared if significant changes occur.

6906: Visflat Monitor

- **Purpose:** Monitor the stability of the camera and filter responses via the VISFLAT channel.
- **Description:** Twice a month, internal flat fields (VISFLATs) will be obtained using the visible calibration channel lamp with the photometric filter set plus a couple of narrow-band filters. The images will be used to monitor WFPC2's flat field response as well as to build a high S/N flat field database, which will provide information on the pixel-to-pixel response in the cameras and any possible long-term contamination-induced changes.

The LRF (FR533N) exposures, one at each gain, taken after DECON will provide a monitor of the ADC's performance. Histograms generated from the ramp filter flats will be used to trace the ADC transfer curve. ON HOLD: In addition to the monitor observations, an initial filter-sweep is done to obtain VISFLATs in all visible filters. These will be compared to the Cycle 5 filter-sweep data to verify that none of the filters are developing any problems, and to provide a check of the calibration channel's long-term stability.

- **Special Requirements:** Uses the VISFLAT calibration channel, whose Welch-Allyn bulb is apparently wearing out. (A back-up exists for the Welch-Allyn bulb.) The Cycle 6 proposal has been redesigned to limit the number of ON/OFF cycles placed on this channel to a level believed safe over 10-15 years. The sweep part of the proposal, which puts the heaviest usage on the lamp, is on hold, pending verification of the lamp health from the short monthly executions. The INTFLAT Monitor (Proposal 6907) can obtain similar information if necessary.
- **Accuracy:** The VISFLAT response is stable to about 0.3%, both in overall level (lamp degradation aside) and in spatial variations. The point of this proposal is to verify this stability on a regular basis and to monitor the lamp degradation.
- **Products:** ISR and TIPS reports will be prepared.

6907: Intflat Monitor

- **Purpose:** Provide backup database of INTFLATS in case VISFLAT channel fails.
- **Description:** This proposal consists of two parts: 1) an INTFLAT filter sweep and, 2) a series of exposure to test the linearity of the camera. 1) The sweep is a complete set of internal flats cycling through both shutter blades and both gains. Signal-to-noise per pixel is estimated to be similar to the VISFLATs (0.6%) but the spatial and wavelength variations in the illumination pattern are much larger. However, the INTFLATs will provide a baseline comparison of INTFLAT vs. VISFLAT, in the event of a calibration channel system failure and temporal variations in the flat fields at the 1% level. In addition, these images will provide a good measurement (better than 1%) of the stability of the gain ratios. 2) The linearity test portion is aimed at obtaining a series of INTFLAT with both gains and both shutters. Since the INTFLATs have significant spatial structure, any non-linearity would appear as a non-uniform ratio of INTFLATs with different exposure times. A set of exposures is also taken with gain 7, shutter B, and CLOCKS=YES.
- **Accuracy:** The signal-to-noise per pixel is similar to that obtained in the VISFLAT program (0.6%) but there are much larger spatial and wavelength variations in the illumination pattern. As a result, this dataset will not form any part of the pipeline calibration. This baseline is necessary in case the VISFLAT channel fails and there are temporal variations in the camera flat-fields at the 1% level.

- **Products:** TIPS reports and ISRs will be prepared if any significant variations are observed.

6908: UV Flat Field Monitor

- **Purpose:** Monitor the stability of UV flat field.
- **Description:** UV flat fields will be obtained with the calibration channel's ultraviolet lamp (UVFLAT) using the UV filter set (F122M, F170W, F160BW, F185W, and F336W). The UV flats will be used to monitor UV flat field stability and the stability of the Woods filter (F160BW) by using F170W as the control. The F336W ratio of VISFLAT (Cycle 6 proposal 6906)/UVFLAT ratio will provide a diagnostic of the UV flat field degradation and tie the UVFLAT and VISFLAT flat field patterns together. Two supplemental dark frames must be obtained immediately after each use of the lamp, in order to check for possible afterimages.
- **Special Requirements:** This uses the limited life UV lamp. In order to prevent excessive degradation of the lamp, the SU duration for each UVFLAT visit should be kept the same as the durations used during Cycle 5 (proposal 6191); the lamp should not remain on for periods of time longer than those used in Cycle 5. To be executed once before and once after the refurbishment mission, shortly after a decontamination.
- **Accuracy:** About 2-8% pixel-to-pixel are expected (depending on filter).
- **Products:** New UV flat fields are made if any changes are detected.

6909: Earth Flats

- **Purpose:** Monitor flat field stability.
- **Description:** As in Cycle 5 program 6187, 4 sets of 200 Earth streak-flats are taken to construct high quality narrow-band flat fields with the filters F160BW, F375N, F502N, F656N and F953N. Of these 200 perhaps 50 will be at a suitable exposure level for de-streaking. The resulting Earth superflats map the OTA illumination pattern and will be combined with SLTV data (and calibration channel data in case of variation) for the WFPC2 filter set to generate a set of superflats capable of removing both the OTA illumination and pixel-to-pixel variations in flatfield. The Cycle 4 plan is being largely repeated except: (1) UV filters are dropped because measurement is generally only of the redleak; (2) F160BW is retained in order to check for developing pinholes; and (3) Crossed filters used as neutral densities are eliminated (illumination pattern is wrong). Specific observations for the Methane Quad filters will also be included.
- **Accuracy:** The single-pixel noise expected in the flat field is 0.3%.
- **Products:** New flat fields to CDBS if changes detected.

6934: Photometric Zeropoint

- **Purpose:** Verify synthetic zeropoint of WFPC2 filters.

- **Description:** Standard stars are observed through all filters longward of F336W (inclusive) with the limit of one orbit per target. Targets include: the spectrophotometric standard GRW+70D5824 in PC and WF3; two stars chosen as standards by other instruments on HST; and two standard star fields, containing 3-4 stars each, commonly used in ground-based photometry. Observations of GRW+70D5824 will be directly comparable to the corresponding observations for cycles 4 and 5 (programs 5572 and 6179) and will verify the stability of the filters as well as improve the accuracy of the calibration. The other standards are observed to provide cross-instrument calibration and in order to increase the range of colors used for photometric verification. This proposal will help all observers who want to do quantitative photometry at the 2% level.
- **Special Requirements:** Specific orientations will be required for the two fields of standards in order to fit the maximum number of stars. All observations should be executed within a week after decontamination.
- **Accuracy:** 2% required, 1% expected for our main spectrophotometric standard GRW+70D5824. Expected accuracy for the other standards is between 2% and 5%, depending on spectral type and filter; most of the error derives from limited knowledge of the transformations between ground-based and WFPC2 photometric systems.
- **Products:** TIPS reports, SYNPHOT updates if necessary, and ISRs will be prepared.

6935: Photometric Transformation

- **Purpose:** (1) Update photometric transformations to Johnson-Cousins system and Strömgren system; (2) Determine spatial dependence of contamination; (3) Check the astrometric solution using M67; (4) Spot check of gain=7 vs. gain=15 ratios; 5) Spot check short vs. long exposure zeropoints.
- **Description:** Three photometric standard star fields in NGC 5139 (ω Cen; metal rich), NGC 2682 (M67; metal poor), and NGC 2100 (young cluster) are observed before and after a decontamination. Four different filter sets are used: (1) The five filters generally used to match the Johnson-Cousins system (F336W, F439W, F555W, F675W, F814W); (2) The wide-band equivalents for the Johnson-Cousins system (F300W, F380W, F450W, F606W, F702W); (3) The Strömgren equivalents (F336W, F410M, F467M, F547M); and (4) Two filters farther toward the UV (F255W, F170W), so that contamination over the full field of view can be measured. F255W is not used for the reddest cluster (NGC 5139). F170W is only used for the bluest cluster (NGC 2100).

  For the brighter clusters (NGC 2682 and NGC 2100) long and short exposures are taken in the UBVRI equivalents both to extend the dynamic range and to check for differences in photometric zeropoints.

  A spot check is included to compare gain=7 and gain=15 is also included for NGC 5139 and NGC 2682.

- **Special Requirements:** The first visit for each target must be taken within 3 days after a decontamination. The second visit, including only the UV filters, must be taken more than 25 days after the first visit, but before the next decontamination.
- **Accuracy:** The photometric transformations should be accurate to 2-5%. The stability of these transformations will be measured to the 1% level. The astrometry should be good to 0.1″ (absolute) and 0.05″ (relative).
- **Products:** ISR and Instrument Handbook. It will also be part of a planned paper on the possibility to do 1% photometry.

6936: UV Throughput and Lyman-α Verification

- **Purpose:** Verify throughput for all UV filters, including Lyman-α test to monitor possible contamination on pick-off mirror.
- **Description:** Spectrophotometric standards are observed shortly before and after a DECON through all the UV filters in each chip and through F160BW crossed with F130LP, F185LP, and F165LP to determine the wavelength dependence of the throughput across the bandpass (for color terms). This proposal is based on the Cycle 5 UV Throughput proposal (6186) but includes also the standard BD+75D325 used in Cycle 4 (proposal 5778) to establish the Lyman-α throughput calibration.
- **Special Requirements:** Timing requirements with respect to decontaminations.
- **Accuracy:** The UV throughput will be measured to better than 3%. Accuracy in Lyman-α throughput is expected to be between 5 and 10%, because of the residual uncertainty of the red leak correction after observations with crossed F122M and F130LP.
- **Products:** TIPS reports, SYNPHOT updates, and ISRs will be prepared if necessary.

6937: CTE Calibration

- **Purpose:** (1) Test whether the exposure-time dependence of the photometric calibration is due to CTE (long vs. short exposure problem); (2) refine flux and background-level dependent aperture corrections.
- **Description:** The globular cluster NGC 2419 will be observed through F555W with a combination of exposure times (between 5 and 1400 s) and preflash levels (0 to 500 e^-). Analysis of cycle 5 CTE calibration (proposal 6192) suggests that magnitude errors due to charge transfer effects are greatly reduced (if not entirely eliminated) at background levels of 160 e^- or greater. CTE effects have been proposed as the solution to reported differences in the magnitudes of stars measured on frames with short exposures vs. long exposures. If CTE is the cause, then the differences should disappear with preflash. We will re-observe the cluster NGC 2419 with and without preflash to test this hypothesis. This dataset will also provide a large

number of stars with which to refine existing measurements of the effects of CTE on the wings of the PSF. A range of preflash levels will be explored at the 60 sec exposure time.

- **Special Requirements:** Observations should be made at the same position and roll angle as the previous NGC 2419 LONG exposures (proposal GO-5481).
- **Accuracy:** The reported short vs. long effect is ~0.05 mag. We wish to reduce this to less than 0.01 mag.
- **Products:** An ISR will be prepared. If appropriate, a special task to correct the CTE effect will be generated.

6938: PSF Characterization

- **Purpose:** Provide a sub-sampled PSF over the full field to allow PSF fitting photometry, test PSF subtraction as well as dithering techniques (c.f. effects of the OTA breathing and CCD gain).
- **Description:** Measure PSF over full field in photometric filters in order to update the TIM and TINYTIM models and to allow accurate empirical PSFs to be derived for PSF fitting photometry. These observations will also be useful in order to test PSF subtraction and dithering techniques at various locations on the CCD chips. With one orbit per photometric filter, a spatial scan is performed over a 4X4 grid on the CCD. The step size is 0.025 arcseconds; this gives a critically sampled PSF over most of the visible range. This program uses the same specially chosen field in ω Cen as the Cycle 5 proposal 6193, but with a few arcsec shift in order to map the PSF variation better. The standard 'photometric' filters are used. Two additional orbits are used to explore the effects of OTA breathing and CCD gain onto dithering and PSF subtraction techniques. Data volume will be a problem, so special tape recorder management will be called for. The proposal also allows a check for sub-pixel phase effects on the integrated photometry.
- **Special Requirements:** This needs the same pointing and orientation as Cycle 5 observations for proposal 6193, thus should be scheduled within a similar time frame.
- **Accuracy:** It provides measurement of pixel phase effect on photometry (sub pixel QE variations exist). The chosen field will have tens of well exposed stars in each chip. Each star will be measured 16 times per filter at different pixel phases. The proposal therefore provides, in principle, a high signal-to-noise, critically sampled PSF. This would leave PSF fitting photometrists in a much better position than now, where pixel undersampling clearly limits the results. The result will be largely limited by breathing variations in focus. It is hard to judge the PSF accuracy that will result. If breathing is less than 5 microns peak-to-peak, the resulting PSFs should be good to about 10% in each pixel. Breathing effects will be investigated (1 additional orbit) as well as the gain dependence (1 additional orbit). PSF fitting results using this calibration would of course be much more accurate. In addition, the test gives a direct measurement of sub-pixel phase effects on photometry, which should be measured to better than 1%.

- **Products:** A PSF library (CDBS) will be assembled, and an ISR will be issued as needed.

6939: Linear Ramp Filters

- **Purpose:** Verify throughput calibration for Linear Ramp Filters at selected wavelengths.
- **Description:** Throughput calibration is obtained by observing the spectrophotometric standard GRW+70D5824 at several filter rotations and wavelengths. This completes the program carried out in Cycle 5, in which some wavelength ranges and rotations could not be covered.
- **Accuracy:** Throughput accuracy should be verified to better than 3%; 1-2% can be achieved.
- **Products:** SYNPHOT throughput tables will be updated if necessary.

6940: Polarizers

- **Purpose:** Verify stability of polarization calibration.
- **Description:** The goal of this proposal is to check for any changes in the polarization calibration since Cycle 5. Observations are made in F555W+POLQ of both polarized and unpolarized stars, in addition to VISFLATs. Data are taken in all four quads of the polarizer, as well as in three rotated positions of the POLQ.
- **Special Requirements:** Requires specific orientations.
- **Accuracy:** 3%.
- **Products:** Update throughput tables if necessary

6941: Astrometry Verification

- **Purpose:** Verify accuracy and stability of geometric transformation and relative astrometry solution.
- **Description:** A very rich star field in ω Cen will be observed in five different positions with relative shifts of 40″ in each coordinate. Positions of more than 2000 stars per chip will be compared between pointings using the three different astrometric solutions provided by Gilmozzi, Holtzman and Trauger, in order to verify and refine their accuracy. (Differences of up to 1 PC pixel exist in some regions of the field of view.) A very densely populated field is chosen in order to achieve better coverage of the field of view, even if at the expense of the accuracy of individual position measurements. Observations will be carried out in three filters, F555W, F300W, and F814W, to provide a verification and/or correction of the wavelength dependence of the solution. The F555W observation is repeated with smaller shifts of 15″ to ensure a better coverage of the PC.
- **Accuracy:** We expect better than 0.01″ and require better than 0.05″ (full field of view).
- **Products:** Improvements will be noted in METRIC and in the aperture reference file if required. An ISR will be issued as needed.

6942: Camera Electronics Verification

- **Purpose:** Verify several aspects of the WFPC2 camera electronics: linearity, gain ratios, effect of CLOCKS, and effect of CTE on extended sources.
- **Description:** Observing a very extended non-uniform target represented by the giant elliptical galaxy NGC 4472. The linearity test is carried out by taking exposures of NGC 4472, centered in WFALL, with a variety of exposure times. Since the galaxy is non-uniform, the ratio of these exposures is directly related to the camera linearity. The exposures will be taken with GAIN=7. However, one exposure will also be taken with GAIN=15. Additional exposures will be taken with CLOCKS=YES and with a preflash. These observations complement those of the internal calibration proposal 6907. The two major advantages of these observations compared to the 6907 ones are the possibility of studying the effect of preflash (since the light distribution of the preflash is different from that of NGC 4472) and the possibility of measuring an absolute response curve, since NGC 4472, unlike the INTFLAT lamp, does not have variations in luminosity. NGC 4472 has been chosen as target galaxy because it is large enough to produce significant signal in all chips and bright enough to allow us to explore the highest counts without excessive integration times.
- **Accuracy:** We expect 0.5% for linearity and CTE, 0.1-0.2% for gain ratios and CLOCKS. We require less than 1% on each item.
- **Products:** ISRs and TIPS reports will be prepared as needed.

6943: Throughput Verification for Narrow Band Filters

- **Purpose:** Direct verification of throughput of narrow band filters through observations of emission line objects.
- **Description:** The current throughput calibration of narrow-band filters is based on filter profiles from data obtained before launch and on observations of continuum sources. This program will verify the accuracy of the calibration, and indirectly the stability of the filters, by observing eight planetary nebulae with strong lines and well-established ground-based spectra. The observations can be executed in SNAPSHOT mode since they will be short and none is specifically required. Some planetary nebulae with existing Cycle 4 and 5 observations will be included for stability verification.
- **Accuracy:** We expect 2% and require 3%.
- **Products:** SYNPHOT tables will be updated and an ISR issued if required.